SELINUS UNIVERSITY
OF SCIENCES AND LITERATURE

Computer, Physics, and Clinical Applications of Spectral Computed Tomography

By ZIMAM A. ROMMAN

A DISSERTATION

Presented to the Department of
Biomedical Imaging Technology
program at Selinus University

Faculty of Computer Science
in fulfillment of the requirements
for the degree of Doctor of Philosophy
in Biomedical Imaging Technology

2023

Abstract

Computed Tomography (CT) has been a fundamental pillar in medical imaging for over five decades. This modality enabled the viewing of internal structures of the body, revolutionizing the diagnosis and treatment of various diseases. CT images are generated using rotating x-ray tube and x-ray detector bank and can made available through mathematical algorithms and signal processing techniques. The x-ray tube serves as the source of radiation and emits x-ray beam made of poly-energetic photons. While this beam nature can allow for image generation of body structures and has been essential for medical diagnostics, it has several limitations, including poor tissue contrast and limited information about chemical composition.

In recent years, the introduction of the Spectral CT has overcome most of these limitations by enabling more exact and detailed characterization of tissues. This innovation is based on the measurement of the energy spectrum of x-ray photons and the detection of changes in their attenuation as they interact with several types of tissues. By supplying more precise information about tissue composition, spectral CT has the potential to improve clinical outcomes and facilitate earlier diagnosis of various conditions, including cancer, cardiovascular disease, and neurological disorders.

This thesis aims to review and supply deeper understandings of the fundamentals principles and imaging requirements including potential artifacts and image quality assessment of Spectral CT. The work will also include the potential clinical applications in the diagnostic and therapeutic fields, adoption insights, and future strategies.

Acknowledgment

In the loving memory of my late father, Ali, I want to express my deep gratitude for the enduring impact he had on my life, even in his absence and I carry his values and wisdom with me always.

I extend my heartfelt appreciation to my mother, Mariam, for her endless love, sacrifices, and encouragement. Her strength and resilience, especially after my father's passing, have been my guiding light.

To my beloved wife, Nida, I am incredibly grateful for your unwavering support, understanding, and patience during the challenging times of my dissertation.

My sons, Ali and Mohammed and my daughter Hala, have been a source of inspiration as well.

I also want to acknowledge my dissertation supervisor Prof. Salvatore Fava for his support.

Table of Contents

List of Tables and Figures

Tables

Figures

CHAPTER 1: Introduction and Aim of the Study

Computed Tomography revolutionized medical imaging by providing detailed cross-sectional images of the human body. It is a non-invasive imaging technique that combines X-ray technology with computer processing to generate high-resolution images. This introduction aims to explore the invention of CT, its value in clinical practice, the increased number of CT procedures with statistics, and its limitations in image quality and diagnosis.

The invention of computed tomography is attributed to the work of British engineer Godfrey Hounsfield and South African physicist Allan Cormack. In the early 1970s, Hounsfield developed the first CT scanner while working at Electric and Musical Industries (EMI) Laboratories. His work earned him the Nobel Prize in Physiology or Medicine in 1979. Cormack, on the other hand, contributed to the development of the mathematical algorithms needed to reconstruct images from the X-ray data obtained through CT scanning.

Computed Tomography involves the use of X-rays and detectors to measure the attenuation of X-ray beams as they pass through the body. The collected data is processed by a computer, which generates detailed cross-sectional images. Hounsfield's invention was a significant milestone in medical imaging, as it allowed physicians to visualize internal structures in a way that was not possible with conventional X-rays.

CT imaging has become an essential tool in clinical practice due to its potential advantages. It provides detailed anatomical information and allows for the visualization of structures that are difficult to assess with other imaging modalities. CT is used in various medical specialties, including radiology, oncology, neurology, cardiology, and trauma care. It aids in the detection, diagnosis, and monitoring of a wide range of diseases and conditions, such as cancer, cardiovascular disorders, neurological disorders, and musculoskeletal injuries.

In the field of oncology, CT plays a crucial role in the staging of tumors, assessing treatment response, and guiding biopsies. In emergency medicine, CT is valuable for evaluating trauma patients and finding internal injuries. In cardiology, CT angiography supplies detailed images of the coronary arteries, aiding in the

diagnosis of coronary artery disease. CT also plays a crucial role in the planning of surgical interventions and radiation therapy, allowing for precise targeting of tumors while minimizing damage to surrounding healthy tissues.

Over the years, there has been a significant increase in the number of CT procedures performed worldwide. This surge can be attributed to several factors, including technological advancements, increased availability of CT scanners, and the growing demand for correct and prompt diagnostic information. According to statistics from the World Health Organization (WHO), the number of CT examinations has been rising steadily, with an estimated 7 billion CT scans performed globally each year.

The widespread adoption of CT imaging can be attributed to its ability to supply fast and correct diagnosis, which leads to improved patient outcomes. The advancements in CT technology, such as faster scanning times, higher spatial resolution, and the development of multi-detector CT scanners, have contributed to the increased use of CT in clinical practice. The accessibility of CT scanners in hospitals and imaging centers has also played a significant role in the rise of CT procedures.

While CT imaging offers exceptional diagnostic capabilities, it does have certain limitations in terms of image quality. One major limitation is the presence of artifacts, which can degrade the clarity and accuracy of the images. Artifacts can arise from various sources, including patient motion, metallic implants, and image reconstruction errors. These artifacts may lead to misinterpretation of the images and potentially affect the accuracy of the diagnosis.

Although CT is a powerful imaging modality, it has limitations when it comes to certain diagnostic challenges. One such limitation is its lower sensitivity in detecting early-stage cancers compared to other imaging techniques such as magnetic resonance imaging (MRI) or positron emission tomography (PET). While CT can supply detailed anatomical information, it may not always reveal the functional or molecular characteristics of tumors, which can be important for exact staging and treatment planning.

Another limitation of CT is its use of ionizing radiation. CT scans involve exposure to X-rays, which carry a small but potential risk of causing radiation-induced cancers,

particularly in patients who undergo repeated scans or are more sensitive to radiation, such as children and young adults. To mitigate this risk, efforts are being made to optimize CT protocols and minimize radiation doses without compromising image quality. Techniques such as automatic exposure control, iterative reconstruction algorithms, and low-dose protocols are being employed to reduce radiation exposure while supporting diagnostic accuracy.

Additionally, CT imaging may face challenges in imaging certain types of tissues or structures. For example, imaging structures with high calcium content, such as bones or calcified plaques, may lead to beam hardening artifacts, which can affect the accuracy of the image interpretation. Similarly, distinguishing between several types of soft tissues with similar densities, such as differentiating between liver lesions or characterizing small nodules in the lungs, can be challenging due to limited tissue contrast in CT imaging.

Furthermore, CT scans may require the use of contrast agents to enhance the visualization of specific structures or abnormalities. While contrast-enhanced CT scans can provide valuable information, the use of contrast agents carries risks, such as allergic reactions or adverse effects on renal function, especially in patients with pre-existing kidney disease. Precautions and proper patient selection are necessary to minimize these risks.

In recent years, efforts have been made to overcome these limitations and enhance the diagnostic capabilities of CT. Dual-energy CT, for example, combines data from different X-ray energy levels to improve tissue characterization and reduce artifacts. Advanced image reconstruction techniques, such as iterative reconstruction algorithms, are being developed to improve image quality, reduce noise, and enhance spatial resolution.

In conclusion, Computed Tomography has revolutionized medical imaging, providing clinicians with detailed and precise cross-sectional images of the human body. It has proven invaluable in diagnosing and monitoring various diseases and conditions across multiple medical specialties. However, it is important to recognize the limitations of CT, including artifacts, radiation exposure, challenges in diagnosing certain conditions, and the need for contrast agents. Ongoing advancements in technology and imaging techniques aim to address these

limitations, further improving the utility and diagnostic accuracy of CT in clinical practice.

Dual-energy spectral computed tomography (DECT) is an advanced imaging technique that has gained significant attention in recent years. This introduction aims to explore the invention of dual-energy spectral CT, its status, and its potential clinical value. By using multiple energy levels, dual-energy spectral CT provides enhanced tissue characterization and improved diagnostic capabilities, opening new avenues in medical imaging.

The invention of dual-energy spectral CT can be traced back to the pioneering work of Dr. Jorgen H. J. Jorgensen in the late 1970s. Dr. Jorgensen proposed the concept of using different energy levels in CT imaging to overcome the limitations of conventional CT, particularly in terms of tissue characterization. His first work laid the foundation for the development of dual-energy spectral CT technology.

Dual-energy spectral CT involves the simultaneous acquisition of two or more CT datasets at different energy levels. This is achieved by using either two X-ray sources with different voltage potentials or a single X-ray source with rapid switching of tube voltage. The acquired datasets are then processed to generate composite images that highlight different tissue properties based on their energy-dependent attenuation characteristics.

Dual-energy spectral CT has rapidly evolved over the past few decades, with significant advancements in both hardware and software. Modern CT scanners are equipped with dual-energy capabilities, allowing clinicians to acquire and analyze data at multiple energy levels. Various algorithms and reconstruction techniques have been developed to extract tissue-specific information and generate material-specific images, improving diagnostic accuracy.

In terms of hardware, dual-energy spectral CT scanners employ advanced detectors capable of discriminating between different energy levels, as well as X-ray sources capable of rapidly switching energy levels or running at multiple energy settings. Additionally, iterative reconstruction algorithms and post-processing techniques have been refined to reduce image artifacts and improve image quality.

Dual-energy spectral CT offers several potential clinical benefits across a wide range of medical specialties. Its ability to differentiate materials based on their

energy-dependent attenuation characteristics provides valuable information for tissue characterization, identification of specific substances, and improved lesion detection. Potential clinical applications of dual-energy spectral CT include:

Oncology:

Dual-energy spectral CT scan aid in the characterization of lesions, differentiation between benign and malignant tissues, and assessment of tumor vascularity. It may also play a role in evaluating treatment response and detecting early signs of recurrence.

Cardiovascular Imaging:

Dual-energy spectral CT enables correct assessment of coronary artery calcifications, characterization of plaque composition, and identification of perfusion defects. It can also supply valuable information for pre-procedural planning in Transcatheter Aortic Valve Replacement (TAVR) and other interventions.

Musculoskeletal Imaging:

Dual-energy spectral CT can aid in the evaluation of gout by distinguishing uric acid crystals from other types of crystal deposits. It also shows promise in assessing bone mineral density and detecting subtle fractures.

Abdominal Imaging:

Dual-energy spectral CT can improve the detection and characterization of liver lesions, particularly in patients with fatty liver disease. It can also aid in the evaluation of renal stones and identification of iodine-enhancing lesions in the kidneys.

Pulmonary Imaging:

Dual-energy spectral CT has potential applications in pulmonary imaging, such as the assessment of pulmonary embolism, characterization of lung nodules, and differentiation of ground-glass opacities.

CHAPTER 2: Literature Search

2.1 All Clinical Applications

Table 1: Description of the method of research in the literature (All applications)

Item	
Date of Search	20-Sep-2023
Sources	PubMed, Cochrane
Search Items	(Spectral CT OR dual energy CT OR dual-energy CT OR dual-energy computed tomography OR dual-energy computed tomography OR DECT)
Period	No restrictions
Inclusion Criteria	Articles published in English

Results:

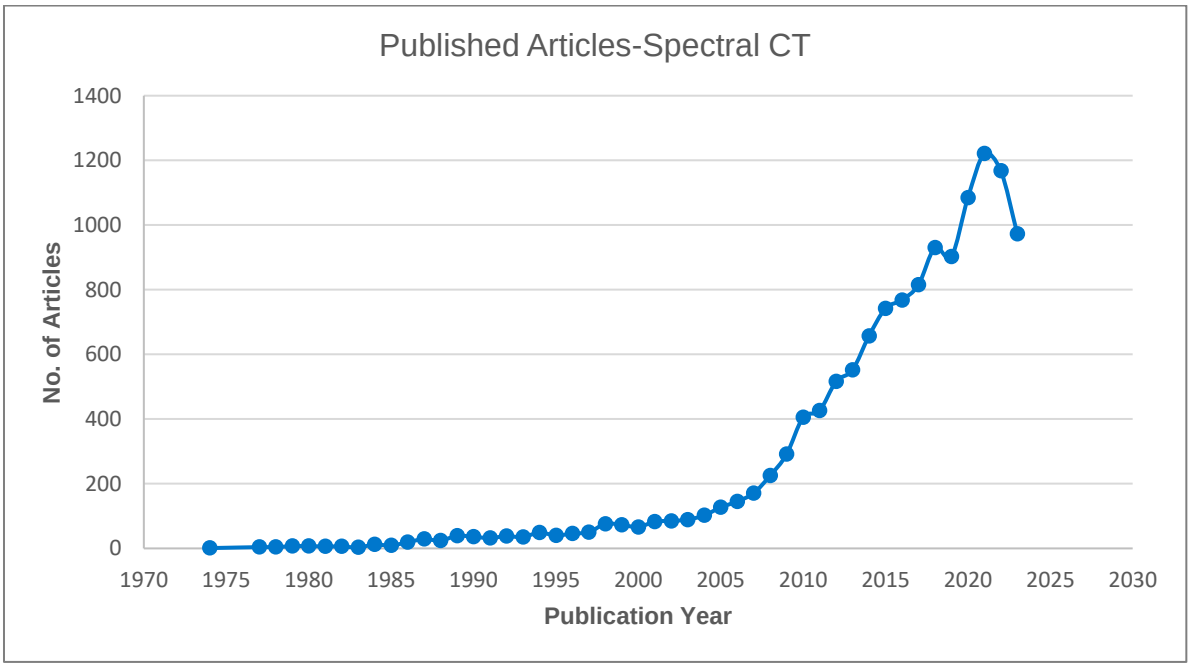

2.2 Abdomen

Table 2: Description of the method of research in the literature (Abdomen)

Item	
Date of Search	20-Sep-2023
Sources	PubMed, Cochrane
Search Items	(Spectral CT OR dual energy CT OR dual-energy CT OR dual-energy computed tomography OR dual-energy computed tomography OR DECT AND Abdomen)
Period	No restrictions
Inclusion Criteria	Articles published in English

Results:

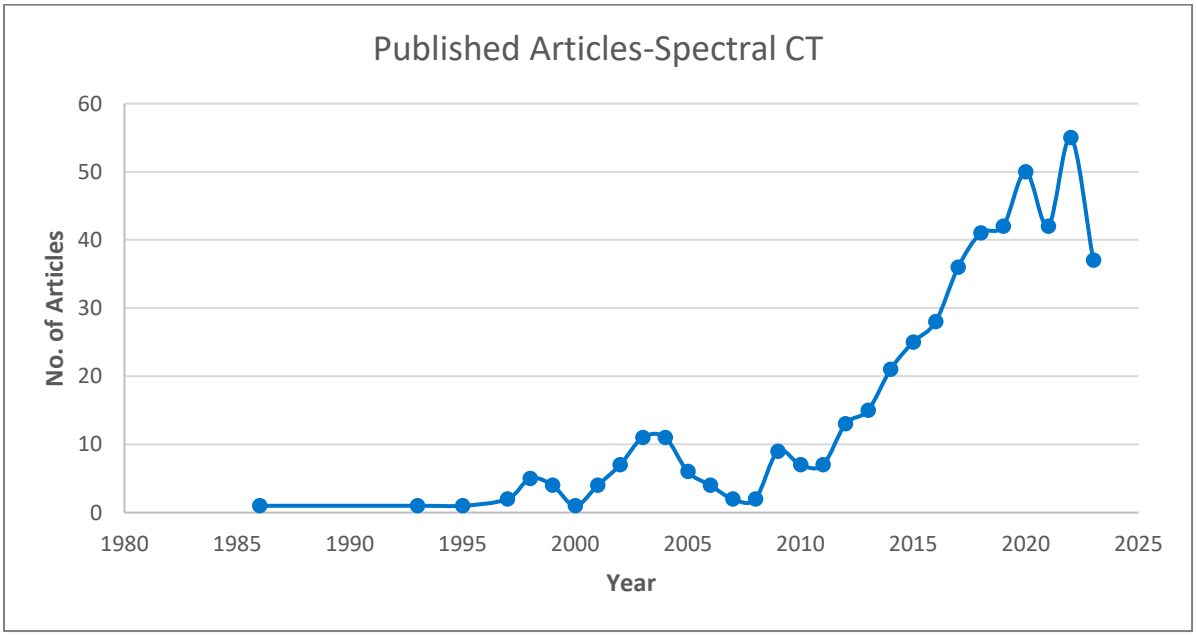

2.3 Chest

Table 3: Description of the method of research in the literature (Chest)

Item	
Date of Search	20-Sep-2023
Sources	PubMed, Cochrane
Search Items	(Spectral CT OR Dual energy CT OR dual-energy CT OR dual-energy computed tomography OR dual-energy computed tomography OR DECT) and (pleura OR lung OR breast OR mediastinum OR thymus OR embolism OR bone metastasis OR esophagus OR esophageal cancer)
Period	No restrictions
Inclusion Criteria	Articles published in English

Results:

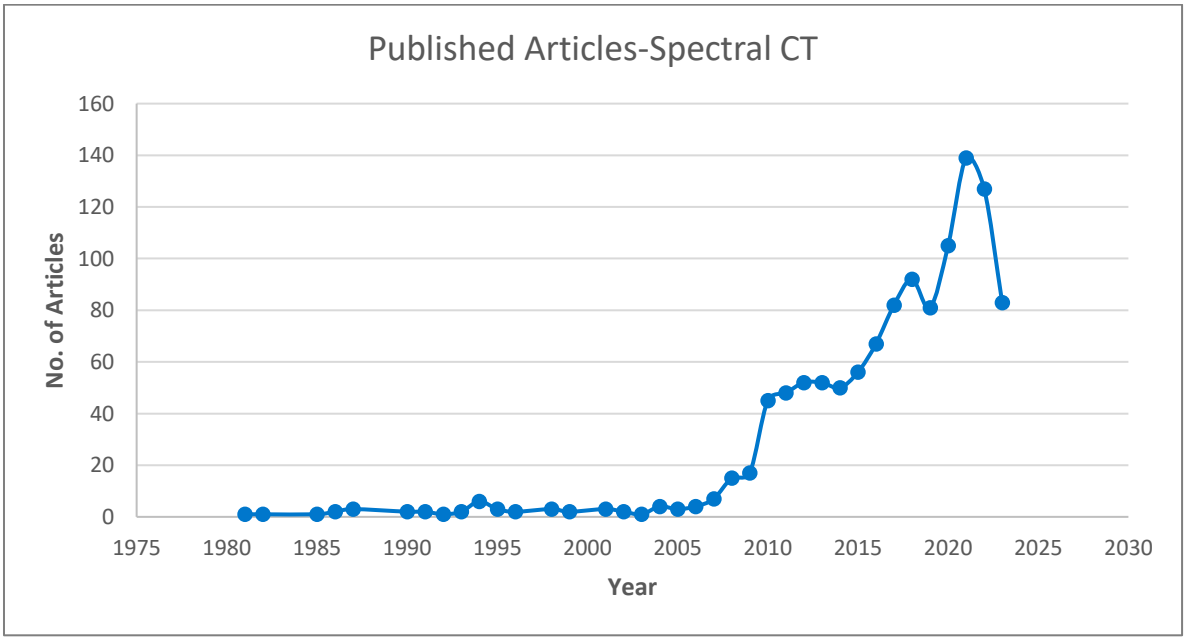

2.4 Heart

Table 4: Description of the method of research in the literature (Heart)

Item	
Date of Search	20-Sep-2023
Sources	PubMed, Cochrane
Search Items	(Spectral CT OR dual energy CT OR dual-energy CT OR dual-energy computed tomography OR dual-energy computed tomography OR DECT) and (Heart OR cardiac OR ventricles OR coronary)
Period	No restrictions
Inclusion Criteria	Articles published in English

Results:

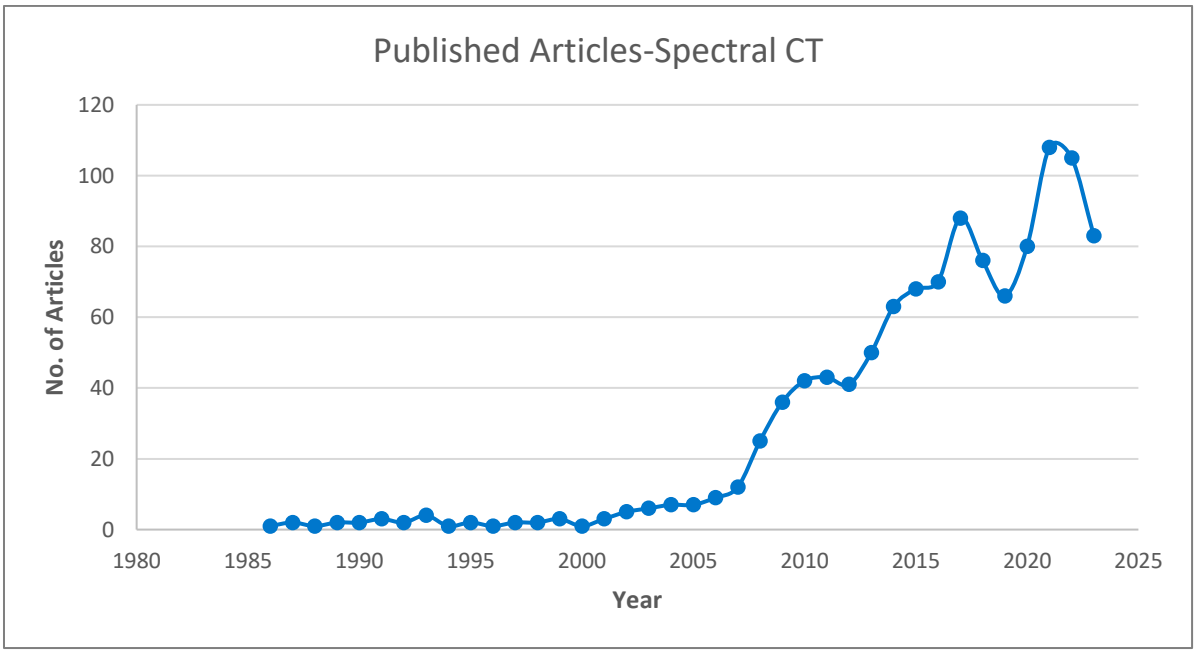

2.5 Neurology

Table 5: Description of the method of research in the literature (Neurology)

Item	
Date of Search	20-Sep-2023
Sources	PubMed, Cochrane
Search Items	(Spectral CT OR dual energy CT OR dual-energy CT OR dual-energy computed tomography OR dual-energy computed tomography OR DECT) and (neuro OR brain OR stroke OR brain infarction)
Period	No restrictions
Inclusion Criteria	Articles published in English

Results:

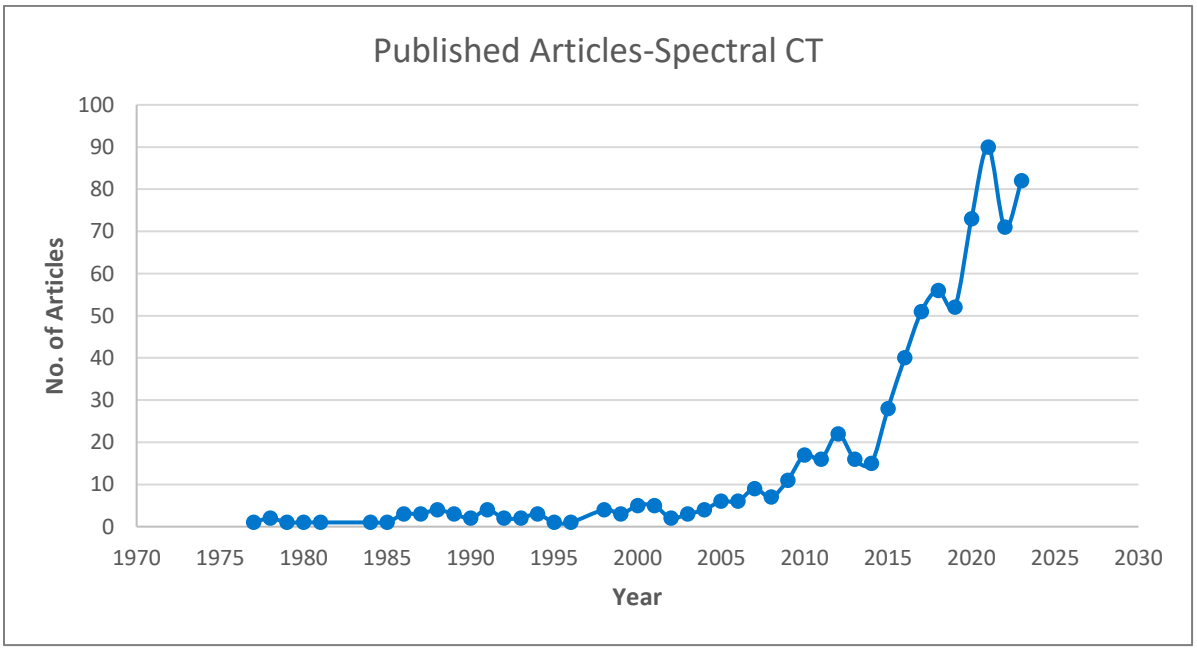

CHAPTER 3: Principles of Conventional Computed Tomography

3.1 Basic CT Components

The X-ray Tube

The X-ray tube handles generating the X-ray beam used in CT imaging, while the detector arrays detect and measure the transmitted X-rays. The X-ray tube typically consists of a rotating anode and a cathode that emits electrons, which are accelerated towards the anode. Detector arrays, made up of scintillation crystals or solid-state detectors, convert the X-rays into electrical signals for image reconstruction.

The Patient Table

The patient table is designed to move the patient smoothly through the CT gantry during image acquisition. It allows for precise positioning and controlled motion, enabling scanning of specific anatomical regions. The table is equipped with features such as motorized movement, indexing, and tilt, ensuring correct alignment and patient comfort.

The Gantry

The gantry is the circular structure through which the X-ray tube and detector arrays rotate around the patient. It supplies mechanical stability and houses various components of the CT system. The rotational movement allows for data acquisition from multiple angles, which is essential for producing cross-sectional images. Modern CT systems offer fast rotation times, enabling rapid image acquisition.

The Data Acquisition System

The data acquisition system consists of electronic components that receive and process signals from the detector arrays. It digitizes the analog signals, performs calibration and corrections, and transfers the data to the image reconstruction system. Advanced data acquisition systems can manage high-speed data transfer, enabling the acquisition of volumetric data in multi-slice and helical CT.

The Image Reconstruction System:

The image reconstruction system processes the acquired projection data and generates cross-sectional images of the patient's anatomy. It employs mathematical algorithms, such as filtered back projection (FBP) or iterative reconstruction techniques, to reconstruct the images. The reconstruction system accounts for factors like beam hardening, scatter, and detector response to produce accurate and high-quality images.

CT Image Acquisition

CT image acquisition involves obtaining a series of projection images by measuring the transmitted X-ray intensities from different angles around the patient. These projection images capture the attenuation characteristics of the tissues within the body.

Single-Slice vs. Multi-Slice CT

Single-slice CT systems acquire one slice of data per rotation, while multi-slice CT systems can simultaneously acquire multiple slices. Multi-slice CT has significantly improved imaging speed, allowing for faster scanning of larger volumes and enabling advanced imaging techniques such as cardiac CT and dynamic perfusion imaging.

Helical CT

Helical CT, also known as spiral CT, involves continuous rotation of the X-ray tube and simultaneous patient table movement. This technique allows for the acquisition of volumetric data and eases faster scanning. Helical CT is particularly useful for studies requiring three-dimensional reconstruction or dynamic imaging.

Cone-Beam CT

Cone-beam CT uses a cone-shaped X-ray beam and a two-dimensional detector array. It is commonly used in dental and maxillofacial imaging, providing high-resolution volumetric data with a single rotation. Cone-beam CT is helpful for imaging smaller regions of interest with reduced radiation dose.

These components and techniques collectively contribute to the image acquisition process in CT, enabling the generation of detailed cross-sectional images of the patient's anatomy.

3.2 Image Reconstruction in CT

Filtered Back Projection

Filtered back projection (FBP) is a widely used image reconstruction algorithm in CT. It involves back projecting the acquired projection data after applying a filtering process to compensate for the non-uniform distribution of X-ray attenuation. FBP is efficient but may result in image artifacts and reduced image quality, particularly in the presence of noise. A common formula of FBP can be expressed as follows:

$$g(x, y) = \int [0, \pi] P(s, \theta) * w(x, y, s, \theta) \, d\theta \quad \ldots\ldots\ldots\ldots (1)$$

where g(x, y) represents the reconstructed image, w(x, y, s, θ) is the weighting function that accounts for the geometry of the CT system, and the integral is taken over all projection angles from 0 to π.

Iterative Reconstruction Algorithms

Iterative reconstruction algorithms iteratively refine a first image estimate to improve image quality. These algorithms model the physics of X-ray interactions and incorporate statistical models to optimize image reconstruction. Iterative techniques have shown promising results in reducing noise, improving image quality, and allowing for dose reduction. However, they are computationally intensive and require longer processing times. A common formula of FBP can be expressed as follows:

$$x\_(k+1) = x\_k + A\text{^}T * (p - A * x\_k) \quad \ldots\ldots\ldots\ldots (2)$$

where x_k stands for the image estimate at iteration k, A is the system matrix that describes the imaging geometry and accounts for the physical properties of the CT system, p represents the measured projection data.

The IR algorithm iteratively updates the image estimate by incorporating the discrepancy between the measured projection data and the forward projection of the current image estimate. The process involves performing forward projection using the system matrix A to simulate the expected projection data, followed by a backprojection of the difference between the measured and estimated projection data.

Advanced Reconstruction Techniques

Advanced reconstruction techniques, such as model-based iterative reconstruction (MBIR) and deep learning-based algorithms, have gained attention in recent years. MBIR incorporates a prior model of the imaged object to iteratively refine the reconstruction, leading to improved image quality and reduced noise. Deep learning algorithms use neural networks trained on large datasets to directly reconstruct high-quality images from raw projection data, bypassing the need for explicit mathematical models. These techniques show potential for further enhancing image quality and reducing radiation dose. Following is an example of MBIR formula:

$$x\_(k+1) = x\_k + \gamma * D\hat{}T * (p - A * x\_k) + \lambda * R\hat{}T * R * (x\_k - s) \quad \ldots\ldots (3)$$

where x_k represents the image estimate at iteration k, γ is a regularization parameter that controls the trade-off between data fidelity and regularization, D is the data fidelity module, which represents the discrepancy between the measured projection data (p) and the forward projection of the current image estimate ($A * x\_k$), λ is a regularization parameter that controls the strength of regularization, R is the regularization module, which enforces certain constraints or penalties on the image estimate, and s represents the prior knowledge or initial guess for the image.

The MBIR framework incorporates both data fidelity and regularization components. The data fidelity module ensures that the estimated image matches the acquired projection data, while the regularization module imposes constraints on the image to promote desirable characteristics like smoothness or sparsity.

The specific implementation details of MBIR, including the design of the data fidelity and regularization modules, can vary among different CT systems and research approaches. Various mathematical techniques, such as total variation regularization, compressed sensing, or statistical models, can be utilized within the modules to achieve the desired image reconstruction quality and properties.

3.3 Image Quality and Optimization

Spatial Resolution

Spatial resolution in CT refers to the ability to distinguish small structures or details within an image. It is influenced by factors such as detector pixel size, focal spot size, and reconstruction algorithm. Higher spatial resolution enables better visualization of anatomical structures and improved diagnostic accuracy.

Spatial resolution is influenced by several key factors. These factors include the size of the X-ray focal spot, detector pixel size, geometric magnification, and patient motion. Each of these factors contributes to the overall spatial resolution of the CT system.

The X-ray focal spot size is a fundamental factor that affects spatial resolution. A smaller focal spot size leads to better spatial resolution as it produces a narrower X-ray beam and reduces blurring. The spatial resolution can be calculated using the formula:

$$\text{Spatial Resolution} = \frac{2(\text{FFS} * \text{DPS})}{\text{SID}} \ldots\ldots\ldots\ldots\ldots\ldots\ldots (4)$$

Where FFS is Focal Spot Size, DPS is the Detector Pixel Size, and SID is the Source-to-Image Distance.

Geometric magnification is another factor that affects spatial resolution. It refers to the increase in object size at the detector plane compared to its actual size due to the geometry of the imaging setup. The formula for calculating geometric magnification is:

$$\text{Geometric Magnification} = \frac{SOD}{\text{SID}} \ldots\ldots\ldots\ldots\ldots\ldots\ldots (5)$$

Where SOD is Source-to-Object Distance

A higher geometric magnification results in improved spatial resolution as it effectively magnifies the object, making smaller details more discernible. The detector pixel size also plays a significant role in spatial resolution. Smaller detector pixels can capture finer details, leading to better spatial resolution. The mathematical formula for calculating the detector spatial resolution is:

$$\text{Detector Spatial Resolution} = \frac{1}{2(DPS)} \ldots\ldots\ldots\ldots\ldots\ldots\ldots (6)$$

Where DPS is the Detector Pixel Size

This formula highlights the inverse relationship between detector pixel size and spatial resolution.

Minimizing patient motion is essential for keeping spatial resolution. Patient movement during image acquisition can introduce blurring and degrade the image

quality. Techniques such as breath-holding instructions or using fast scanning protocols can help mitigate motion artifacts and preserve spatial resolution.

In addition to these factors, other aspects like reconstruction algorithms, slice thickness, and image post-processing techniques can influence the final spatial resolution in CT. Advanced iterative reconstruction algorithms and high-resolution image reconstruction kernels can enhance spatial resolution by reducing image noise and optimizing image reconstruction processes.

Contrast Resolution

Contrast resolution refers to the ability of CT to distinguish between tissues with different X-ray attenuation properties. It depends on factors such as X-ray tube voltage, beam filtration, and image reconstruction algorithms. Enhancing contrast resolution enables better differentiation between tissues with similar attenuation coefficients, aiding in the detection of subtle pathologies.

Contrast resolution is influenced by several key factors, including X-ray tube voltage, image noise, patient size, and reconstruction algorithms. Each of these factors contributes to the overall contrast resolution of the CT system.

X-ray tube voltage is a significant factor affecting contrast resolution. The attenuation of X-rays by different tissues varies with tube voltage. Higher tube voltages result in greater penetration of X-rays, leading to reduced attenuation and decreased contrast resolution. The relationship between tube voltage (kVp), attenuation coefficient (μ), and contrast resolution (CR) can be expressed using the formula:

$$\mathrm{CR}\ \alpha \frac{kVp}{\mu} \ldots\ldots\ldots\ldots\ldots\ldots\ldots (6)$$

This formula illustrates that increasing the tube voltage enhances contrast resolution by increasing the attenuation differences between tissues.

Image noise has a direct impact on contrast resolution. Higher levels of noise can obscure subtle differences in tissue attenuation and degrade contrast resolution. The relationship between image noise (N), contrast resolution (CR), and pixel value standard deviation (σ) can be described by the formula:

$$\mathrm{CR}\ \alpha \frac{1}{(\mathrm{N} * \sigma)} \ldots\ldots\ldots\ldots\ldots\ldots\ldots (7)$$

Reducing image noise through techniques such as dose optimization, advanced noise reduction algorithms, and right image reconstruction parameters improves contrast resolution.

Patient size also affects contrast resolution. Larger patients tend to show increased X-ray attenuation, which can reduce the contrast differences between tissues. To account for this, it is common to adjust acquisition parameters such as tube current (mA) or tube voltage (kVp) based on patient size to optimize contrast resolution.

Reconstruction algorithms play a crucial role in optimizing contrast resolution. Advanced iterative reconstruction techniques and noise reduction algorithms can enhance contrast resolution by suppressing image noise while preserving image details. These algorithms use mathematical formulations and optimization algorithms to iteratively refine the reconstructed image.

It's important to note that contrast resolution can also be influenced by factors like image display settings, slice thickness, and post-processing techniques. Appropriate windowing, image enhancement, and advanced visualization tools can further enhance the perception of contrast differences in CT images.

In conclusion, contrast resolution is a fundamental parameter in CT imaging that enables differentiation between tissues with slight attenuation differences. It is influenced by factors such as X-ray tube voltage, image noise, patient size, and reconstruction algorithms. Mathematical formulas supply insights into the relationships between these factors and contrast resolution. Optimizing contrast resolution enhances the visualization of subtle tissue variations, aids in accurate diagnosis, and improves the overall clinical utility of computed tomography.

Noise

Noise in computed tomography (CT) images is an inherent and undesirable element that can affect image quality and diagnostic accuracy. It manifests as random fluctuations or variations in pixel values, obscuring minute details and reducing image clarity. In this essay, we will explore the concept of noise in CT images, its sources, characteristics, and mathematical formulas used to quantify and mitigate it.

Noise in CT images can arise from several sources, including X-ray photon statistics, electronic noise, patient motion, and system imperfections. These sources contribute to the overall noise characteristics in CT images.

The primary source of noise in CT images is the statistical nature of X-ray photon interactions. X-ray photons follow a Poisson distribution, resulting in inherent statistical variations in the number of detected photons. This statistical fluctuation translates into image noise. The relationship between the mean number of detected photons (N) and the standard deviation of image noise (σ) can be expressed by the square root relationship:

$$\sigma = \sqrt{N} \dots\dots\dots\dots\dots\dots\dots (8)$$

This formula indicates that the standard deviation of image noise increases with the square root of the mean number of detected photons. Hence, reducing image noise can be achieved by increasing the number of detected photons, either by optimizing acquisition parameters or by using advanced image reconstruction algorithms.

Electronic noise is another source of noise in CT images. It originates from electronic components within the CT system, such as the detectors and analog-to-digital converters. Electronic noise can introduce a baseline noise level that adds to the overall image noise. The standard deviation of electronic noise is represented by the parameter σe.

The total noise in a CT image is a combination of the statistical noise (σ) and the electronic noise (σe). The total noise (σtotal) can be calculated using the formula:

$$\sigma total = \sqrt{(\sigma^2 + \sigma e^2)} \dots\dots\dots\dots\dots\dots\dots (9)$$

System imperfections, such as detector artifacts, calibration errors, or electronic instabilities, can also contribute to image noise. These imperfections can introduce structured noise patterns or uneven noise distributions in CT images, which can be challenging to quantify using simple mathematical formulas. However, they can be mitigated through calibration procedures and advanced image processing techniques.

To mitigate noise and improve image quality, various techniques are employed in CT imaging. These include dose optimization, iterative reconstruction algorithms, and noise reduction filters. Iterative reconstruction algorithms use mathematical

optimization techniques to refine the image estimate iteratively, suppressing noise while preserving image details. Noise reduction filters, such as Gaussian filters or adaptive smoothing algorithms, selectively reduce noise while keeping edge sharpness.

In conclusion, noise is an inherent aspect of CT images arising from the statistical nature of X-ray photon interactions and various system-related factors. Mathematical formulas help quantify and analyze the characteristics of noise in CT images. Mitigating noise through optimization of acquisition parameters, advanced image reconstruction algorithms, and noise reduction filters contributes to improved image quality, enhanced diagnostic accuracy, and better patient care in computed tomography.

Artifacts

Image artifacts in computed tomography (CT) can significantly affect the quality and diagnostic accuracy of the images. There are several types of artifacts commonly met in CT scans. Motion artifacts occur due to patient movement during image acquisition, respiratory and cardiac motion, or equipment-related issues. These artifacts can lead to blurring, ghosting, and reduced image sharpness, resulting in decreased diagnostic confidence and potential misinterpretation of findings.

Another type of artifact is beam-hardening artifacts, which arise from variations in X-ray beam attenuation. These artifacts cause streaking and shading in the images, particularly in high-density structures. They can obscure anatomical structures, result in inaccurate Hounsfield unit measurements, and affect density calculations, leading to potential diagnostic inaccuracies. Beam Hardening Correction: Beam hardening artifacts can be mitigated using correction algorithms, such as the water correction algorithm. This algorithm is based on the Beer-Lambert law:

$$I(\mathrm{x}) = I_{\circ}(x) * e^{(-\mu(x)*t)} \dots\dots\dots\dots\dots\dots\dots (10)$$

where I(x) is the attenuated intensity at position x, I_0(x) is the incident intensity, μ(x) is the linear attenuation coefficient, and t is the thickness of the object being imaged.

Metal artifacts are another common issue in CT imaging, caused by metallic objects within the patient's body. These artifacts produce streaks, shadows, and signal dropout, often interfering with the visibility and alignment of structures. Implants, dental fillings, and surgical clips are common sources of metal artifacts. These

artifacts can alter the image appearance, obscure anatomy, and potentially lead to false-positive findings.

The partial volume effect is another type of artifact that occurs when a voxel holds multiple tissue types. It results in blurring and loss of minute details, particularly at boundaries between structures. The limited spatial resolution and voxel size contribute to this artifact, potentially leading to reduced image clarity and inaccurate tissue characterization.

To mitigate these artifacts, various strategies and technological advancements are employed in CT imaging. Motion artifacts can be addressed through patient education and cooperation, respiratory gating, cardiac synchronization techniques, and advanced motion correction algorithms. Beam hardening artifacts can be reduced by using spectral CT techniques to account for beam hardening effects, as well as employing metal artifact reduction algorithms and optimizing scan protocols and parameters.

Metal artifacts can be mitigated through advanced metal artifact reduction techniques, dual-energy CT imaging, and iterative reconstruction algorithms. Addressing the partial volume effect involves improving spatial resolution, employing smaller voxel sizes, utilizing advanced reconstruction algorithms, and implementing multi-slice CT and thin-section acquisitions.

In conclusion, image artifacts in computed tomography can have significant implications for image quality and diagnostic accuracy. Understanding the diverse types of artifacts, their causes, and effects is crucial for radiologists and technologists to make accurate interpretations. By employing mitigation strategies and using advancements in CT technology, healthcare professionals can minimize the impact of artifacts and enhance the diagnostic capabilities of CT imaging. Ongoing research and technological advancements continue to improve image quality, pushing the boundaries of CT as a valuable tool in medical imaging.

3.4 Radiation Dose Considerations

Dose Metrics and Measurement

Various dose metrics are used to quantify and assess radiation dose in CT. These include the CT dose index (CTDI), dose-length product (DLP), and size-specific

dose estimates (SSDE). CTDI is the dose profile along the central axis of the CT beam, while DLP accounts for the length of the scanned region. SSDE adjusts the dose estimate based on patient size to ease dose comparisons across different-sized patients. Accurate dose measurement and monitoring are crucial for optimizing radiation dose in CT.

Dose Modulation Techniques

(1) Automatic Tube Current Modulation (ATCM):

Automatic Tube Current Modulation adjusts the tube current during CT scanning based on the patient's anatomy and attenuation characteristics. It aims to reduce radiation dose in areas with lower attenuation, while keeping proper image quality in regions of higher attenuation. ATCM techniques include:

a- Localizer-Based Modulation: This technique uses pre-scan radiographs to assess patient attenuation and adjusts the tube current, accordingly, optimizing dose distribution.

b- z-Axis Modulation: z-Axis modulation modulates the tube current along the patient's longitudinal axis, adapting it to variations in patient size and anatomy. It ensures that the radiation dose is appropriately tailored to each section of the patient's body.

(2) Tube Voltage Modulation:

Tube voltage modulation, also known as automatic tube potential selection, varies the tube voltage based on patient size and desired image quality. Lower tube voltages reduce radiation dose while preserving image quality, particularly in patients with lower body mass or for specific imaging tasks. The relationship between radiation dose and tube voltage can be expressed by the equation:

$$\text{Dose } \alpha\ kVp^n \ldots\ldots\ldots\ldots\ldots\ldots\ldots (11)$$

where Dose stands for radiation dose, kVp is the tube voltage, and n is an exponent reflecting the relationship between tube voltage and dose reduction.

(3) Iterative Reconstruction:

Iterative reconstruction algorithms optimize image quality while reducing noise, enabling dose reduction without compromising diagnostic accuracy. These algorithms employ statistical models and iterative calculations to improve image

quality and reduce artifacts. The reconstruction process can be represented by the equation:

$$\text{Minimize } \|Ax - b\| + R(x) \dots\dots\dots\dots\dots\dots\dots (12)$$

where A represents the system matrix, x is the unknown image to be reconstructed, b is the measured projection data, and R(x) represents regularization terms that promote noise reduction.

Benefits of Dose Modulation Techniques

(1) Radiation Dose Reduction:

Dose modulation techniques minimize radiation exposure during CT scans. ATCM and tube voltage modulation adapt the radiation dose to the patient's specific anatomy and imaging requirements, reducing unnecessary exposure. Iterative reconstruction algorithms further contribute to dose reduction by improving image quality at lower radiation doses. The reduction in radiation dose can be quantified by comparing the dose-length product (DLP) values before and after implementing dose modulation techniques.

(2) Image Quality Enhancement:

Dose modulation techniques aim to support or improve image quality while reducing radiation dose. ATCM ensures consistent image quality across different anatomical regions, preventing overexposure in areas with higher attenuation and keeping adequate image quality in regions with lower attenuation. Tube voltage modulation optimizes the balance between image noise and contrast, improving image quality in specific patient populations. Iterative reconstruction algorithms enhance image quality by reducing noise and artifacts, compensating for the lower radiation dose.

Impact on Clinical Practice and Patient Care:

(1) Diagnostic Accuracy:

Dose modulation techniques preserve diagnostic accuracy in CT imaging. By optimizing the radiation dose according to patient-specific factors, these techniques ensure that relevant anatomical details are captured while minimizing potential artifacts and noise. This improves the accuracy of diagnostic interpretations and reduces the likelihood of false-positive or false-negative findings.

(2) Radiation Risks Reduction:

Dose modulation techniques mitigate the potential risks associated with radiation exposure, particularly in vulnerable patient populations such as children and pregnant women. By reducing unnecessary radiation dose, these techniques help minimize the long-term risks of radiation-induced malignancies. The effective radiation dose can be quantified using dose indices such as the Computed Tomography Dose Index (CTDI) and the Size-Specific Dose Estimate (SSDE).

(3) Workflow Efficiency:

Dose modulation techniques improve workflow efficiency in radiology departments. With optimized protocols and reduced radiation dose, patient throughput can be increased without compromising image quality or patient safety. This results in improved resource utilization and reduced waiting times for patients.

Pediatric CT Imaging

Pediatric computed tomography plays a vital role in diagnosing and managing various medical conditions in children. However, the increased radiosensitivity of pediatric patients raises concerns about radiation-induced risks. This essay discusses the unique challenges associated with pediatric CT imaging, the mathematical formulas used to estimate radiation dose, and strategies for optimizing dose while maintaining diagnostic image quality.

(1) Radiosensitivity and Radiation Dose Estimation:

Children are more radiosensitive than adults due to their rapidly dividing cells and longer life expectancy. Estimating the radiation dose received during a pediatric CT scan is crucial for risk assessment and dose optimization. The following mathematical formulas are commonly used in pediatric CT:

CTDI (Computed Tomography Dose Index) is a measure of the radiation dose delivered per unit scan length. It is calculated using the equation:

$$\mathrm{CTDI} = CTDI_{vol} * \mathrm{pitch} \quad \ldots\ldots\ldots\ldots\ldots\ldots\ldots (13)$$

where $CTDI_{vol}$ represents the volume weighted CTDI value, and pitch is the ratio of table feed per rotation to the beam collimation width.

SSDE (Size-Specific Dose Estimate) considers the child's size and provides a more accurate estimate of the effective radiation dose. It is calculated using the equation:

$$\text{SSDE} = \frac{CTDI_{vol} * \text{DLP}}{a * b * c} \ldots\ldots\ldots\ldots\ldots\ldots\ldots (14)$$

where DLP is the dose-length product, “a” is the scan length, “b” is an age correction factor, and “c” is a size correction factor adjust for pediatric patient characteristics.

(2) Strategies for Dose Optimization in Pediatric CT:

Tailoring CT protocols to the specific clinical indication and patient age is crucial for dose optimization. The choice of proper scan parameters, such as tube current, tube voltage, and slice thickness, can significantly influence the radiation dose.

AEC (Automatic Exposure Control) systems automatically adjust tube current based on patient size and attenuation. They help achieve consistent image quality while minimizing unnecessary radiation dose. AEC systems use mathematical algorithms to optimize tube current modulation.

Iterative reconstruction algorithms improve image quality and reduce noise, enabling dose reduction in pediatric CT. These algorithms use statistical models and iterative calculations to enhance image quality without compromising diagnostic accuracy.

(3) Pediatric Imaging Guidelines:

Professional societies and regulatory bodies provide guidelines specific to pediatric imaging. These guidelines emphasize the use of alternative imaging modalities when proper and the justification of CT scans in pediatric patients. They also encourage the adoption of dose reference levels and regular audit programs to ensure dose optimization.

(4) Balancing Image Quality and Radiation Dose:

Achieving a balance between image quality and radiation dose is essential in pediatric CT imaging. Dose reduction measures should not compromise diagnostic accuracy. Quality assurance programs, ongoing education, and collaboration between radiologists, technologists, and medical physicists are crucial for maintaining image quality while minimizing radiation dose.

Conclusion:

Pediatric CT imaging requires special consideration due to the increased radiosensitivity of children. Estimating radiation dose using mathematical formulas

like CTDI and SSDE provides valuable information for risk assessment. Implementing dose optimization strategies, such as protocol optimization, AEC, iterative reconstruction, and adherence to pediatric imaging guidelines, helps reduce radiation exposure while preserving diagnostic image quality. Continuous advancements in technology, further research, and adherence to radiation safety principles are vital in ensuring the safe and effective use of CT imaging in pediatric patients.

Emerging Trends and Future Directions

(1) Dual-Energy CT:

Dual-energy CT utilizes two different X-ray energy spectra to provide more information about tissue composition and material identification. It enables improved tissue characterization, virtual non-contrast imaging, and enhanced visualization of contrast agents.

(2) Photon-Counting CT:

Photon-counting CT detectors have the potential to revolutionize CT imaging by providing higher spatial resolution, improved contrast resolution, and energy discrimination capabilities. These detectors can enhance image quality while potentially reducing radiation dose.

(3) Artificial Intelligence and Machine Learning in CT:

Artificial intelligence (AI) and machine learning techniques are being increasingly applied to CT imaging for image reconstruction, noise reduction, artifact correction, and automated image analysis. AI algorithms can aid in improving image quality, optimizing protocols, and aiding in the detection and diagnosis of pathologies.

(4) Functional CT Imaging:

Functional CT techniques, such as perfusion imaging and CT angiography, provide information about blood flow, tissue perfusion, and vascular dynamics. These techniques enable the assessment of organ function and the characterization of tumors and ischemic diseases.

(5) Ultra-High-Resolution CT

Advancements in detector technology and image reconstruction algorithms are driving the development of ultra-high-resolution CT, which offers superior spatial resolution for detailed visualization of small structures and early detection of abnormalities.

These emerging trends and future directions in CT technology hold significant promise for further improving image quality, diagnostic accuracy, and patient care in the field of medical imaging. Continued research and technological advancements will shape the future of CT imaging.

.

CHAPTER 4: Principles of Spectral Dual Energy CT

4.1 Rationale

CT uses a polychromatic X-ray tube with peak energy (kVp), kVp being the kilovoltage applied between the cathode and anode of the X-ray tube. In 120 kVp setting for example, the propagating electrons towards anode acquire a maximum kinetic energy of 120 keV at this tube setting, before interacting with atomic electrons in the anode. The interaction results in deceleration of electrons emitting polychromatic X-ray spectrum, with a maximum X-ray energy equal to the voltage difference between the cathode and the anode, superimposed by a broad distribution of X-ray energy distribution below the maximum of 120 keV. Conventional CT determines tissue attenuation that is measured in Hounsfield units (HU) or CT numbers, the values obtained from a linear transformation of the attenuation coefficient of the material in each voxel. It is difficult to differentiate between different tissue types, as linear attenuation coefficient is not unique to any given material, but depends on material composition, the interacting photon energies, and the mass density of the material. Hence, materials with different elemental composition can have identical CT numbers. However, dual energy CT acquires data at 2 different energy spectra, to perform tissue characterization by utilizing the differences in their attenuations at different energies. To achieve this goal, the systems should use different spectral sources or a method of discriminating the received spectra and record the data separately and this is achieved in different ways by different vendors.

4.2 Vendor Offerings

Several leading medical imaging vendors have developed spectral DECT systems, each with its unique features and capabilities. Following are the main 3 approaches:

(1) Systems that utilize two distinct X-ray sources with different energy spectra, allowing for simultaneous acquisition of dual-energy data.

(2) Systems wilt detector technology that allows for the energy-sensitive separation of the X-ray photons, providing material decomposition capabilities.

(3) Systems that integrate a fast-switching X-ray tube, enabling rapid alternation between high and low energy acquisitions. These vendor offerings highlight the diversity and innovation within the spectral DECT field.

4.3 Spectral Image Generation

Spectral images are synthesized usually through material decomposition and material separation using basis images or raw data.

4.3.1 Material Decomposition

Separation of two varied materials is not always possible with conventional CT imaging. Specific concentrations of iodine and calcium for example will have same HU values making them indistinguishable. However, differentiation of the materials having different atomic numbers that look similar on conventional CT image can be achieved by examining with two different energies. The fact that the X-ray attenuation of any material is a linear combination of Compton scatter attenuation and photoelectric attenuation helps Dual Energy (DE) CT in basis material decomposition (BMD). It can be assumed that the energy dependence of these 2 effects is fixed across all materials, but their relative contribution to the overall attenuation changes for different materials. Photoelectric attenuation has a strong dependence on energy when compared to Compton scatter that has a weak dependence. In materials with higher atomic number, where photoelectric effect is the predominant factor, the attenuation of the X-ray photons is larger. DE CT uses the variability of the K-edge of varied materials and therefore the difference in attenuation of the X-ray photons.15 The most utilized high atomic number materials for decomposition are iodine and calcium with their K-edge values of 33 keV and 4 keV respectively. These high atomic number materials can be discriminated from soft tissue that has a sufficiently different and lower K-edge of 0.01-0.53 keV due to their lower atomic numbers. Brain parenchyma, brain hemorrhage, and CSF that constitutes the soft tissues in neuroimaging, all have low atomic numbers.DE CT scanners express different materials as basis pair. The most common basis pairs utilized is a combination of iodine and water. Compton scatter dominates in the attenuation of water with some contribution from photoelectric effect. In contrast, photoelectric effect dominates in the attenuation of iodine and hence strongly depends on X-ray photon energy. Using this base pair, every material in the body is

represented as a linear combination of water and iodine. Even though the human body does not physically consist entirely of water and iodine, the algorithm presumes that each material specific X-ray attenuation as a combination of X-ray attenuation of water and iodine. The image maps created based on base pairs are useful for material decomposition. The concept can be shown by the coordinate system with the CT numbers measured from two different energy spectra as the x- and y-axis, with specific material plotted in a two-dimensional space. Following is diagram (Fig1) illustrating the methos of material decomposition:

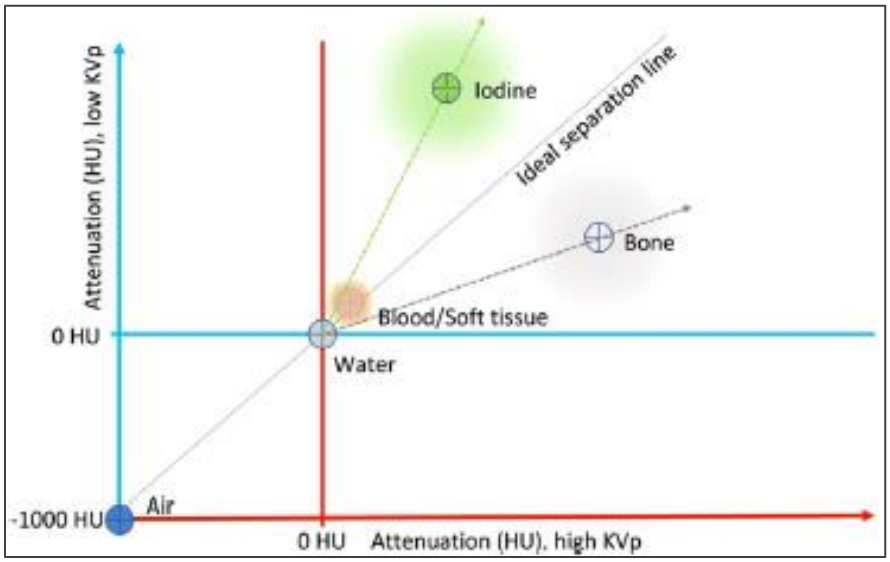

Figure 1: Diagram of basis material decomposition (BMD) postprocessing algorithm. Computed tomography number measurements of different concentrations of iodine and calcium. Dual-energy space with low kV data on the y-axis and the high-kV data on the x-axis. Slope defines separation based on difference in densities of two materials in Hounsfield units. [72].

4.3.2 Material Separation

Material separation algorithms define a slope between the density values at both acquired spectra and differentiate materials based on the photoelectric effect within a certain density range—that is, colors are assigned on both sides of the slope (Fig. 2). Examples for these algorithms include kidney stone differentiation (i.e., differentiation of uric acid from magnesium or calcium or the differentiation of iodine and calcium. Another possibility is to drop certain substances from a dataset by identifying the substance and then filling in, for example, air density for the corresponding voxels (e.g., eliminate calcium for bone removal from angiographic datasets.

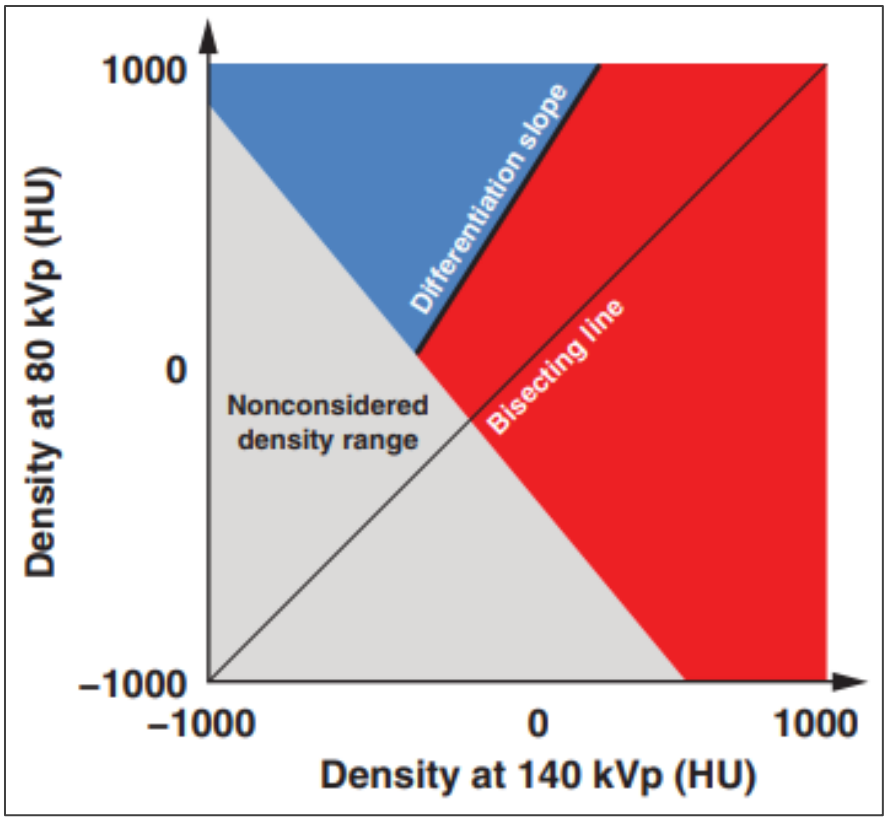

Figure 2: Diagrams of postprocessing algorithms. Algorithm is used to differentiate two materials from one another. Slope defines separation based on difference in densities of two materials in Hounsfield units. Two materials are color-coded in red or blue. [73]

4.3.3 Spectral CT Image Examples

On the following page, clinical examples are included to illustrate the methods of image generation:

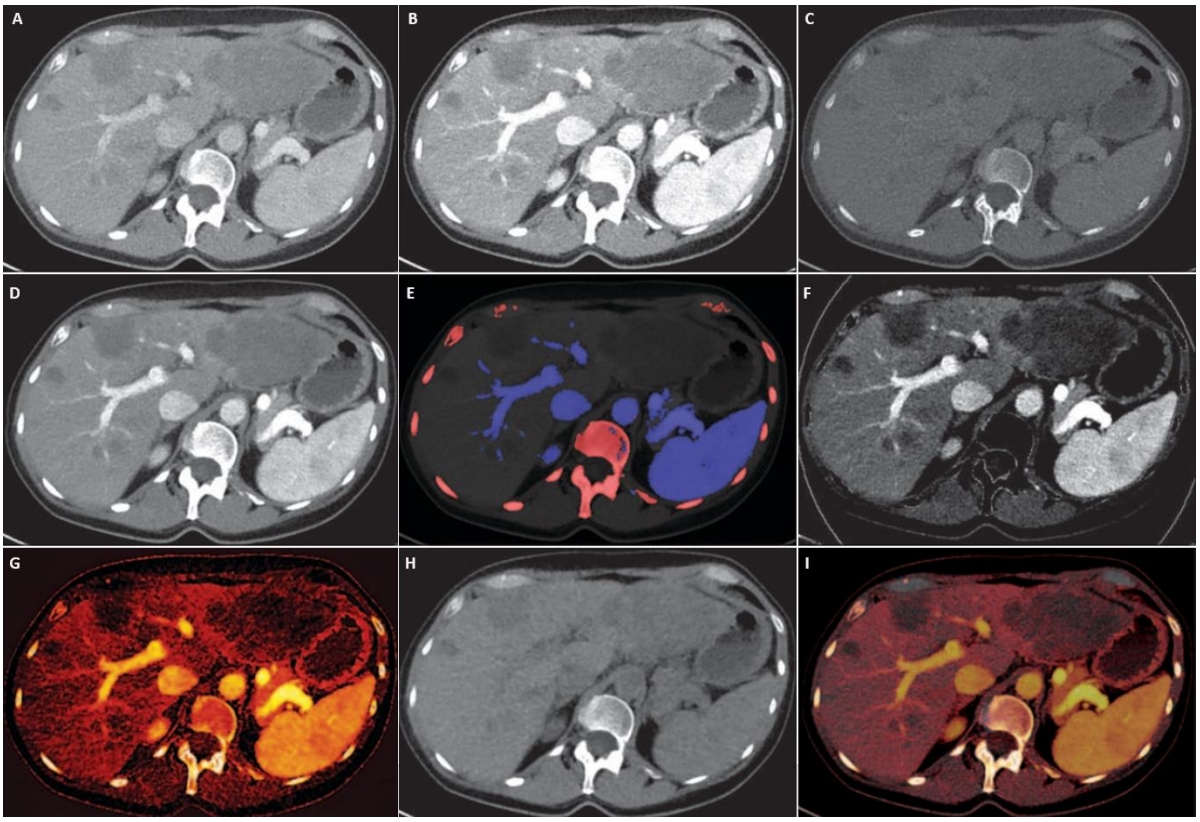

Figure 3: Clinical example dataset obtained on dual-source CT scanner using 0.4-mm stannum filter at 140 kVp and 71 mAs and 100 kVp and 69 mAs with overall CT dose index of 5.7 mGy. Images were generated with Syngo dual-energy software (version VE32B, Siemens Healthcare) of 72-year-old woman with liver metastasis from colorectal cancer. [73]

A: High energy base image
B: Low energy base image
C: 140 keV monoenergetic image
D: Optimum energy monoenergetic image
E: Algorithm differentiates iodine (blue) from calcium (red)
F: Angiographic image after bone removal
G: Algorithm quantifies iodine by color-coding iodine in orange
H: Virtual unenhanced image after iodine subtraction
I: Fusion of color-coded iodine image and unenhanced image

4.4 Technology Challenges

Spectral DECT faces various technological challenges that affect its widespread implementation. One such challenge is the exact calibration of energy spectra to ensure reliable material decomposition. Efficient data acquisition and processing are crucial for achieving robust and artifact-free spectral images. Managing the increased radiation dose associated with acquiring multiple energy scans is another technical consideration. Overcoming these challenges requires advancements in hardware design, image reconstruction algorithms, and dose optimization techniques.

4.5 Adoption Challenges

The widespread adoption of spectral DECT faces several challenges that need to be addressed. One significant challenge is the first cost of acquiring spectral DECT systems. These systems are typically more expensive than conventional CT scanners, making them less accessible to smaller healthcare facilities and clinics. Efforts to reduce costs and make spectral DECT more economically practical will be crucial for its broader adoption.

In addition to cost, the integration of spectral DECT into existing clinical workflows presents logistical challenges. Radiologists and technologists need to be trained in the acquisition, interpretation, and analysis of spectral DECT images. Standardized protocols and reporting guidelines should be set up to ensure consistency and facilitate data exchange between institutions.

Furthermore, collaboration between radiologists, physicists, and other healthcare professionals is necessary to optimize imaging protocols, address quality control issues, and establish clinical guidelines for the proper utilization of spectral DECT. These efforts will ensure that spectral DECT is used effectively and safely in clinical practice.

4.6 Clinical Value

Spectral DECT holds significant promise in various clinical domains. Its ability to differentiate and quantify materials can aid in the characterization and classification of pathological tissues, improving diagnostic accuracy. Applications include oncology, cardiovascular imaging, musculoskeletal imaging, and renal imaging,

among others. Spectral DECT may enhance the detection of subtle lesions, enable more accurate tissue characterization, and provide valuable functional information, potentially influencing treatment decisions and patient outcomes.

4.7 Image Quality Limitations

Despite its numerous advantages, spectral DECT has some image quality limitations. Beam hardening artifacts can arise due to the different energy spectra used, leading to streaks and inaccuracies in the reconstructed images. Noise amplification is another challenge, especially in low-dose protocols. These limitations can affect the reliability and interpretability of spectral DECT images and require ongoing research and development efforts to mitigate their impact.

4.8 Future Directions and Research Opportunities

The field of spectral DECT continues to evolve, offering exciting avenues for future research and development. Improving hardware designs, such as developing more efficient X-ray sources and advanced detectors, can enhance image quality and reduce radiation dose. Advancements in reconstruction algorithms and image processing techniques can help address artifacts and noise amplification, improving the accuracy and interpretability of spectral DECT images.

Research efforts can focus on expanding the clinical applications of spectral DECT. Exploring its potential in areas such as neuroimaging, pulmonary imaging, and interventional radiology can uncover new insights and further establish its clinical value. Investigating the integration of spectral DECT with other imaging modalities, such as magnetic resonance imaging (MRI) or positron emission tomography (PET), may enable multimodal imaging approaches and comprehensive patient assessments.

Additionally, conducting rigorous clinical trials and outcome studies can provide evidence of the clinical benefits and cost-effectiveness of spectral DECT. Collaborations between academic institutions, industry partners, and regulatory bodies can facilitate the validation and standardization of spectral DECT protocols, leading to wider adoption and utilization in routine clinical practice.

4.9 Regulatory and Safety Considerations

As with any advanced imaging technology, regulatory and safety considerations are paramount. Regulatory bodies need to set up guidelines and standards for spectral DECT systems, ensuring their safety and efficacy. Dose optimization strategies and radiation protection protocols should be developed to minimize patient exposure and keep the ALARA (As Low as Reasonably Achievable) principle.

Clinicians and radiologists should be aware of the potential risks and benefits associated with spectral DECT. Understanding the proper clinical indications and the limitation of the technology is crucial for its responsible and effective use. Collaboration between radiology departments, medical physicists, and radiation safety officers is essential to implement comprehensive quality assurance programs and ensure adherence to best practices.

4.10 Economic and Workflow Considerations

The economic viability and integration of spectral DECT into clinical workflows are important considerations for its successful adoption. Cost-effectiveness studies can assess the impact of spectral DECT on patient outcomes, healthcare resource use, and overall healthcare costs. Demonstrating its clinical value and potential cost savings may facilitate reimbursement and increase accessibility for patients.

Integrating spectral DECT into existing clinical workflows requires careful planning and optimization. Radiology departments need to streamline protocols, establish dedicated reading and interpretation workflows, and provide adequate training to radiologists and technologists. Collaboration with information technology specialists can help in the seamless integration of spectral DECT data into picture archiving and communication systems (PACS) and Electronic Medical Records (EMR).

4.11 Limitations and Considerations in Clinical Implementation

While spectral DECT holds immense promise, there are several considerations and limitations that need to be acknowledged for its successful clinical implementation. One such consideration is the increased complexity of image interpretation. Radiologists and clinicians must undergo training to effectively analyze and interpret spectral DECT images, as the material-specific information requires a nuanced understanding of tissue characteristics and pathologies.

Another limitation is the potential for increased radiation dose associated with spectral DECT acquisitions. The use of multiple energy levels and more scans can result in a higher cumulative radiation exposure for patients. Therefore, careful optimization of protocols and dose reduction strategies, such as iterative reconstruction algorithms and tailored acquisition techniques, are crucial to minimize radiation dose while supporting diagnostic image quality.

Furthermore, the integration of spectral DECT into clinical practice causes the establishment of standardized protocols and reference ranges for material-specific measurements. Consistency in acquisition techniques, calibration, and data analysis across different institutions and vendors is crucial for accurate and reliable comparisons of spectral DECT findings and for enabling multicenter studies and research collaborations.

4.12 Clinical Applications and Benefits

Spectral DECT has shown significant potential in various clinical applications. In oncology, it offers improved tissue characterization, enabling the differentiation of benign and malignant lesions, the assessment of tumor vascularity, and the detection of small metastatic lesions. Spectral DECT can aid in the evaluation of cardiovascular disease by providing accurate quantification of calcifications, plaque composition, and myocardial perfusion.

Musculoskeletal imaging benefits from the ability to differentiate between diverse types of tissue, such as bone, cartilage, and soft tissue, facilitating the detection of fractures, osteoarthritis, and other musculoskeletal pathologies. In renal imaging, spectral DECT can enhance the characterization of renal stones, enabling accurate stone composition analysis and tailored treatment planning.

Moreover, spectral DECT has the potential to improve image-guided interventions, such as guiding needle placements, evaluating tissue perfusion, and assessing treatment response. By providing functional and metabolic information, spectral DECT may aid in treatment planning and monitoring, leading to more personalized and targeted therapies.

4.13 Image Quality and Artifact Considerations

Beam hardening artifacts can occur due to differences in X-ray attenuation between high and low energy acquisitions, leading to streaks and inaccuracies in the reconstructed images. Advanced correction algorithms and hardware improvements can mitigate these artifacts and enhance image quality.

Noise amplification is another challenge, particularly in low-dose protocols, as the material decomposition algorithms may amplify the noise inherent in the data. Advanced denoising techniques and iterative reconstruction algorithms can help mitigate noise and improve image quality without compromising spatial resolution or diagnostic accuracy.

Additionally, patient-specific factors, such as body habitus and metal implants, can introduce image artifacts and affect the accuracy of material decomposition. Careful patient positioning, tailored acquisition techniques, and artifact reduction algorithms can minimize these effects and improve the reliability of spectral DECT images.

4.14 Future Directions and Emerging Technologies

The field of spectral DECT continues to evolve rapidly, with ongoing research and development efforts aimed at overcoming existing challenges and expanding its clinical applications. Emerging technologies, such as photon-counting detectors, hold the potential to further enhance spectral DECT capabilities by providing increased energy resolution and improved material decomposition accuracy.

Further advancements in artificial intelligence and machine learning algorithms can aid in automated image analysis, quantification, and tissue classification, thereby streamlining the interpretation workflow and reducing inter-observer variability. Integration with other imaging modalities, such as PET or MRI, can enable complementary information fusion and ease comprehensive imaging assessments.

Moreover, advancements in dose optimization techniques, such as model-based iterative reconstruction and adaptive dose modulation, can help minimize radiation dose while supporting diagnostic image quality. Continued research into optimizing dose management and developing robust quality assurance programs will contribute to the safe and effective implementation of spectral DECT in clinical practice.

4.15 Conclusion

Spectral Dual-Energy Computed Tomography (DECT) is a significant advancement in CT imaging, providing material-specific information and expanding the diagnostic capabilities of conventional CT. This introduction has discussed the vendor offerings, technology challenges, adoption challenges, clinical value, and image quality limitations associated with spectral DECT.

While challenges such as image interpretation complexity, radiation dose management, and standardization need to be addressed, spectral DECT holds great promise in various clinical applications. Its ability to differentiate tissues, characterize lesions, and provide functional information has the potential to improve diagnostic accuracy, guide treatment decisions, and enhance patient outcomes.

Future research should focus on overcoming existing limitations through advancements in hardware design, reconstruction algorithms, and dose optimization strategies. Collaboration between academia, industry, and regulatory bodies is crucial for standardization, validation, and widespread adoption of spectral DECT. With continued innovation and clinical validation, spectral DECT is poised to revolutionize diagnostic imaging and contribute to advancements in healthcare.

CHAPTER 5: Clinical Applications of Spectral CT

5.1 Clinical value in Oncology

Oncology, the branch of medicine dedicated to the study and treatment of cancer, has seen transformative advancements in diagnostic imaging with the introduction of Spectral Computed Tomography. This revolutionary imaging technique has redefined the way oncologists diagnose and treat various forms of cancer, enhancing both precision and patient outcomes.

One of the most significant applications of Spectral CT in oncology is its ability to differentiate between different tumor types with remarkable accuracy. Traditional CT scans often struggle to distinguish between tumors of similar densities. However, Spectral CT's dual-energy or multi-energy capabilities enable the quantification of tissue composition, making it possible to discriminate between tumor types based on their elemental composition. This capability aids oncologists in tailoring treatment plans specific to the cancer type, which can have a profound impact on patient outcomes.

Another vital aspect of Spectral CT in oncology is its role in assessing tumor perfusion. Accurate assessment of blood flow within tumors is crucial for understanding their aggressiveness and response to treatment. Spectral CT can provide dynamic contrast-enhanced images that reveal the perfusion characteristics of tumors in real-time. This information aids oncologists in making informed decisions about the choice and efficacy of therapies, such as targeted chemotherapy or radiation therapy.

Furthermore, Spectral CT plays a pivotal role in monitoring a patient's response to cancer therapy. Oncologists can use it to assess changes in tumor size, density, and perfusion over time. This capability is particularly valuable when evaluating the effectiveness of treatments, helping to find early signs of response or resistance. Real-time monitoring of treatment response allows for prompt adjustments in therapeutic regimens, optimizing patient care.

In addition to tumor characterization and treatment monitoring, Spectral CT aids in precise localization for radiation therapy planning. By differentiating between tumor and healthy tissues with greater accuracy, Spectral CT helps radiation oncologists

design treatment plans that maximize tumor irradiation while sparing adjacent healthy tissues. This results in more targeted and effective radiation therapy, reducing side effects and improving the patient's quality of life.

In conclusion, Spectral CT has appeared as a notable change in the field of oncology. Its ability to differentiate between tumor types, assess tumor perfusion, monitor treatment response, and aid in radiation therapy planning has significantly improved the diagnosis and treatment of cancer. As this technology continues to evolve, its impact on oncology is expected to grow, ultimately leading to more personalized and effective cancer care. With Spectral CT, oncologists have a powerful tool at their disposal, offering new hope and improved outcomes to cancer patients worldwide.

On the following page, clinical examples are included to illustrate the value of the spectral CT:

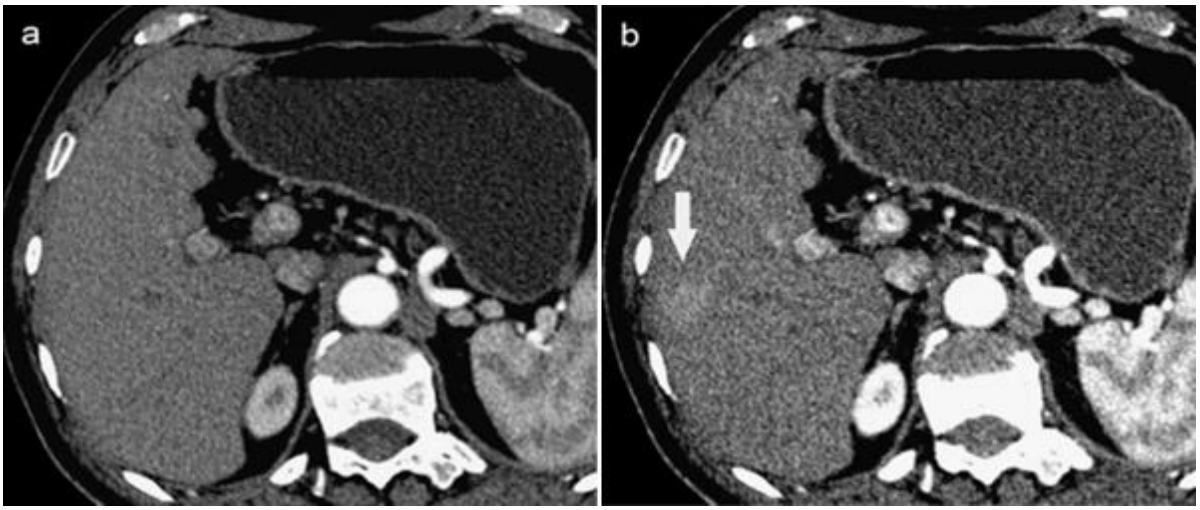

Figure 4: a Conventional CT image, b monochromatic image at 40 keV of a 73-year-old man (slice thickness 1.25 mm). a on the axial contrast-enhanced conventional CT image, no lesion is visible. b Axial contrast-enhanced monochromatic image at 40 keV shows a hepatic lesion (arrow), which is more conspicuous. [53]

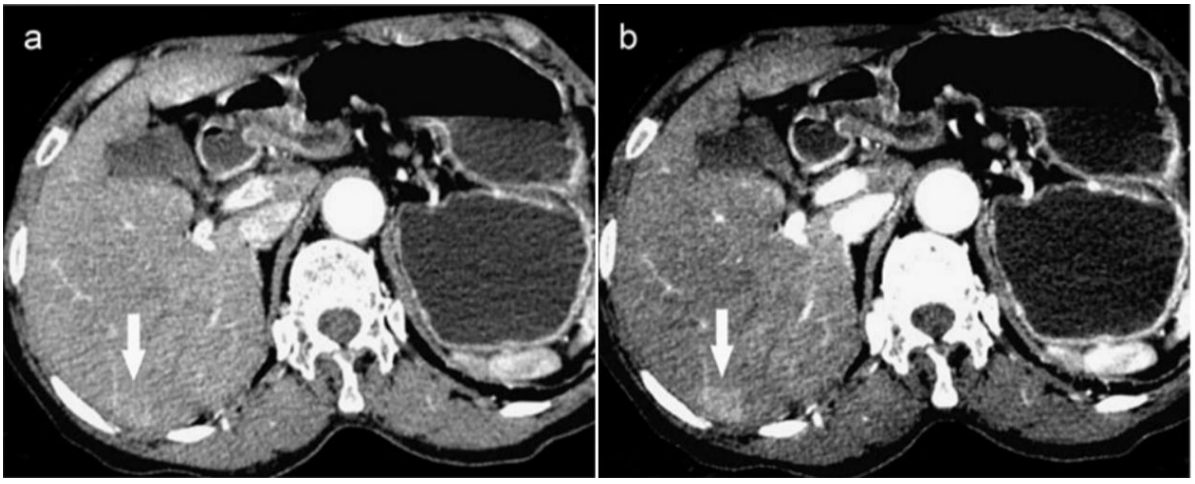

Figure 5: a Conventional CT image, b monochromatic image at 40 keV of a 66-year-old woman (slice thickness 1.25 mm). a On the axial contrast-enhanced conventional CT image, the lesion is less visible than that on the contrast-enhanced monochromatic image at 40 keV (arrow) (b). [53]

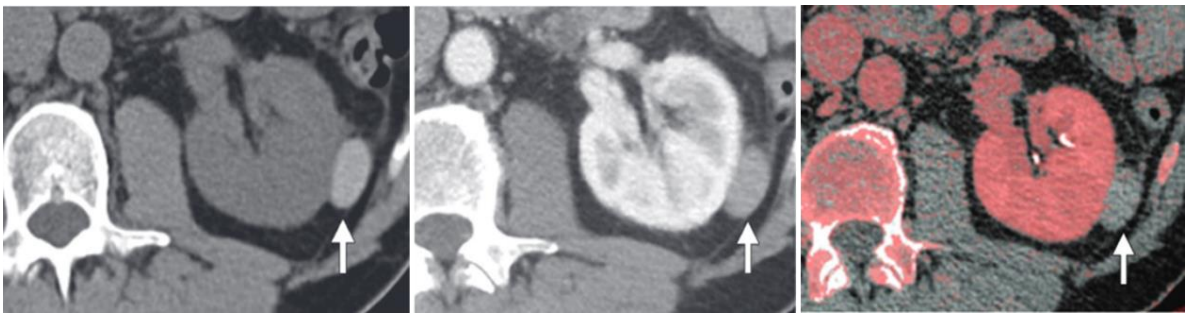

Figure 6: Hyper-attenuating cyst. (left) TUE CT image shows a hyperattenuating exophytic lesion in the left kidney (arrow). (middle) At contrast-enhanced CT, the lesion (arrow) demonstrates questionable enhancement (attenuation difference of 14 HU). (right) Corresponding iodine CT image with a color overlay shows no appreciable iodine within the lesion, a finding indicative of a hyperattenuating cyst. The lesion remained unchanged 6 months later. [54]

5.2 Clinical value in Cardiology

Cardiovascular diseases are still a leading cause of mortality worldwide, emphasizing the critical need for accurate and advanced imaging techniques. Spectral Computed Tomography has appeared as a powerful tool in the field of cardiology, offering a range of applications that have revolutionized cardiovascular imaging and patient care.

One of the primary applications of Spectral CT in cardiology is coronary artery imaging. Coronary artery disease (CAD) is a prevalent cardiovascular condition, and the ability to visualize coronary arteries with precision is vital for diagnosis and treatment planning. Spectral CT's multi-energy capabilities provide enhanced contrast and spatial resolution, enabling cardiologists to assess coronary artery stenosis and plaque composition more accurately. This has led to improved diagnostic accuracy and the ability to identify patients who may benefit from interventions like percutaneous coronary intervention (PCI) or coronary artery bypass grafting (CABG).

Myocardial perfusion imaging is another critical aspect of cardiology where Spectral CT shines. By tracking the passage of contrast agents through the myocardium, Spectral CT allows cardiologists to assess myocardial blood flow and detect regions of ischemia or infarction. This information is invaluable for diagnosing conditions like myocardial infarction and evaluating the extent of coronary artery disease. It guides treatment decisions and helps predict patient outcomes.

Pulmonary embolism (PE) detection is yet another significant application of Spectral CT in cardiology. PE is a life-threatening condition, and prompt and accurate diagnosis is crucial. Spectral CT's ability to differentiate between clot material and surrounding tissue aids in finding and characterizing pulmonary emboli. It provides cardiologists with the information needed to assess the severity of PE and figure out proper treatment strategies, such as anticoagulation therapy or catheter-directed thrombolysis.

Furthermore, Spectral CT can contribute to cardiac risk assessment by quantifying coronary artery calcium (CAC) scores. CAC scores are valuable predictors of cardiovascular events. Spectral CT can accurately assess and quantify coronary artery calcium deposits, allowing cardiologists to find patients at higher risk of future

cardiac events. This information can guide preventive measures, such as lifestyle modifications and statin therapy, to reduce the risk of heart disease.

In conclusion, Spectral CT has ushered in a new era in cardiology by providing advanced imaging capabilities that significantly enhance cardiovascular diagnosis and treatment. From precise coronary artery imaging and myocardial perfusion assessment to pulmonary embolism detection and risk stratification through CAC scoring, Spectral CT empowers cardiologists with the tools they need to make informed decisions and improve patient outcomes. As this technology continues to evolve, it holds promise for even further advancements in the field of cardiology, offering hope for millions of individuals affected by cardiovascular diseases.

On the following page, clinical examples are included to illustrate the value of the spectral CT:

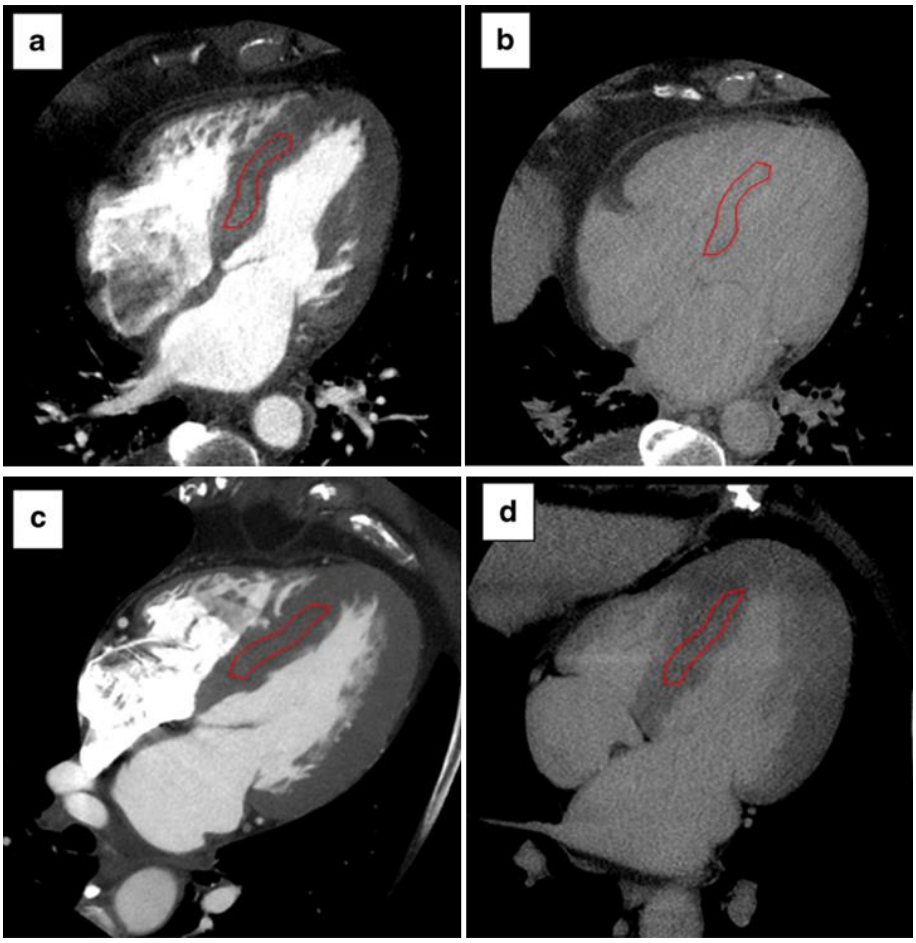

Figure 7: Examples of arterial (a, c) and 5-minute (b, d) DECT images obtained in one patient with CA (top row) and one patient with CH (bottom row). Myocardium iodine concentration (MIC) measured on arterial acquisition within the inter-ventricular septum (red line) was in the same range in the CA (2.76 mg/mL) and CH (3.28 mg/mL) patient. The CA patient showed a much higher MIC on delayed acquisition (3.44 mg/mL) than the CH patient (1.86 mg/mL). [55]

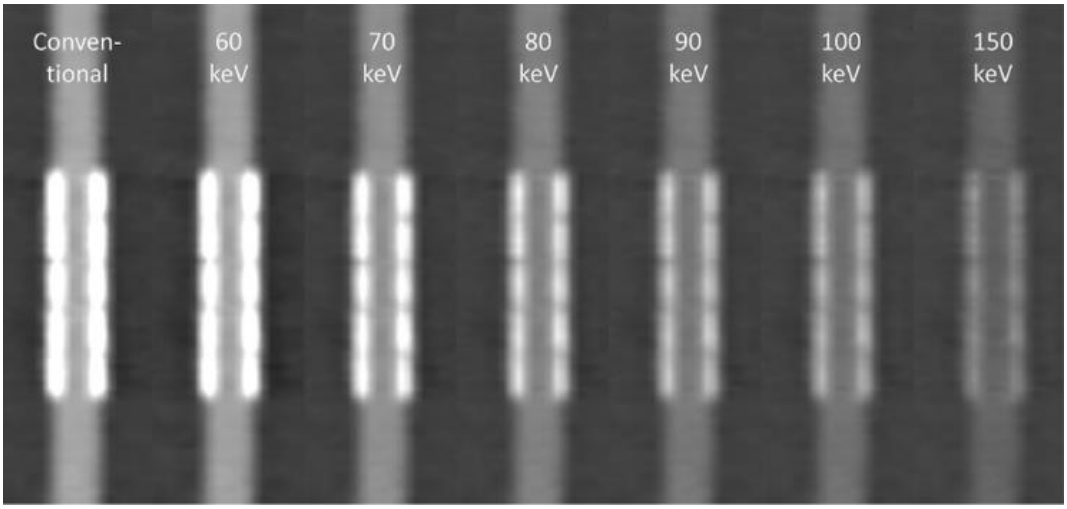

Figure 8: Identical raw data of a Nitinol stent ("Radius"; diameter 3.0 mm, length 20 mm, strut thickness 0.09 mm) reconstructed with different algorithms (CD images and monoenergetic reconstructions at different keV-levels) showing reduced image noise in lower keV monoenergetic reconstructions and reduced attenuation differences as well as increased visible lumen diameter in higher keV monoenergetic reconstructions compared to the conventional reconstruction method.[56]

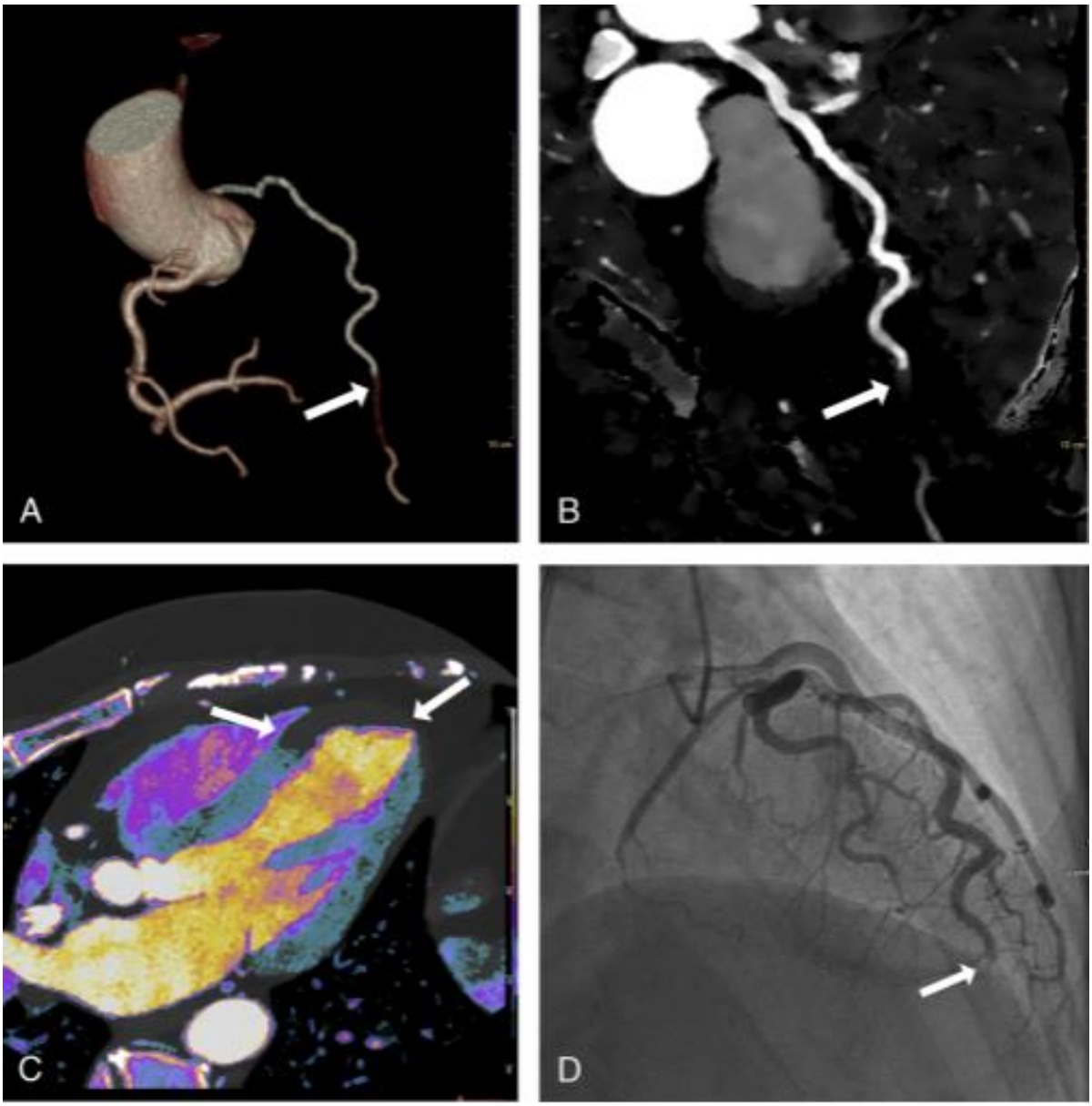

Figure 9: A, Volumetric 3D shaded surface display shows lack of opacification of the distal LAD. B, Iodine Density image shows lack of intraluminal contrast in the distal LAD segment from occlusion. There is a downstream lower iodine density contrast from retrograde flow via collaterals. C, Iodine Density color image fused on virtual non-contrast image show lack of iodine in the distal antero-septal segment of myocardium corresponding to distal LAD territory. D, Conventional coronary angiogram showing occlusion of the distal LAD confirming culprit lesion. [61]

5.3 Clinical value in Neurology

Neurology, the medical specialty dedicated to the study and treatment of neurological disorders, has experienced remarkable progress with the introduction of Spectral Computed Tomography. This innovative imaging technology is playing a pivotal role in the diagnosis and treatment of various neurological conditions, offering advantages that were previously unattainable.

One of the most notable applications of Spectral CT in neurology is its ability to aid in stroke imaging. Stroke is a medical emergency, and prompt diagnosis is crucial for effective treatment. Spectral CT's multi-energy capabilities enable the rapid identification of ischemic regions within the brain. By differentiating between normal and ischemic tissues, it helps neurologists figure out the extent of brain damage and decide on the most proper therapeutic interventions, such as thrombolysis or mechanical thrombectomy. This capability has revolutionized stroke care, leading to better outcomes and reduced disability in stroke patients.

Brain tumor characterization is another area where Spectral CT is making a significant impact. Differentiating between several types of brain tumors is challenging due to their similar appearances on conventional CT scans. However, Spectral CT's ability to quantify tissue composition based on elemental composition provides neurologists with valuable information for precise tumor diagnosis. It aids in distinguishing between benign and malignant tumors and guides treatment planning, ensuring that patients receive the most proper therapies, such as surgery, radiation, or chemotherapy.

Cerebral angiography, a vital diagnostic procedure in neurology, has also received help from Spectral CT technology. Traditional angiography involves the injection of contrast agents into blood vessels to visualize vascular abnormalities in the brain. Spectral CT's real-time imaging capabilities allow neurologists to obtain dynamic angiographic images non-invasively. This reduces the risks associated with invasive procedures and enhances the diagnostic accuracy of cerebrovascular conditions, such as aneurysms, arteriovenous malformations (AVMs), and stenosis.

Furthermore, Spectral CT has proven to be instrumental in the assessment of intracranial hemorrhage. Hemorrhagic strokes and traumatic brain injuries often require urgent intervention. Spectral CT's ability to distinguish between several

types of hemorrhages, such as subarachnoid, subdural, or intraparenchymal hemorrhages, enables neurologists to make rapid and precise diagnoses. This information guides treatment decisions, including surgical interventions, if necessary, and improves patient outcomes.

In conclusion, Spectral CT has appeared as a momentous change in the field of neurology. Its applications in stroke imaging, brain tumor characterization, cerebral angiography, and intracranial hemorrhage assessment have significantly advanced neurological diagnosis and treatment. By providing neurologists with enhanced imaging capabilities and more precise information, Spectral CT is improving the quality of care and outcomes for patients with neurological disorders. As technology continues to evolve, it holds the promise of further advancements in neurology, offering hope to individuals affected by neurological conditions.

On the following page, clinical examples are included to illustrate the value of the spectral CT:

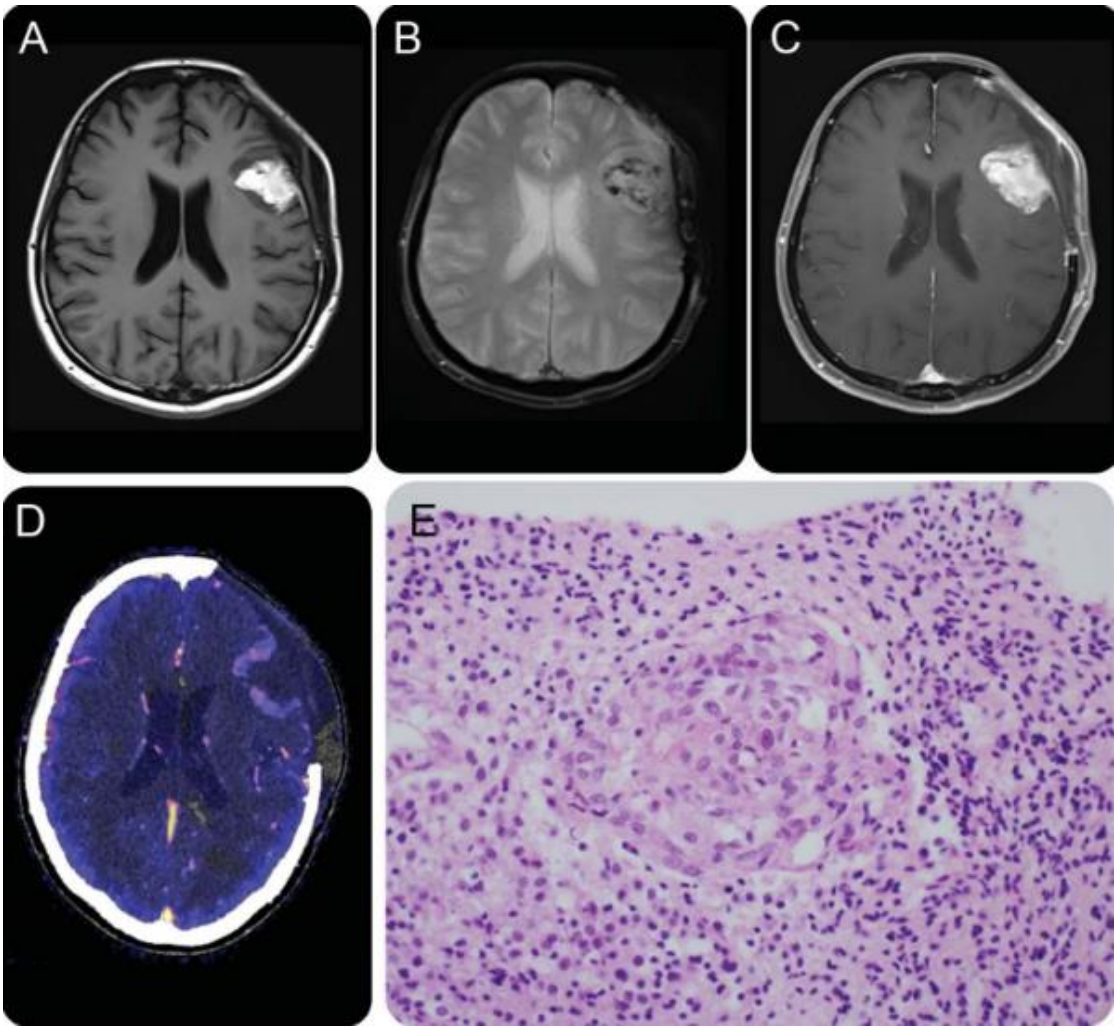

Figure 10: Because the signal intensity at the previous resection site is hyperintense on pre-contrast T1 image (A) due to hemorrhage (B; T2 gradient recalled echo), it is difficult to identify the tumoral enhancement (C; postcontrast T1). However, dual energy CT iodine-overlay image (D) reveals the previously undetectable enhancement along the periphery. Biopsy was consistent with glioblastoma multiforme. [57]*

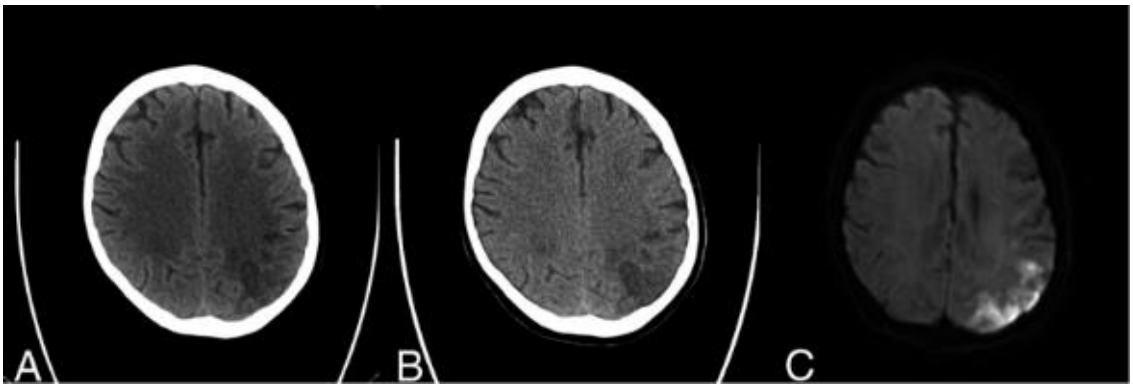

Figure 11: A sample case of a 66-year-old male patient who presented with right-sided weakness and numbness (NIHSS 7). His medical history included diabetes mellitus, hypertension, hyperlipidemia, prior smoking, and prior ischemic stroke, for which the patient used dual-antiplatelet therapy. The time between last seen well and CT was 14 hours. The time between CT and DWI was 12 hours. Conventional NCCT (A) and virtual NCCT (B) show early ischemic changes in the left parietal lobe (ASPECTS region M6). In the same region, DWI (C) shows hyperintensity, indicating diffusion restriction compatible with ischemia. [58]

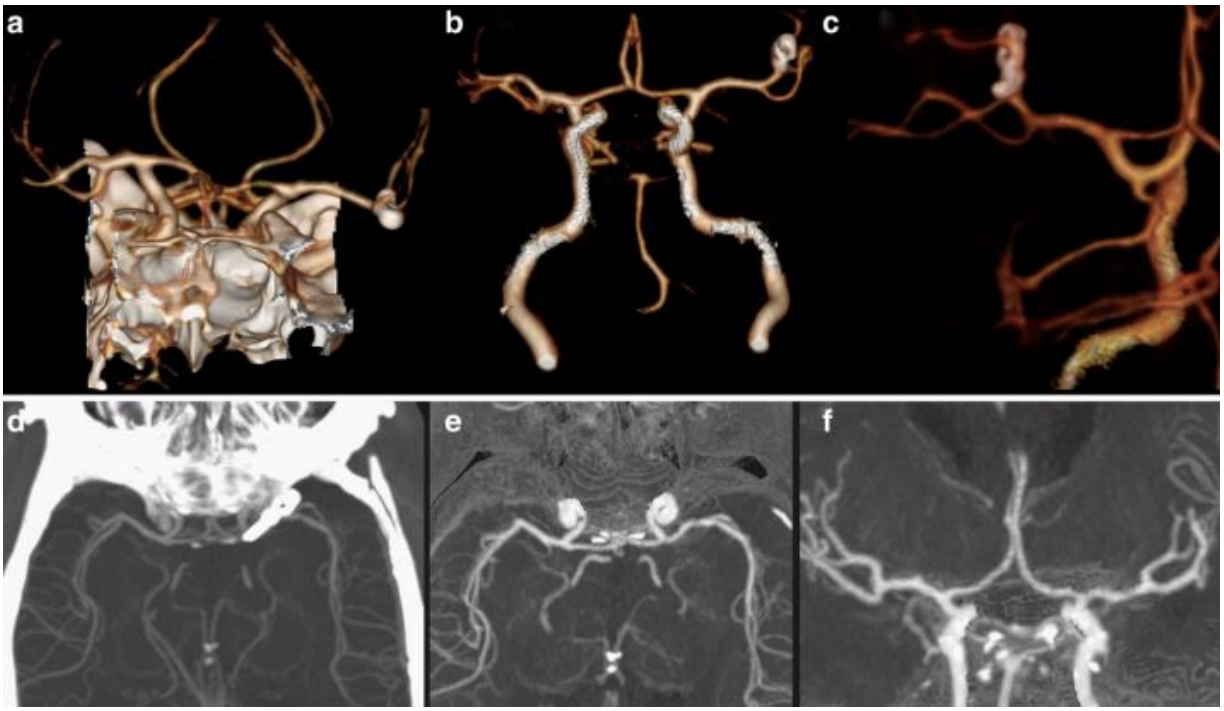

Figure 12: DECTA of 50-year-old male after clipping left MCA aneurysm before (a) and after automated bone removal (b, c—detail). The surgical clip was not removed by the automated bone removal. DECTA 80/Sn140 kVp, 310/155 mAs, CTDI 26.34 mGy, DLP 467 mGycm; 95 cc iodinated contrast 300 mg/ml; injection rate 5.5 cc/s; 40 cc saline flush 5.5 cc/s. DECTA of 51-year-old male after clipping of left carotid aneurysm before (d) and after automated bone removal (e, f). The surgical clip is removed by the automated bone removal. DECTA 80/Sn140 kVp, 310/155 mAs, CTDI 26,34 mGy, DLP 366 mGycm; 95 cc iodinated contrast 300 mg/ml; injection rate 5.5 cc/s; 40 cc saline flush 5.5 cc/s. [59]

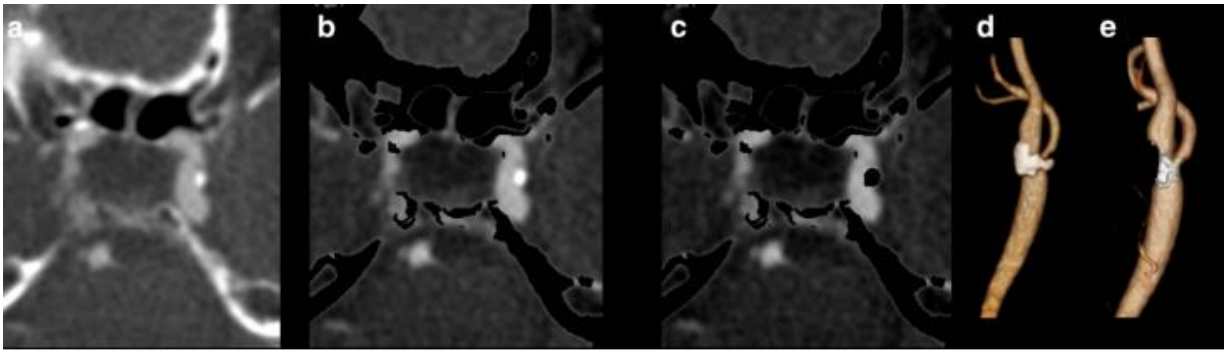

Figure 13: Detailed images of DECTA (a) at the cavernous part of the internal carotid artery (ICA), bone-removed DECTA with calcifications (b) and bone-removed DECTA without calcifications (c). Volume rendered images of carotid bifurcation with (d) and without (e) calcified plaques. DECTA 100/Sn140 kVp, 95/96 mAs, CTDI 5.9 mGy, DLP 211 mGycm; 95 cc iodinated contrast 300 mg/ml; injection rate 5.5 cc/s; 40 cc saline flush 5.5 cc/s. [59]

5.4 Clinical value in Abdominal Imaging

Abdominal imaging plays a critical role in diagnosing a wide range of medical conditions, from liver diseases to gastrointestinal disorders. The advent of Spectral Computed Tomography has brought about significant advancements in abdominal imaging, offering improved diagnostic accuracy and treatment planning across various abdominal pathologies.

One of the primary applications of Spectral CT in abdominal imaging is its role in liver lesion characterization. Liver lesions, both benign and malignant, can be challenging to differentiate on conventional CT scans. However, Spectral CT's dual-energy or multi-energy capabilities allow for enhanced tissue characterization. By analyzing the unique elemental composition of liver lesions, radiologists can distinguish between cysts, hemangiomas, focal nodular hyperplasia (FNH), hepatocellular carcinoma (HCC), and other lesions with greater confidence. This precise characterization aids in the development of tailored treatment plans, optimizing patient care.

Spectral CT has also proven to be invaluable in the detection and characterization of renal stones. Kidney stones are a common cause of abdominal pain, and their correct diagnosis and localization are crucial for effective treatment. Spectral CT's ability to differentiate between various stone types, such as calcium oxalate, uric acid, or struvite stones, aids urologists in selecting the most proper treatment strategies. Additionally, Spectral CT offers improved sensitivity in detecting even small urinary tract stones, minimizing the risk of missed diagnoses and recurrent stone formation.

Gastrointestinal (GI) imaging is another area where Spectral CT is making a significant impact. Disorders of the GI tract often require detailed imaging to assess conditions like inflammatory bowel disease (IBD), diverticulitis, or bowel obstructions. Spectral CT's enhanced contrast resolution and reduced beam hardening artifacts contribute to clearer images of the GI tract, improving diagnostic accuracy. Furthermore, the technology enables virtual non-contrast imaging, cutting the need for added scans while reducing radiation exposure for patients. This is particularly important in patients who require serial imaging for chronic GI conditions.

In the assessment of vascular pathologies within the abdomen, such as abdominal aortic aneurysms (AAA) or mesenteric ischemia, Spectral CT offers superior diagnostic capabilities. Its ability to supply accurate 3D reconstructions of vascular structures aids vascular surgeons in preoperative planning. Additionally, Spectral CT can quantify iodine uptake in vascular lesions, providing valuable information about perfusion patterns. This is crucial for assessing the severity of vascular diseases and guiding treatment decisions.

In conclusion, Spectral CT has ushered in a new era in abdominal imaging, offering unprecedented precision and diagnostic capabilities. Whether it's characterizing liver lesions, detecting renal stones, evaluating GI disorders, or assessing vascular pathologies, Spectral CT has revolutionized the field of abdominal imaging. By providing clinicians with enhanced imaging tools and reducing the need for multiple scans, it is improving the overall quality of care for patients with abdominal conditions. As technology continues to evolve, the promise of further advancements in abdominal imaging holds immense potential for patients and healthcare providers alike.

On the following page, clinical examples are included to illustrate the value of the spectral CT:

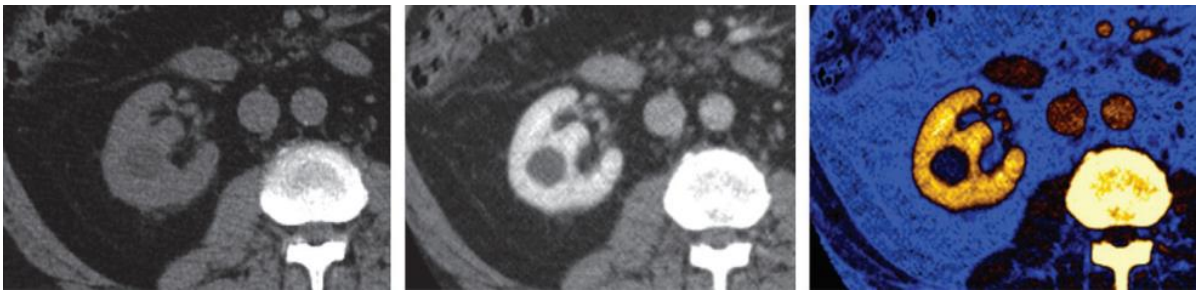

Figure 14: (left) Conventional nonenhanced, (middle) contrast-enhanced, and (right) color-coded iodine overlay images in a patient with a renal cyst. Although contrast enhancement may be ascertained by positioning a region of interest on both (a) conventional nonenhanced and (b) contrast-enhanced images, (c) color-coded iodine overlay image provides direct color-coded visualization of iodine content within the image. Note lack of iodine signal intensity within the cyst, denoting absence of contrast enhancement. [60]

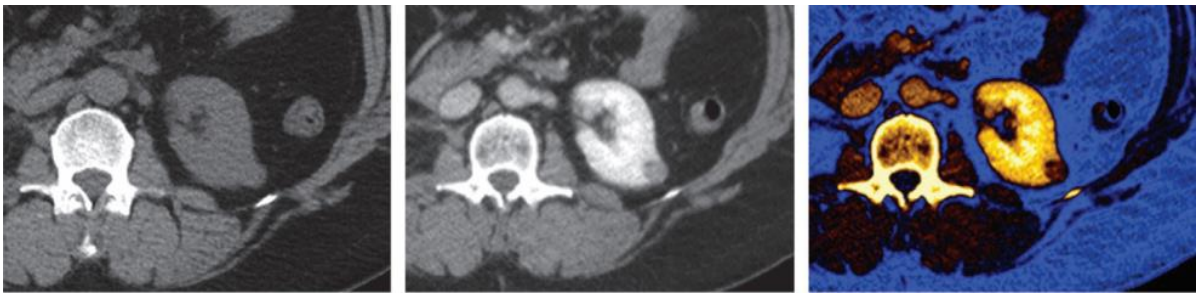

Figure 15: (left) Conventional nonenhanced, (middle) contrast-enhanced, and (right) color-coded iodine overlay images in a patient with an enhancing renal neoplasm. Note presence of iodine signal intensity within the lesion, consistent with lesion enhancement. [60]

Figure 16: (left) Conventional nonenhanced, (middle) contrast-enhanced, and (right) 80-keV virtual monochromatic images in a patient with a small intraparenchymal renal cyst. A surreptitious increase in CT number (pseudo enhancement) is seen on the contrast-enhanced image (b), due to failure of the reconstruction algorithm to correct for beam-hardening. By reducing beam-hardening effects, the virtual monochromatic image mitigates pseudo enhancement. [60]

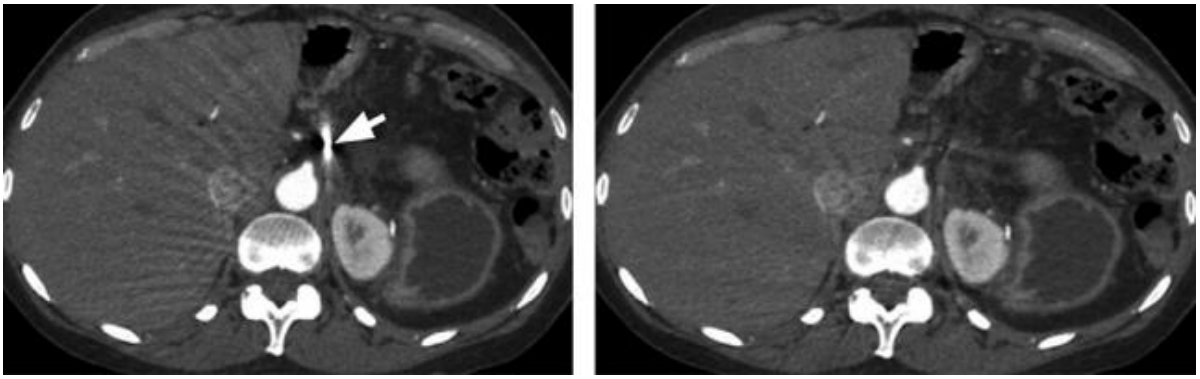

Figure 17: Effectiveness of a metal artifacts reduction algorithm in clinical practice. Virtual monochromatic images at 70 keV (left) without MARS and (right) with MARS. Note substantial correction of beam-hardening and photon starvation artifacts with MARS, due to a metal clip (arrow). [60]

5.5 Clinical value in Orthopedics and Musculoskeletal System

Orthopedic medicine focuses on the diagnosis and treatment of musculoskeletal conditions, which often involve bones, joints, and soft tissues. Spectral Computed Tomography has appeared as a powerful tool in the field of orthopedics, providing advanced imaging capabilities that have transformed the way orthopedic practitioners diagnose and manage a wide range of musculoskeletal disorders.

One of the primary applications of Spectral CT in orthopedics is the evaluation of bone density. Accurate assessment of bone density is crucial for diagnosing osteoporosis and figuring out fracture risk. Spectral CT's ability to quantify bone mineral density (BMD) with precision offers orthopedic specialists a valuable tool for early detection and management of osteoporosis. This is especially important in the aging population, where fractures and bone health are significant concerns.

Spectral CT also excels in soft tissue imaging, a vital aspect of orthopedic diagnostics. Soft tissue injuries, such as ligament and tendon tears, are common in orthopedic practice. Traditional CT scans often struggle to provide detailed soft tissue contrast. However, Spectral CT's improved contrast resolution allows orthopedic surgeons to visualize soft tissue injuries more clearly. This enhances the accuracy of diagnosis and eases treatment planning, whether it involves surgical repair or conservative management.

Cartilage assessment is another area where Spectral CT has proven invaluable in orthopedics. Cartilage plays a crucial role in joint function, and its damage or degeneration can lead to conditions like osteoarthritis. Spectral CT's ability to provide high-resolution images of cartilage and detect early changes in its composition enables orthopedic specialists to intervene promptly and implement strategies to preserve joint function. This is particularly important in sports medicine, where athletes often need precise assessments of cartilage health.

Furthermore, Spectral CT is increasingly being used in orthopedics to aid in the planning of orthopedic surgeries, such as joint replacement procedures. By supplying detailed 3D reconstructions of bones and joints, it allows orthopedic surgeons to perform virtual surgical simulations. These simulations help optimize implant positioning, select right implant sizes, and predict potential challenges

during surgery. This level of preoperative planning contributes to improved surgical outcomes and patient satisfaction.

In conclusion, Spectral CT has become an indispensable tool in the field of orthopedics, offering advanced capabilities for bone density assessment, soft tissue imaging, cartilage assessment, and surgical planning. Orthopedic practitioners can use the technology to enhance diagnostic accuracy, provide prompt interventions, and optimize surgical procedures. As Spectral CT technology continues to evolve, its applications in orthopedics are expected to expand further, offering orthopedic specialists new avenues for improving musculoskeletal care and patient outcomes.

On the following page, clinical examples are included to illustrate the value of the spectral CT:

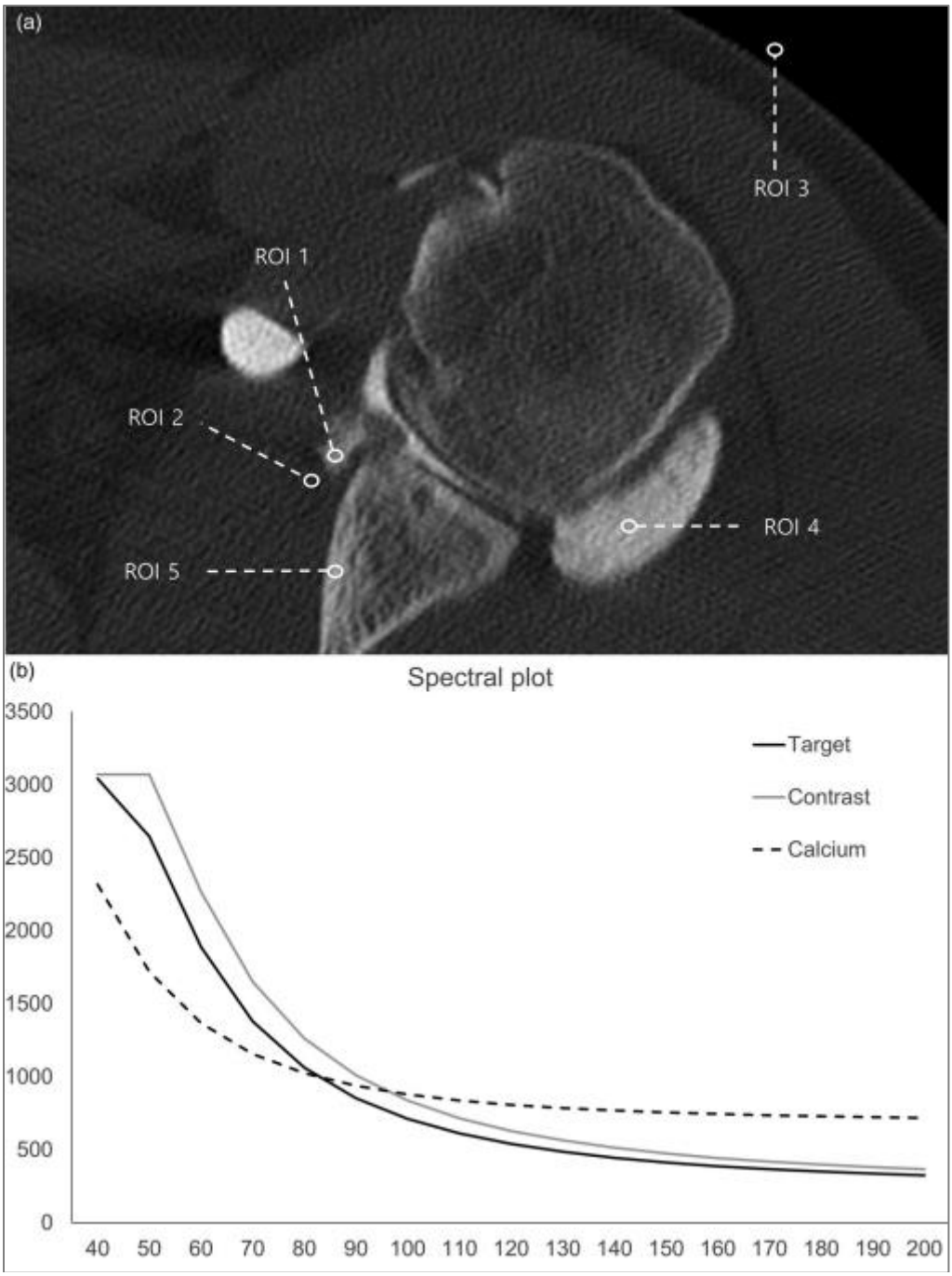

Figure 18: Circular ROIs were placed on a single slice that included the target lesion for image evaluation. The mean Hounsfield unit value was plotted against the monochromatic energy levels in the range of 40–200 keV (spectral plot). (a) ROIs with equal sizes are overlayed on the target lesion (ROI 1), the soft tissue adjacent to the target lesion (ROI 2), the air space (ROI 3), the location in which the contrast media solution filled the glenohumeral joint recess (ROI 4), and the cortical bone of the glenoid (ROI 5). (b) Spectral plots of the target lesion, cortical bone, and contrast media solution are shown. The target lesion shows a curve like that of the contrast media solution, indicating that the target lesion is likely contrast medium. ROI, region of interest. [62]

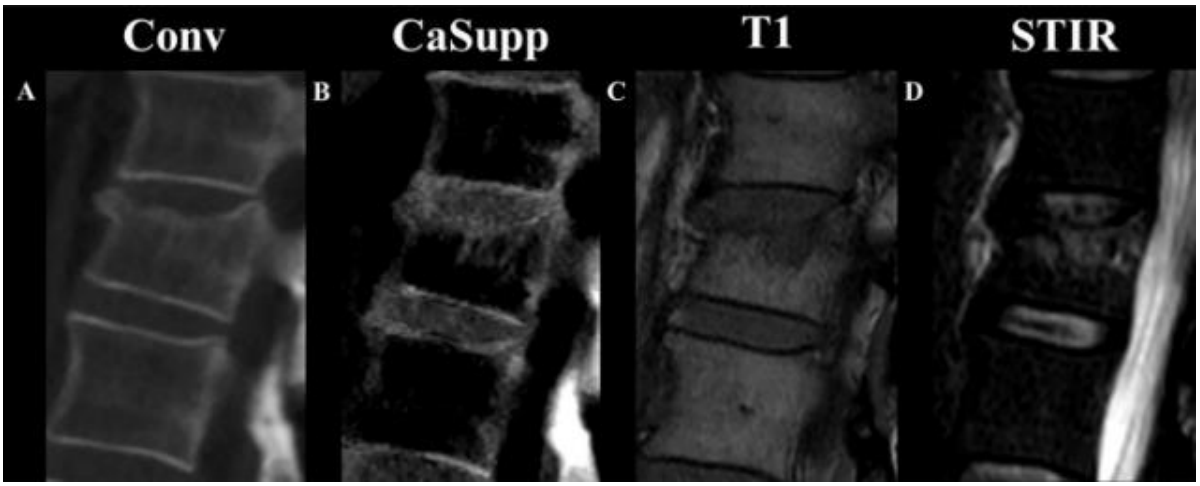

Figure 19: Sagittal conventional CT image (A), sagittal CaSupp (CaSupp-I 90; B), sagittal T1-weightrf sequence (C), and sagittal STIR sequence (D) show an acute fracture at L1 with extensive BME and loss of height. [63]

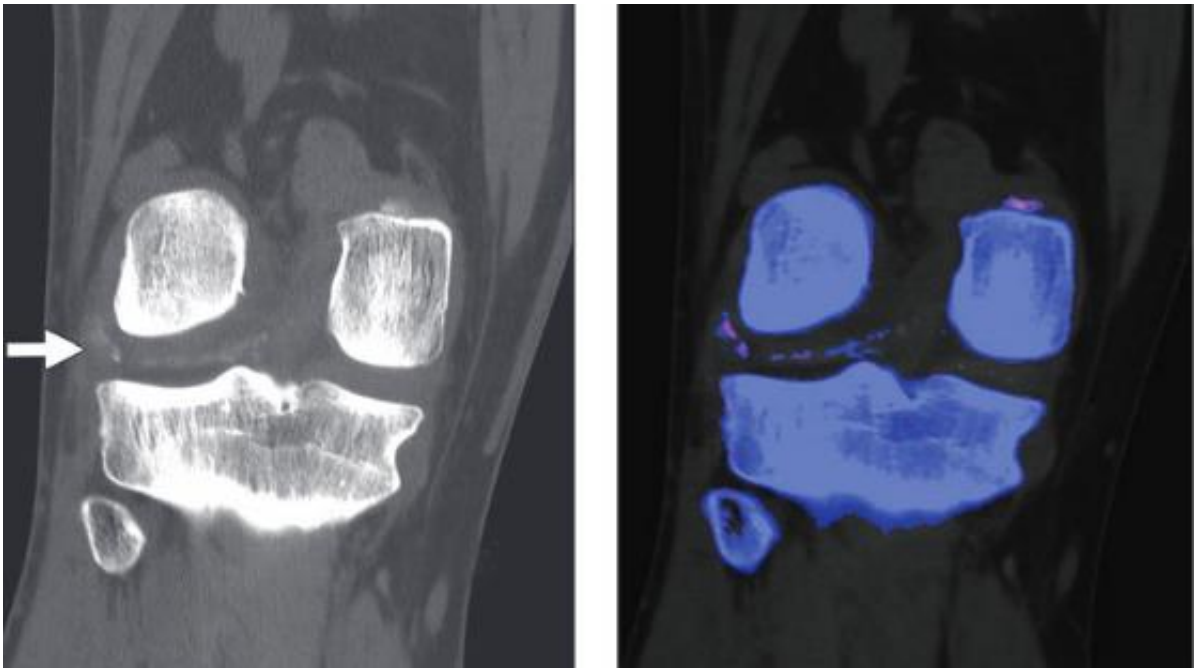

Figure 20: 49-year-old man with chondrocalcinosis. (Left), Conventional unenhanced coronal CT image of knee shows extensive mineralization (arrow) in posterior horn of lateral meniscus and along popliteus tendon. (Right), Dual-energy CT image postprocessed for gout shows that almost all this mineralization is related to calcium deposition (purple) rather than urate crystal deposition, which should be green in color, consistent with chondrocalcinosis. [64]

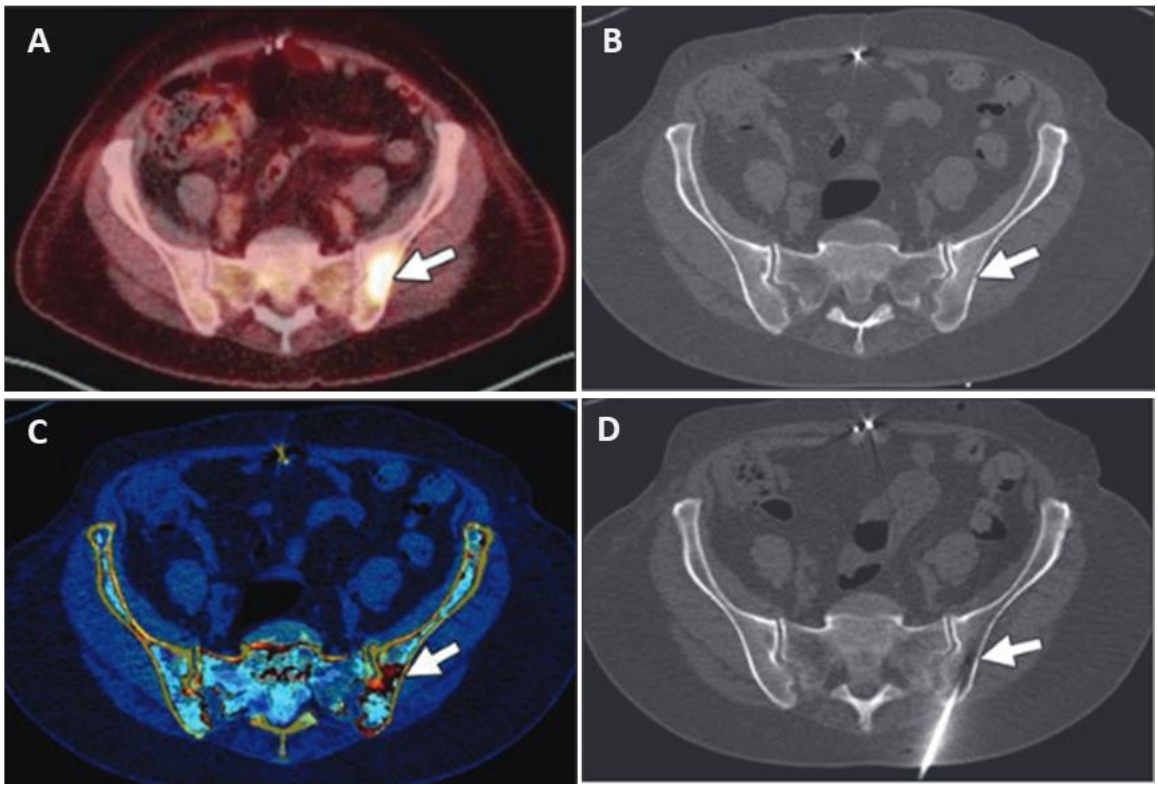

Figure 21: 73-year-old woman with metastatic small cell carcinoma. A–C, FDG-avid lesion (arrows) is seen in left iliac bone on axial fused PET/CT image (A), is not visible on conventional unenhanced axial CT image (B) but is visible on dual-energy CT (DECT) image (C) postprocessed for bone marrow visualization. D, Lesion visualization using DECT allowed targeted CT-guided biopsy, which confirmed metastatic small cell carcinoma (arrow) from primary lung tumor. [64]

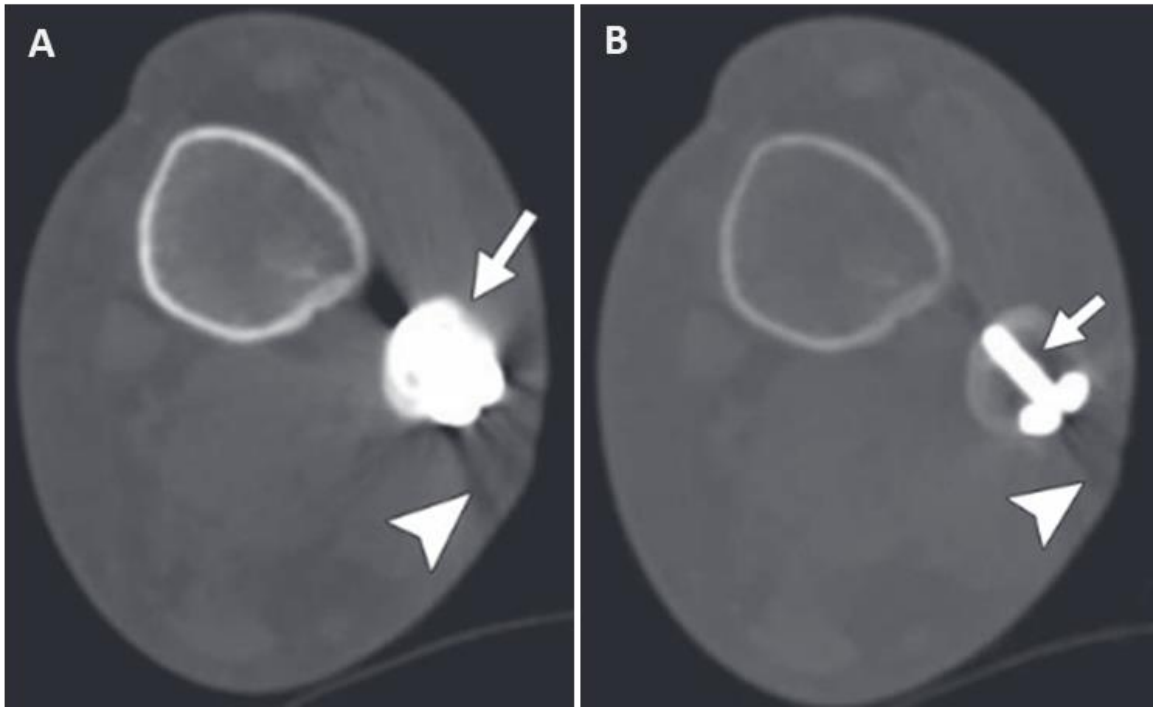

Figure 22: 37-year-old man with history of ankle injury and placement of plates and screws. A, Conventional CT image in axial plane shows fibular screw (arrow), which is not well defined. There is metal artifact (arrowhead) adjacent to screw. B, Virtual monoenergetic image obtained at 200 keV shows improved definition of hardware (arrow) and decreased artifact (arrowhead). [64]

5.6 Clinical value in Pulmonology

Pulmonology, the branch of medicine dedicated to the diagnosis and treatment of respiratory disorders, has seen remarkable advancements with the introduction of Spectral Computed Tomography. This innovative imaging technology has redefined the way pulmonologists diagnose and manage a wide range of pulmonary conditions, offering enhanced accuracy and improved patient care.

One of the primary applications of Spectral CT in pulmonology is in the staging and diagnosis of lung cancer. Lung cancer is a leading cause of cancer-related mortality worldwide, and correct staging is crucial for treatment planning. Spectral CT's multi-energy capabilities enable pulmonologists to assess lesions with greater precision, differentiating between benign and malignant pulmonary nodules. Furthermore, it aids in the detection of lymph node involvement and distant metastases, which are vital factors in finding the stage of the disease. This information guides treatment decisions, whether it involves surgery, radiation therapy, chemotherapy, or targeted therapies.

In the realm of chronic obstructive pulmonary disease (COPD), Spectral CT plays a vital role in assessing disease severity and progression. COPD is a complex condition that affects both the airways and lung parenchyma. Spectral CT provides improved visualization of lung parenchyma, enabling pulmonologists to quantify emphysema and assess lung density. This information aids in the characterization of disease severity and guides treatment decisions, such as pulmonary rehabilitation or surgical interventions like lung volume reduction surgery (LVRS).

Pulmonary embolism (PE) is another area where Spectral CT has made significant strides in pulmonology. PE is a life-threatening condition that requires prompt and accurate diagnosis. Spectral CT's ability to differentiate between clot material and surrounding lung tissue is crucial for finding and characterizing pulmonary emboli. Additionally, it provides information about the perfusion status of lung segments affected by the embolism, which aid s in risk stratification and treatment decisions, including anticoagulation therapy or catheter-directed thrombolysis.

Furthermore, Spectral CT enhances the evaluation of interstitial lung diseases (ILDs), a group of disorders that affect the lung's interstitium. Conventional CT scans may not provide sufficient detail for the correct diagnosis and classification of

ILDs. Spectral CT's improved contrast resolution and tissue characterization capabilities enable pulmonologists to visualize and differentiate various ILDs more effectively. This leads to more exact diagnoses and enables targeted treatment strategies, such as immunosuppressive therapy or anti-fibrotic medications.

In conclusion, Spectral CT has become an indispensable tool in pulmonology, offering advanced capabilities for lung cancer staging, COPD assessment, pulmonary embolism detection, and the evaluation of interstitial lung diseases. Pulmonologists can use this technology to enhance diagnostic accuracy, provide personalized treatment plans, and improve patient outcomes. As Spectral CT technology continues to evolve, its applications in pulmonology are expected to expand further, offering new possibilities for advancing respiratory care and patient well-being.

On the following page, clinical examples are included to illustrate the value of the spectral CT:

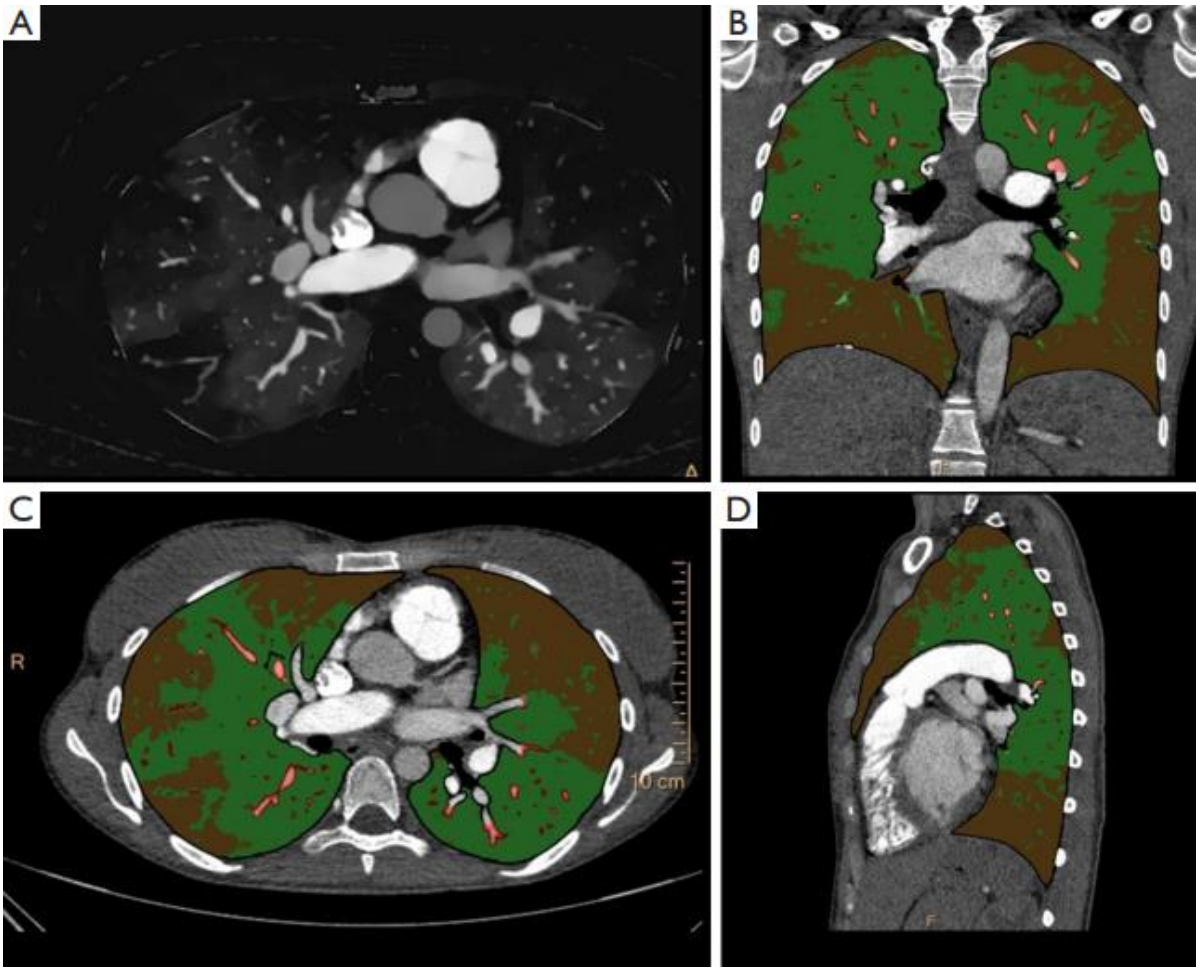

Figure 23: Exemplary assessment of iodine density-based lung segmentation in a patient with chronic thromboembolic pulmonary hypertension. (A) Iodine density image. (B-D) Color-coded images from the automatic quantification based on iodine density. Color coding as follows: red, vessel; green, normal perfused lung regions; brown, mal-perfused lung regions. [65]

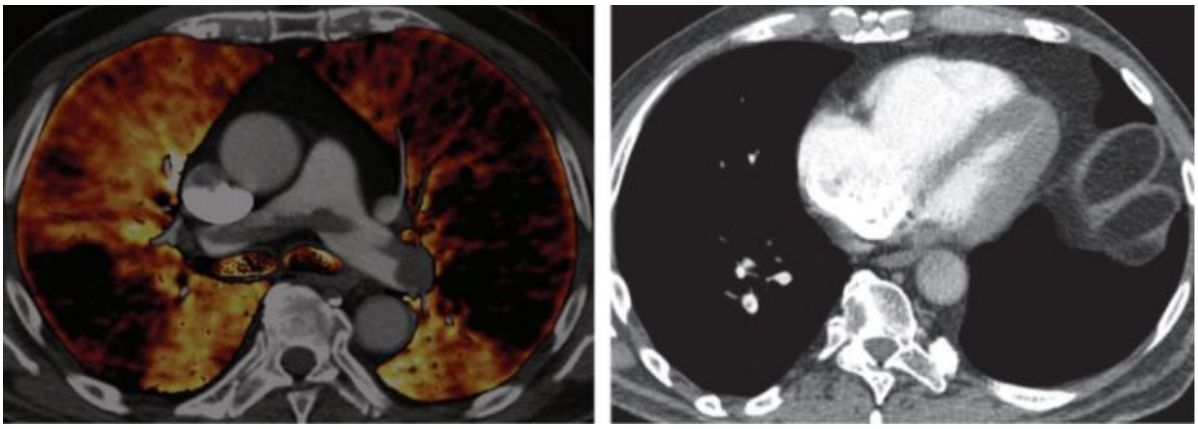

Figure 24: Correlation of perfusion defect size with pulmonary embolism severity in a 55-year-old man who presented with collapse. (left) Axial fused PBV image shows a saddle embolus with extensive bilateral perfusion defects. (right) Axial mixed (100-kVp and Sn 140-kVp) DECT image shows an enlarged right-to-left ventricular ratio and posterior deviation of the interventricular septum, findings consistent with a massive pulmonary embolus. [66]

5.7 Clinical value in Urology

Urology, the medical specialty dedicated to the diagnosis and treatment of disorders of the urinary system and male reproductive organs, has undergone significant transformations with the integration of Spectral Computed Tomography, This cutting-edge imaging technology is reshaping the way urologists approach the diagnosis and management of a diverse range of urological conditions, offering enhanced precision and patient care.

One of the most prominent applications of Spectral CT in urology is its ability to provide detailed and accurate imaging of the kidneys. Kidney diseases, including renal masses and urolithiasis (kidney stones), are common urological concerns. Spectral CT's dual-energy or multi-energy capabilities offer improved contrast resolution, enabling urologists to differentiate between several types of renal masses. Whether distinguishing between benign cysts and solid tumors or characterizing distinct types of renal cell carcinomas, Spectral CT provides essential information for diagnostic accuracy and treatment planning.

For urolithiasis, Spectral CT's ability to differentiate between different stone types, such as calcium oxalate, uric acid, or struvite stones, is invaluable. Urologists can tailor their treatment strategies based on stone composition, optimizing the choice of interventions, including lithotripsy, ureteroscopy, or percutaneous nephrolithotomy (PCNL). This targeted approach enhances the efficiency of stone management, minimizes complications, and improves patient outcomes.

Spectral CT is also making significant contributions to prostate imaging, an area of urology critical for the diagnosis and management of prostate cancer. Prostate cancer is a leading cause of cancer-related mortality in men. Spectral CT's enhanced imaging capabilities enable urologists to visualize the prostate gland with improved clarity. It aids in the detection of prostate lesions, helps targeted prostate biopsies, and assists in the staging of prostate cancer. Additionally, Spectral CT's ability to provide functional imaging data, such as perfusion and vascular parameters, enhances the assessment of tumor aggressiveness and guides treatment decisions, including surgery, radiation therapy, or active surveillance.

In the assessment of bladder cancer, Spectral CT offers advantages in both diagnosis and treatment planning. Accurate staging and localization of bladder

tumors are crucial for determining therapies, such as transurethral resection (TURBT), intravesical chemotherapy, or radical cystectomy. Spectral CT's ability to provide detailed images of the urinary bladder and its contents aids urologists in precisely defining the extent of the disease and planning surgical procedures.

Furthermore, Spectral CT contributes to urological interventions by aiding in the localization of foreign bodies, such as ureteral stents or kept surgical instruments. In cases of urological trauma or complications, Spectral CT's ability to reduce artifacts and improve soft tissue contrast assists urologists in finding and managing these challenges efficiently.

In conclusion, Spectral CT is a transformative technology in the field of urology, offering advanced capabilities for kidney imaging, urolithiasis management, prostate cancer diagnosis, bladder cancer staging, and urological interventions. Urologists can use this technology to enhance diagnostic accuracy, tailor treatment strategies, and improve patient outcomes. As Spectral CT technology continues to evolve, its applications in urology are expected to expand further, offering new opportunities to advance urological care and patient well-being.

On the following page, clinical examples are included to illustrate the value of the spectral CT:

Figure 25: Axial CT images in 69-year-old man with urinary calculus (arrow) in the right kidney. (left) TNE image shows the calculus (3 3 3 mm). (middle) Excretory phase dual-energy image of the corresponding section also shows the calculus, but it cannot be distinguished reliably from contrast medium. (right) After optimal iodine subtraction, the calculus can be detected on the corresponding VNE image (arrow). [67]

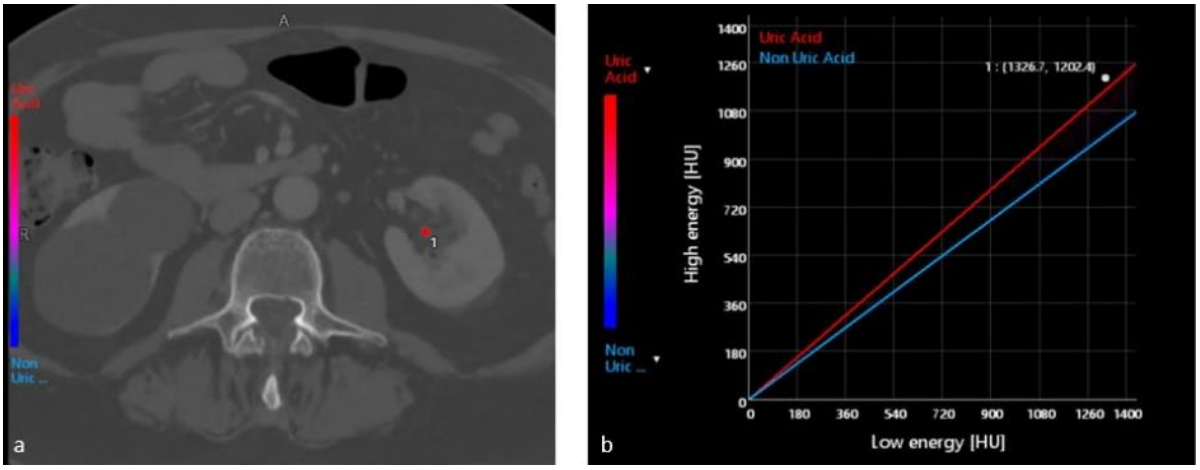

Figure 26: Left kidney stone segmented. The composition was revealed to be uric acid (b). [68]

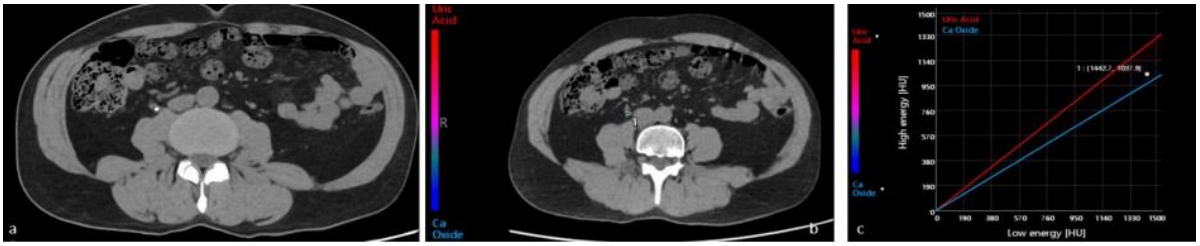

Figure 27: Stone composition analysis. (a) Intraurethral hyperdense stone; (b) automatic segmentation of the stone; (c) in the graphic, the stone is placed next to the calcium oxide. [68]

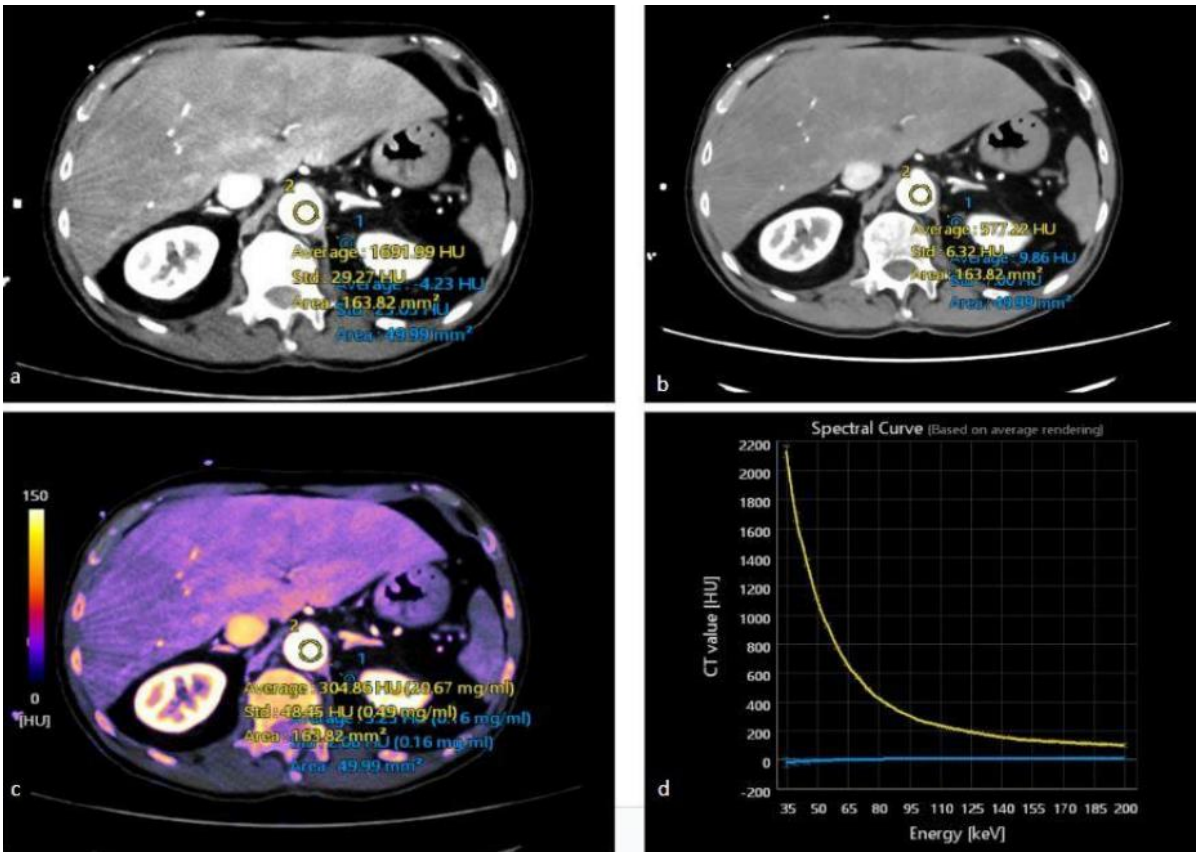

Figure 28: Example of a spectral attenuation curve of a small left renal cyst. (a) Monochromatic image at 40 keV; (b) monochromatic image at 80 keV; (c) iodine map showing no contrast enhancement within the cyst, confirmed by the flat-curve-type of the cyst in blue (d), compared with the upward-curve-type of the aorta in yellow that shows a rise in Hounsfield units for low energy levels. [68]

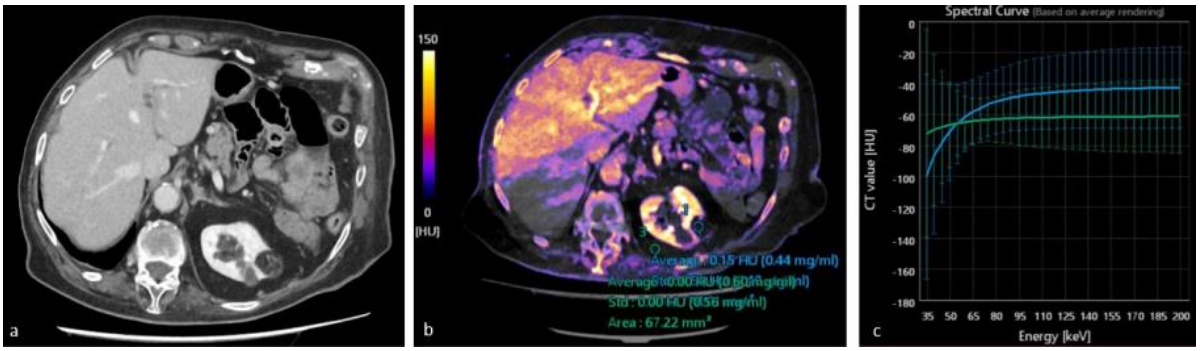

Figure 29: (a) Left renal lesion with prevalent fat tissue density, but with inhomogeneous content; (b) the color-coded overlay-iodine map demonstrates the absence of intralesional contrast enhancement, confirmed by the iodine analysis (c). The lesion was characterized as an angiomyolipoma. The curve of angiomyolipoma (blue) shows a reduction in the attenuation values at lower energies with attenuation values in line with that of the fat tissue (green). [68]

5.8 Clinical value in Pediatrics

Pediatrics is a specialized field of medicine that focuses on the unique healthcare needs of infants, children, and adolescents. In recent years, Spectral Computed Tomography has appeared as a revolutionary tool in pediatric imaging, offering advantages that are particularly valuable when caring for young patients.

One of the key applications of Spectral CT in pediatrics is its role in improving diagnostic accuracy in various clinical scenarios. Pediatric patients often present with complex and diverse conditions, ranging from congenital anomalies to acquired diseases. Spectral CT's multi-energy capabilities enable pediatric radiologists to obtain detailed anatomical and functional information in a single scan. This is especially beneficial when diagnosing conditions like congenital heart defects, where precise anatomical assessments are crucial for treatment planning.

In pediatric cardiology, Spectral CT has been instrumental in supplying non-invasive assessments of congenital heart diseases. By offering high-resolution images of the heart and its structures, Spectral CT assists cardiologists in characterizing cardiac abnormalities, such as ventricular septal defects or Tetralogy of Fallot. Additionally, it aids in the assessment of coronary artery anomalies, guiding interventional procedures or surgical corrections.

Another area where Spectral CT has made a significant impact in pediatrics is in the evaluation of congenital abnormalities. Congenital anomalies can affect various organ systems, including the brain, heart, spine, and kidneys. Spectral CT's superior contrast resolution and reduced radiation dose are particularly helpful in pediatric patients. For example, in pediatric neuroimaging, Spectral CT can provide detailed images of the brain, enabling the early detection and management of conditions like hydrocephalus or brain malformations.

Spectral CT is also transforming the way pediatric oncologists diagnose and monitor childhood cancers. Pediatric cancers often require precise staging and follow-up assessments. Spectral CT's ability to differentiate between tumor types and evaluate treatment response is invaluable in pediatric oncology. It allows oncologists to tailor treatment plans to the specific cancer type, monitor changes in tumor characteristics over time, and make prompt adjustments to therapy.

Moreover, Spectral CT is enhancing diagnostic confidence in pediatric gastroenterology. Gastrointestinal disorders in children can be challenging to diagnose, as they may present with nonspecific symptoms. Spectral CT's advanced imaging capabilities provide pediatric gastroenterologists with clearer visualization of the GI tract, enabling them to detect abnormalities such as malrotation, intussusception, or inflammatory bowel disease more accurately. This leads to prompt diagnosis and prompt intervention, ultimately improving the quality of care for pediatric patients.

In conclusion, Spectral CT has appeared as a game-changer in pediatric imaging, offering advanced capabilities for diagnosing congenital anomalies, evaluating heart defects, monitoring cancer treatment, and assessing gastrointestinal disorders in children. Its high-resolution images, reduced radiation exposure, and functional assessments are transforming pediatric healthcare, enabling healthcare providers to deliver precise and effective care to young patients. As Spectral CT technology continues to evolve, its applications in pediatrics are expected to expand further, offering new possibilities to enhance the well-being of children and adolescents.

On the following page, clinical examples are included to illustrate the value of the spectral CT:

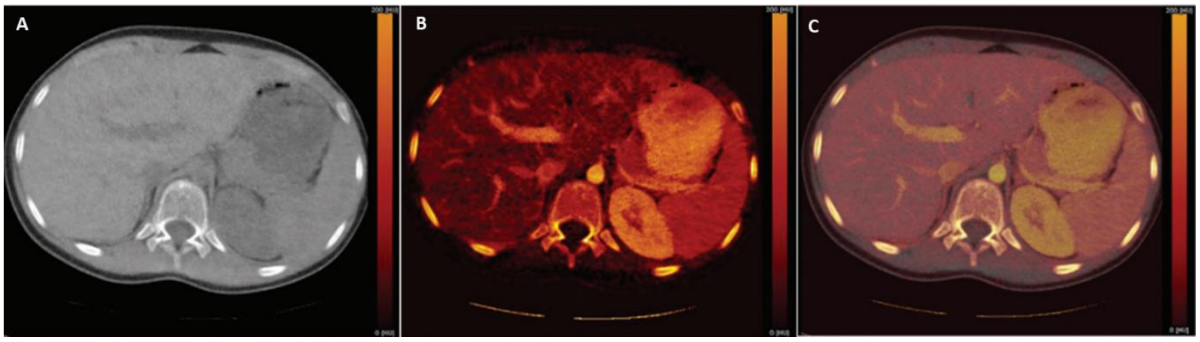

Figure 30: Representative postprocessed iodine specific images in a healthy 7-year-old boy. (a) Virtual nonenhanced CT image is created by using subtraction of iodine content. (b) Iodine map image displays color-coded iodine content. (c) Iodine overlay image superimposes color-coded iodine map on gray-scale virtual nonenhanced image. Iodine content in stomach is related to use of oral contrast material that had iodine material. [69]

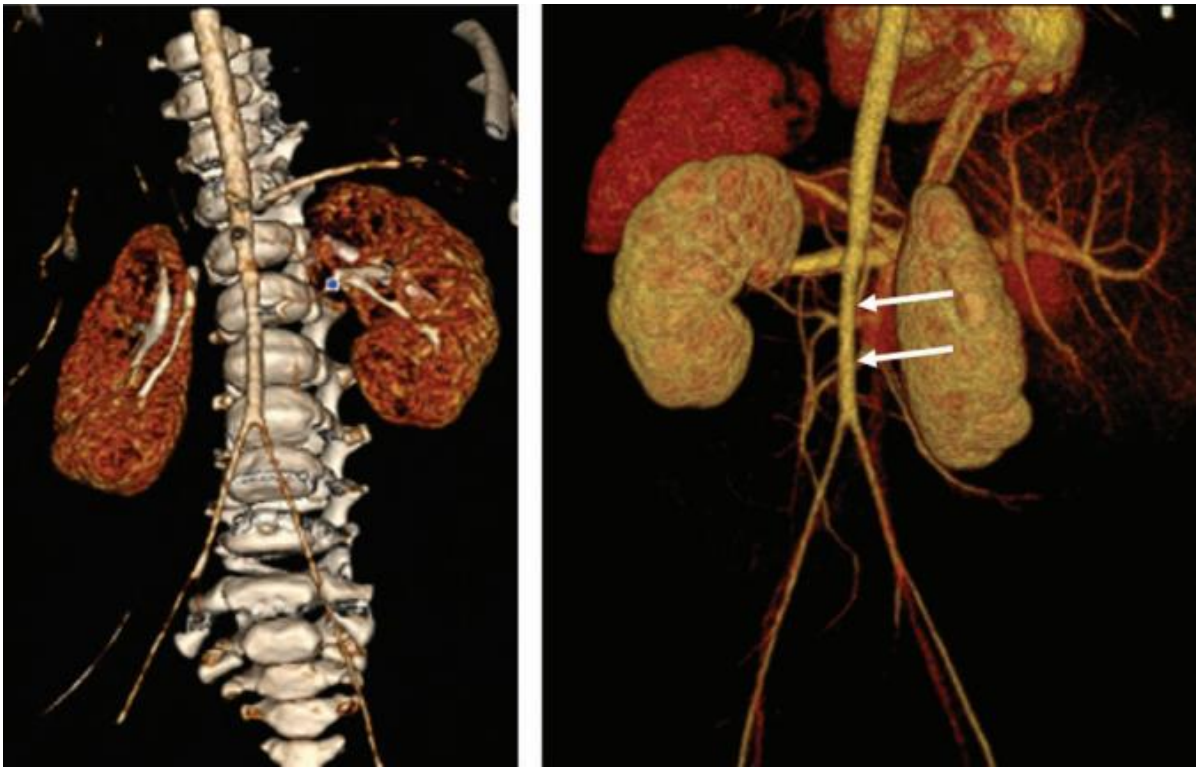

Figure 31:Images show automated bone subtraction in a 6-month-old boy with hypertension. (left) Coronal angiogram before bone subtraction. (right) Coronal angiogram after automated bone removal improves visualization of abdominal aorta and its branches. Tapering of abdominal aorta (arrows) distal to origin of superior mesenteric artery with associated decreased caliber of iliac arteries is consistent with mid-aortic syndrome. [69]

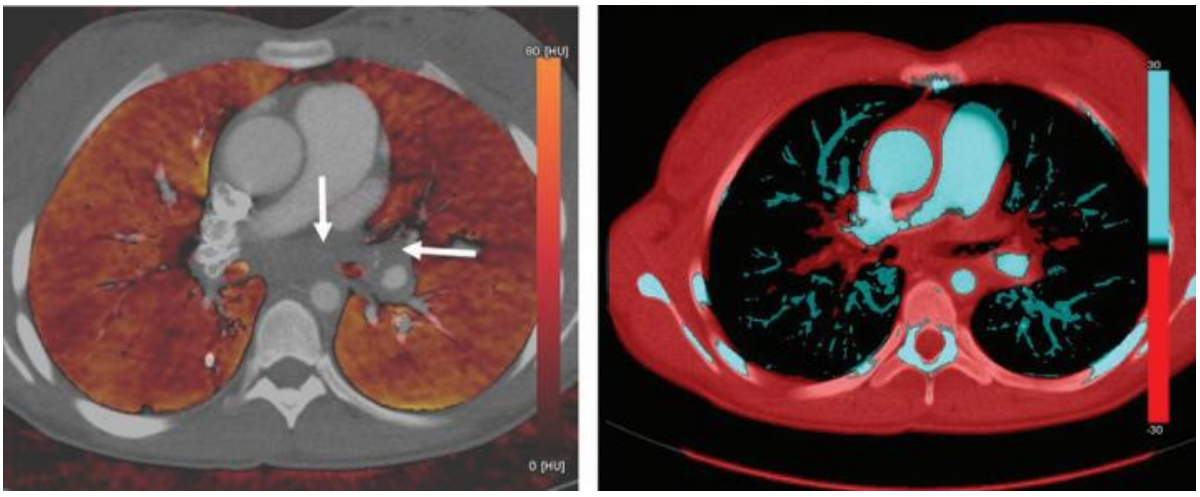

Figure 32: Images show normal lung perfusion and vessel analysis in a 15-year-old girl. (left) Normal lung perfusion is color coded orange and has homogeneous color distribution. Iodine content is low in middle mediastinum and left hilum (arrows) due to fibrosing mediastinitis. (right) Normal lung vessel image in the same patient. Pulmonary arteries that have relatively high iodine content are color coded in blue and pulmonary veins that have relatively low iodine content are color coded red. [69]

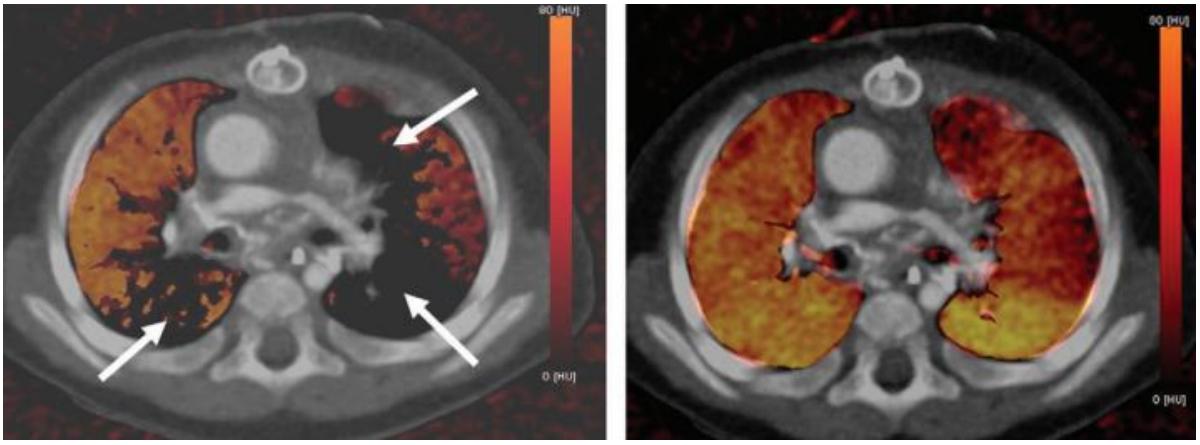

Figure 33: Images show technical artifacts due to incorrect CT algorithm threshold in a 4-month-old boy with tetralogy of Fallot. (left) Iodine defects (arrows) are seen when maximum CT number is set at 2600 HU. (right) Lung parenchyma is nearly normal when CT threshold value is set at 2300 HU except for anterior and lateral parts of left upper lobe, which show small perfusion defects. In young children, higher maximum Hounsfield units are needed to compensate for higher lung density in this population. Iodine enhancement in dependent posterior portions of lungs is slightly higher than that of anterior regions, which is considered normal gravity-related perfusion gradient. [69]

5.9 Gynecology

Gynecology is a medical specialty dedicated to the health of the female reproductive system. In recent years, Spectral Computed Tomography (Spectral CT) has appeared as a valuable tool in gynecological imaging, offering advanced capabilities that enhance the diagnosis and management of various gynecological conditions.

One of the primary applications of Spectral CT in gynecology is the evaluation of pelvic masses and tumors. Ovarian cysts and tumors, uterine fibroids, and other pelvic masses are common gynecological concerns. Spectral CT's multi-energy capabilities provide detailed imaging of these masses, allowing gynecologists to differentiate between benign and malignant lesions. This is essential for deciding on the right course of action, whether it involves monitoring, surgical removal, or further diagnostic tests.

In the assessment of endometriosis, a chronic condition characterized by the growth of endometrial tissue outside the uterus, Spectral CT offers advantages in visualization and diagnosis. Endometriosis often presents with pelvic pain and infertility. Spectral CT's ability to supply enhanced contrast resolution helps gynecologists identify endometrial implants and adhesions more accurately. This contributes to early diagnosis and tailored treatment plans, which may include medical management or surgical interventions.

Spectral CT also plays a vital role in gynecological oncology, particularly in the staging and monitoring of gynecological cancers such as cervical, ovarian, and uterine cancers. Accurate staging is crucial for deciding on the extent of the disease and guiding treatment decisions, including surgery, radiation therapy, or chemotherapy. Spectral CT's ability to provide detailed anatomical and functional information aids gynecologists in staging gynecological cancers and monitoring the response to treatment.

Furthermore, Spectral CT contributes to the evaluation of pelvic inflammatory diseases (PID) and tubo-ovarian abscesses. PID is an infection of the female reproductive organs, while tubo-ovarian abscesses are pus-filled pockets that can form in the fallopian tubes or ovaries. Spectral CT's high-resolution imaging

capabilities aid gynecologists in diagnosing these conditions accurately and guiding right treatment strategies, which may include antibiotics or surgical drainage.

In conclusion, Spectral CT has become an asset in gynecological imaging, offering advanced capabilities for diagnosing and managing pelvic masses, endometriosis, gynecological cancers, and inflammatory conditions. Gynecologists can use this technology to enhance diagnostic accuracy, provide personalized treatment plans, and improve the overall quality of care for women's reproductive health. As Spectral CT technology continues to evolve, its applications in gynecology are expected to expand further, offering new possibilities for advancing women's health and well-being.

On the following page, clinical examples are included to illustrate the value of the spectral CT:

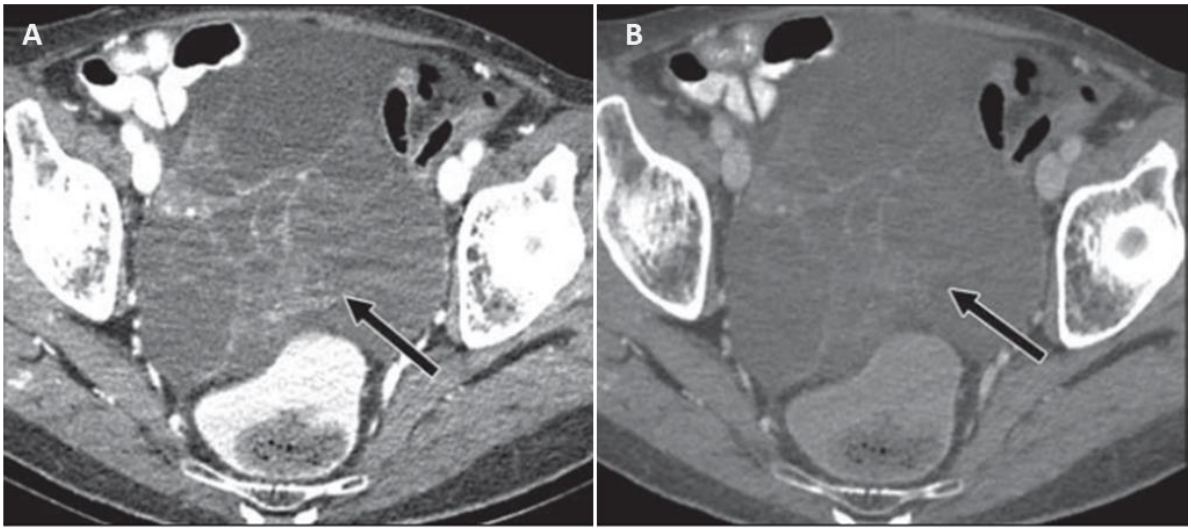

Figure 34: 74-year-old woman with stage IIIC mucinous ovarian cancer. A and B, Axial contrast-enhanced dual-energy CT monochromatic images obtained at 50 keV (A) and 140 keV (B). Internal architecture of tumor is better seen on 50-keV image (A). Note that multiple septations (arrow, A and B) are better seen on lower energy image (A). Improved conspicuity on lower–kiloelectron volt images may help assess adnexal lesions and differentiate simple cysts from more complex cysts. [70]

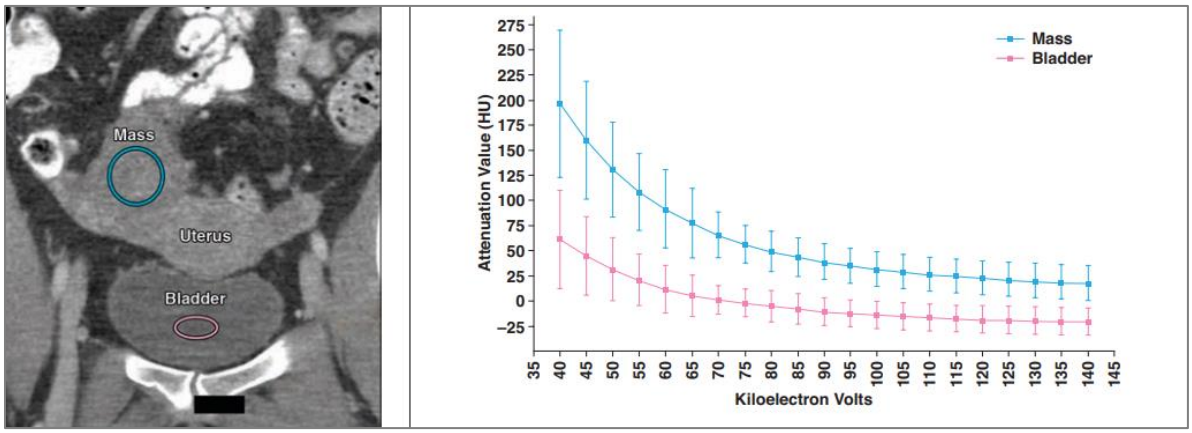

Figure 35: 52-year-old woman with high-grade ovarian cancer. (left), Monochromatic coronal reformatted contrast-enhanced dual-energy CT (DECT) image obtained at 70 keV (similar to image obtained at 120 kVp) shows hypo-attenuated mass in left ovary and bladder. Two ROIs have been drawn on this CT image, with one ROI (blue circle) in mass in right ovary and other ROI in bladder (pink oval). (right), Graph shows DECT spectral attenuation curves for hypo-attenuated mass (corresponding to ROI [blue circle] in A) in right ovary and bladder (corresponding to ROI [pink oval] in left image). Significant difference is noted between curve for hypo-attenuated mass (blue curve) in right ovary and bladder (pink curve), suggesting that mass and bladder have different spectral attenuation curves and, hence, have different materials. Note that curves diverge at lower–kiloelectron volt values, suggesting that they may be better differentiated at lower energies. Horizontal lines within boxes denote mean values, and vertical lines and whiskers denote 95% CIs. [70]

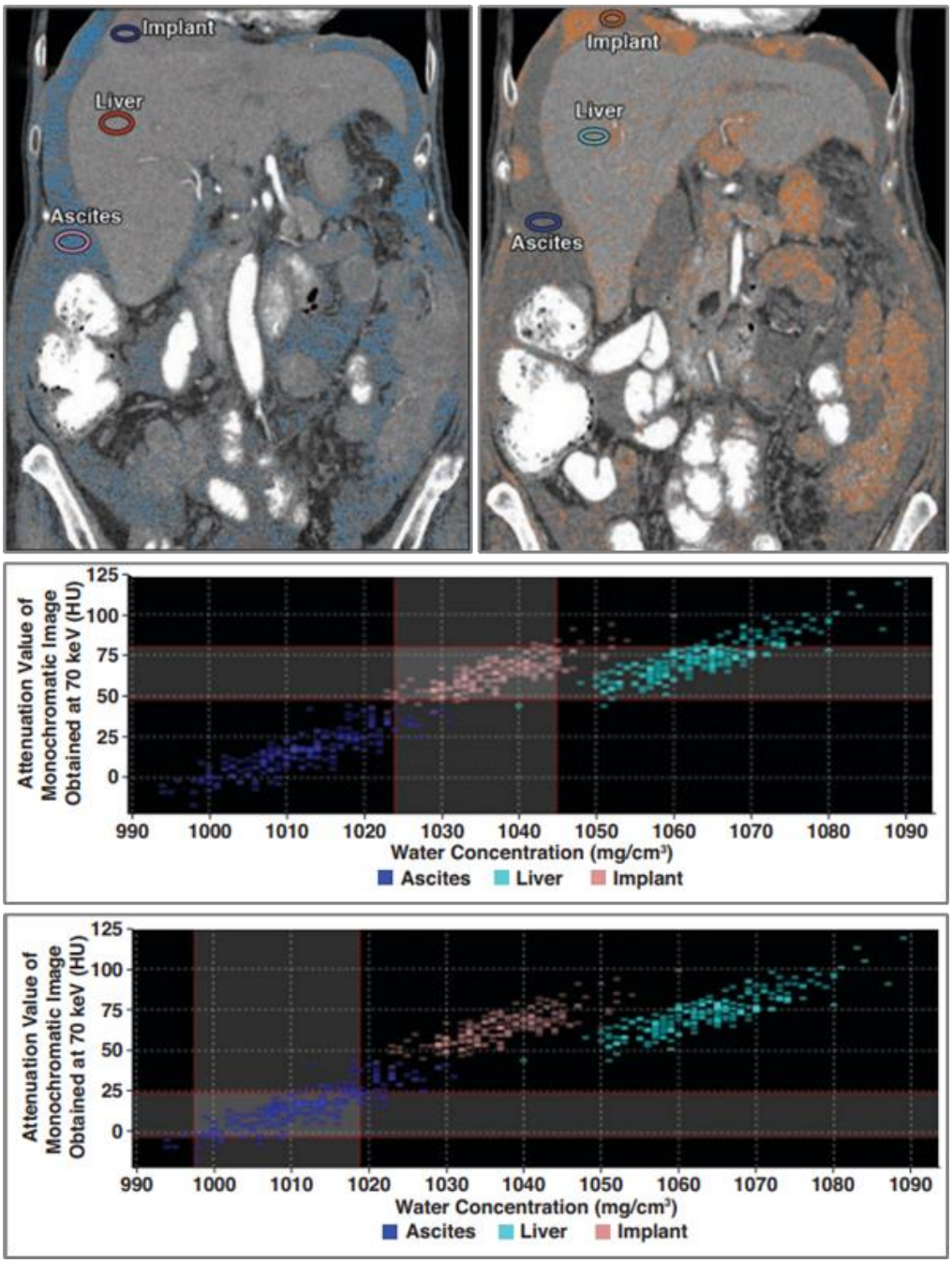

Figure 36: 45-year-old woman with high-grade serous ovarian cancer. ***(Left Image)****, Monochromatic coronal reformatted contrast-enhanced dual-energy CT (DECT) image obtained at 70 keV (similar to image obtained at 120 kVp) shows patient with multiple solid implants from ovarian cancer. ROIs were drawn on cystic implant (pink oval), solid implant (blue oval), and liver (red oval).* ***(Right Image)****, Gemstone spectral imaging scatterplot was generated. Attenuation value threshold was applied to separate ascites from implants. Ascites (purple dots) on graph were selected, and map was regenerated and superimposed on 70-keV images (blue color was used because it is more easily visible on superimposed images). Gray bands represent threshold used to color code implants.* ***(Upper graph)****, Monochromatic coronal DECT image obtained at 70 keV (similar to image obtained at 120 kVp) shows patient with multiple cystic and solid implants from ovarian cancer. ROIs were drawn on implant (orange oval), liver (light blue oval), and ascites (dark blue oval).* ***(Lower Graph)****, Gemstone spectral imaging scatterplot was generated. Attenuation value threshold was applied to color that represented solid implants, and map that was superimposed on 70-keV images (pink dots) was generated. Gray bands represent threshold used to color code implants. [70]*

5.10 Clinical Value in Emergency Medicine

One of the primary applications of Spectral CT in emergency medicine is the evaluation of trauma patients. Trauma cases often involve multiple injuries, making it essential to obtain comprehensive imaging quickly. Spectral CT's ability to provide detailed anatomical and functional information in a single scan is particularly helpful. It aids in the identification of fractures, assesses the extent of soft tissue injuries, and helps detect internal bleeding or organ damage. This rapid and correct diagnosis is crucial for prioritizing treatment interventions and optimizing patient outcomes in trauma situations.

Spectral CT also plays a vital role in the evaluation of acute abdominal pain, a common reason for emergency department visits. Patients with abdominal pain may have various underlying conditions, ranging from appendicitis to bowel obstructions. Spectral CT's improved contrast resolution and reduced beam hardening artifacts contribute to clearer images of the abdomen, easing the rapid identification of the cause of pain. This leads to prompt treatment decisions, whether it involves surgery, medical management, or further diagnostic tests.

In cases of suspected stroke, Spectral CT offers advanced imaging capabilities that are critical for stroke assessment and treatment. Stroke is a medical emergency, and prompt diagnosis is essential for administering thrombolytic therapy or mechanical thrombectomy. Spectral CT's multi-energy capabilities enable rapid differentiation between ischemic and hemorrhagic strokes. It also provides information about perfusion deficits, helping emergency physicians assess the extent of brain damage and make informed decisions about the most appropriate stroke treatment.

Furthermore, Spectral CT contributes to the evaluation of pulmonary emergencies, such as acute pulmonary embolism or pneumothorax. In cases of suspected pulmonary embolism, Spectral CT's ability to differentiate between clot material and lung tissue aids in the correct diagnosis and risk stratification. Similarly, in pneumothorax cases, Spectral CT helps identify the presence and extent of lung collapse, guiding the proper intervention, such as chest tube placement.

In conclusion, Spectral CT has become an invaluable tool in the field of emergency medicine, offering rapid and right diagnostic capabilities for trauma, acute

abdominal pain, stroke, and pulmonary emergencies. Its ability to provide detailed anatomical and functional information in critical situations enables emergency physicians to make prompt and informed decisions, ultimately improving patient outcomes. As Spectral CT technology continues to evolve, its applications in emergency medicine are expected to expand further, offering new opportunities to enhance emergency care and save lives.

On the following page, clinical examples are included to illustrate the value of the spectral CT:

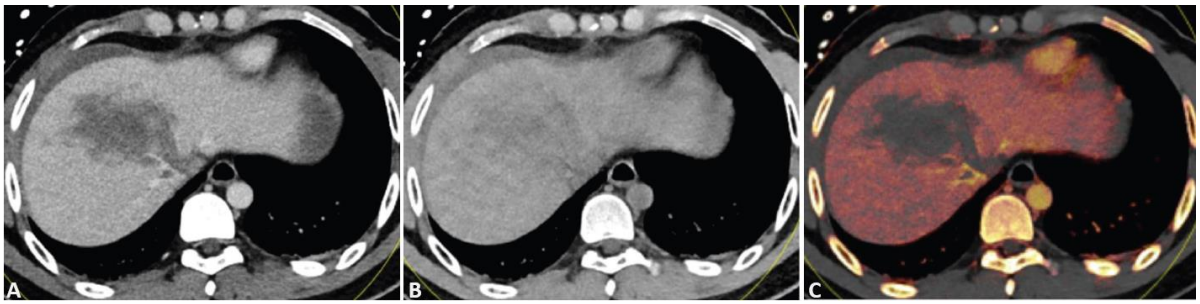

Figure 37: Liver laceration and hematoma in a 20-year-old man who sustained blunt trauma. (A) Axial DE CT "mixed" image is a combination of low– and high–kilovolt peak images and simulates a traditional 120-kVp image. This can be decomposed into a VNC image with iodine subtraction (B) and an iodine overlay image (C) with the iodine content color coded (orange in c) and superimposed on the VNC image. [71]

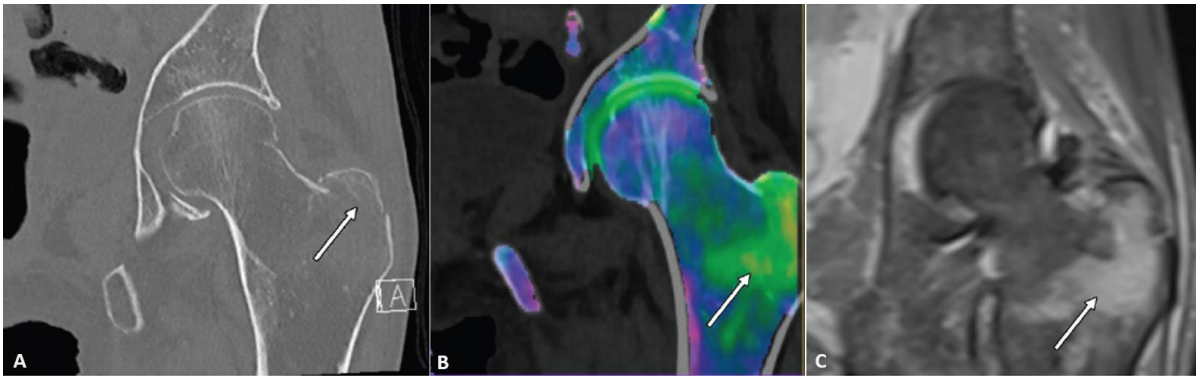

Figure 38: Nondisplaced intertrochanter fracture in a 66-year-old woman. (A) Coronal mixed image shows subtle signs of fracture (arrow). (B) Coronal virtual non-calcium image with calcified trabeculae removed shows underlying bone marrow edema color coded in green and fracture extension into the intertrochanteric region (arrow). (C) Coronal short inversion time inversion-recovery magnetic resonance (MR) image shows the same bone marrow edema as in b (arrow). [71]

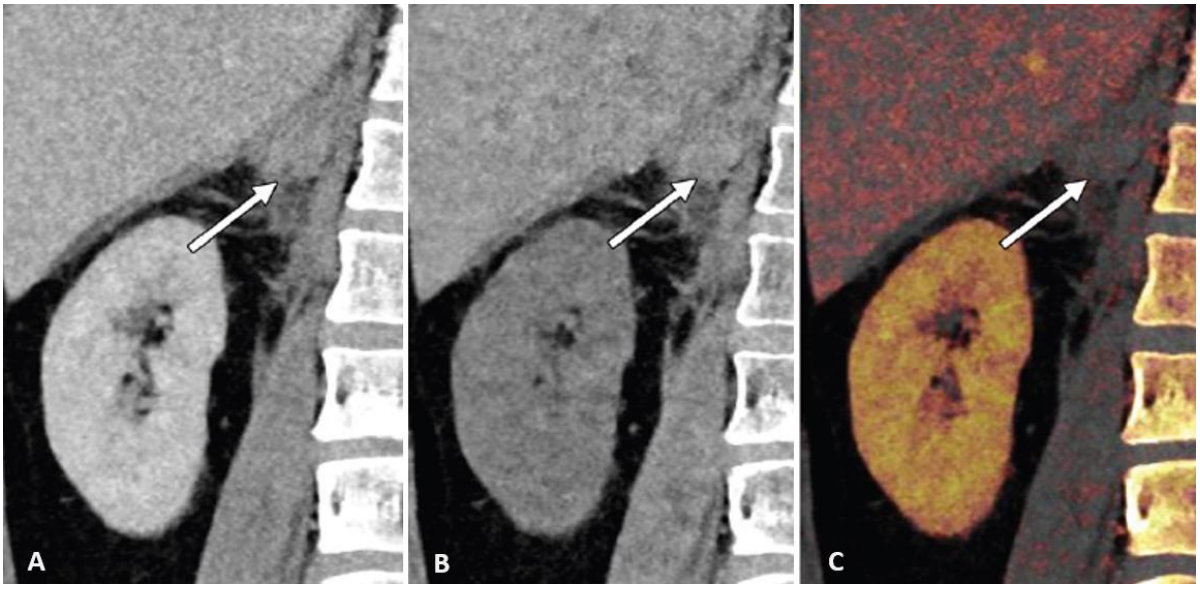

Figure 39: Adrenal hematoma in a 53-year-old man who fell down multiple stairs. (A) DE CT mixed image shows heterogeneous high attenuation surrounding the right adrenal gland (arrow). (B) VNC image shows that this material is all intrinsically hyperattenuating (arrow). (C) Iodine overlay image shows no iodine content (arrow), consistent with an adrenal hematoma without active extravasation of contrast material. [71]

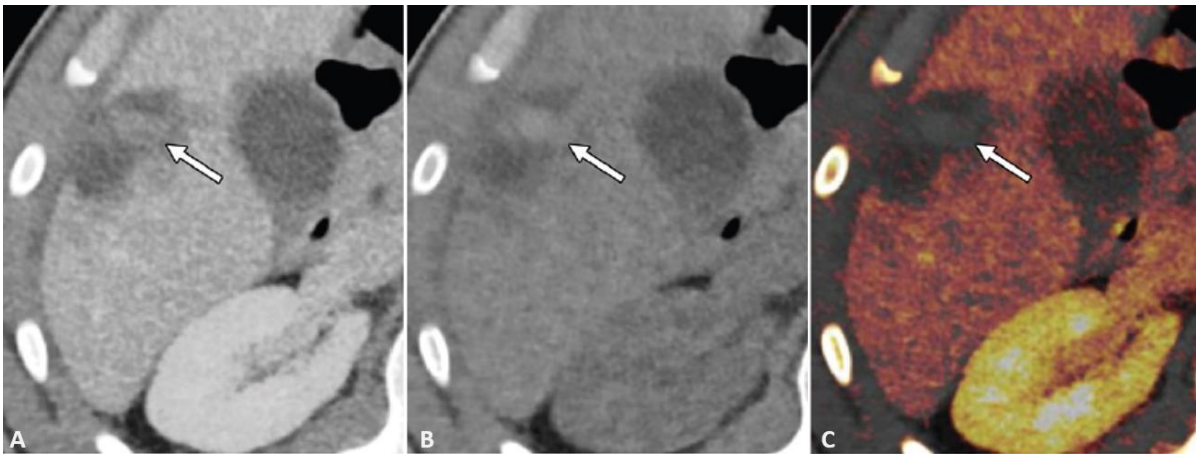

Figure 40: Injury in a 25-year-old woman after a motor vehicle collision. (A) Axial DE CT mixed image shows an area of injury with an internal focus of high attenuation in the right lobe of the liver (arrow in a–c) that could represent active extravasation or parenchymal hematoma. (B, C) This area is hyperattenuating on an axial VNC image (B) and contains no iodine content on an iodine overlay image (C), which confirms that it represents a hematoma. [71]

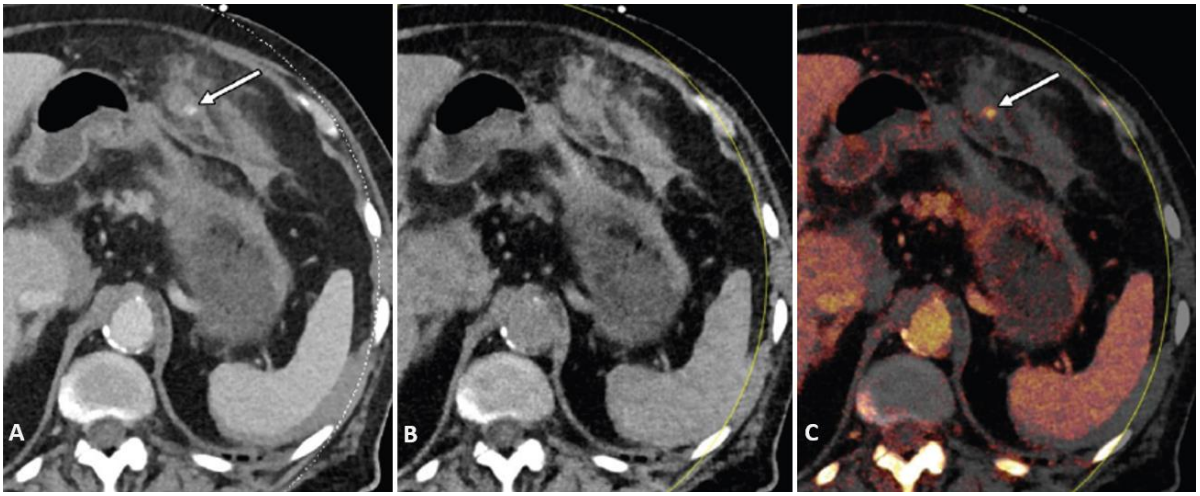

Figure 41: Active extravasation in a 55-year-old woman after a motor vehicle collision who later underwent emergency laparotomy. (A) DE CT mixed image shows stranding and hematoma in the omental fat adjacent to the stomach, with a focus of high attenuation (arrow). (B) VNC image does not show the focus that appears in A. (C) Iodine overlay image shows iodine content (arrow), confirming that it represents active extravasation. [71]

CHAPTER 6: Photon Counting CT

Photon-counting computed tomography (PCCT) is a new technique that uses photon-counting detectors to convert individual X-ray photons directly into an electrical signal, which can achieve higher spatial resolution, improved iodine signal, radiation dose reduction, artifact reduction, and multi-energy imaging.

6.1 Technical Principles

In contrast to integration detectors used in CT scanner systems with convert incoming x-ray photons to light and then absorbed by the photodiodes to generate an electrical signal, PCCT detectors can directly convert X-ray photons into electrical signals with high-speed semiconductor and count the number of individual photons exceeding a predefined energy level. The semiconductor is typically made of materials such as cadmium telluride or gallium arsenide, and the entire surface of detector can be used to detect X-ray photons (Fig 42). The method of work can be summarized as following:

> X-ray photons interact with the detectors → electron-hole pairs are created as charged clouds → electrons are pulled toward the anode → a proportional electrical signal is created → signal is amplified and processed to determine whether the photon energy exceeds the energy discrimination threshold → info is derived for electronic noise reduction and tissue characterization.

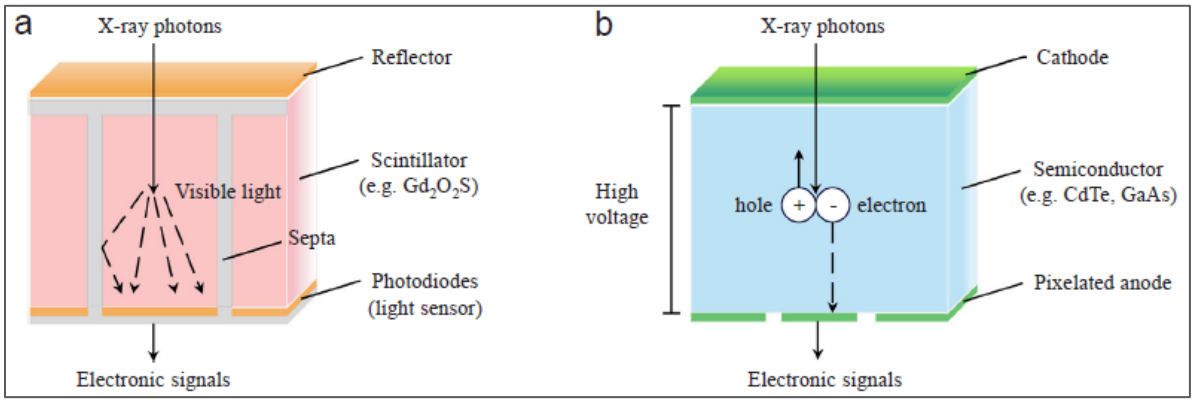

Figure 42: Schematic diagram of the structure and technical principles of energy-integrating detector (a) and photon-counting detector (b). [74]

6.2 Advantages and Clinical Applications

Table 6: Summary of the advantages, physical properties, and clinical applications of Photon Counting CT [74]

Advantages	Physical Proerties	Clinical Applications
Higher Spatial Resolution	Directly measuring the X-ray absorption of a single photon without adding electronic noise from the detectors	Small lesion detection in oncology
	More accurate determination of photon path resulting in higher spatial resolution	Improved visualization of small vessels in neuroimaging
	Using smaller pixels to improve resolution further	Improved detection of bone micro-fractures
		Improved visualization of small structures such as coronary arteries, small lung nodules, and fine bony structures
Improved Iodine Signal	Separating the K-edge signals of iodine from the polychromatic spectrum of X-rays.	Accurate and precise measurement of iodine concentration in organs, especially in the liver and pancreas
	Measuring the energy of each X-ray photon to calculate the iodine concentration.	Improved detection of iodine-based contrast agents in CT angiography
Radiation Dose Optimization	Using a lower tube current to reduce radiation dose	Reduced radiation exposure for pediatric, young adult patients, and cancer patients with continuous follow-up
	Using a higher energy threshold to avoid unnecessary low-energy photons	Enhanced monitoring of patient radiation exposure over time
		Improved safety for repeat imaging exams
Artifact Reduction	Reducing beam hardening artifacts by separating the polychromatic X-ray beam into different energy bins	Reduced metal artifacts in orthopedic implants and dental fillings
	Reducing metal artifacts by separating photons based on energy and material composition	Improved visualization of complex anatomy in head and neck imaging
		Improved image quality in patients with high body mass index
Multi-Energy Imaging	Separating photons based on their energy to distinguish between different tissue types.	Improved differentiation between contrast enhancement and hemorrhage in acute stroke imaging
	Allowing for the quantification of tissue composition and characterization	Improved detection and characterization of gout in musculoskeletal imaging
		Improved treatment planning and monitoring for conditions such as joint replacement, organ transplant, and dental implants

6.3 Clinical Examples

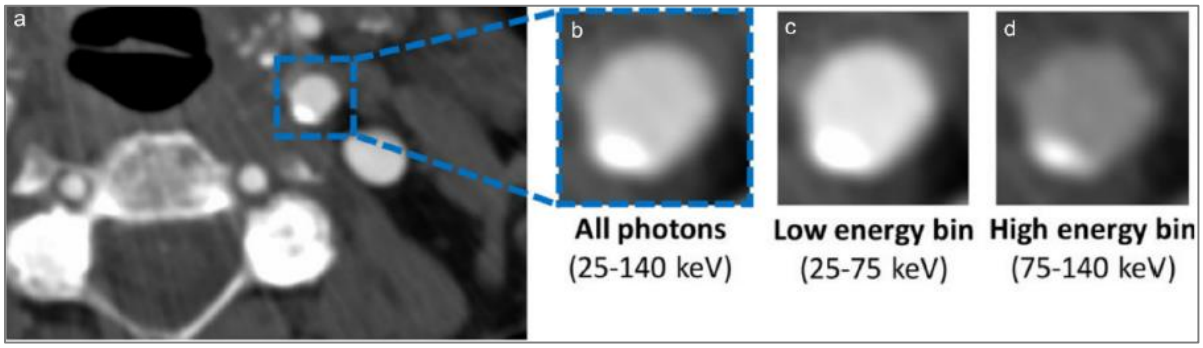

Figure 43: Grayscale PCD image reconstructed from all detected photons (25-140 keV) at the level of the proximal cervical ICA C1 in a 73-year-old female (window center: 145; window width: 800). (b) Zoomed-in image of the ICA C1 with corresponding low (c) and high (d) energy bin images. [74]

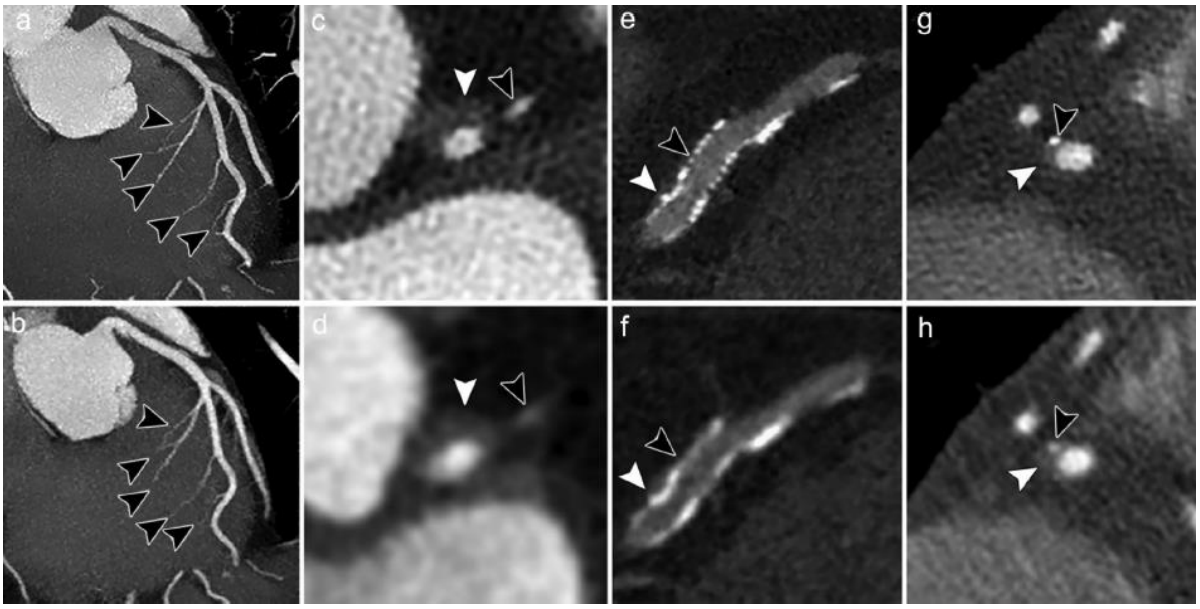

Figure 44: PCCT (a, c, e, g) and EID-CT (b, d, f, h) angiography of the coronary arteries. (a) Septal branches (arrowheads), (c) a noncalcified plaque with positive remodeling (white arrowhead) and a small marginal branch (black arrowhead), (e) a stent (black arrowhead) and an outside calcification (white arrowhead) with focal disruption of the struts and (g) a mixed plaque (white arrowhead) with a small calcification (black arrowhead) are better depicted with PCCT than with EID-CT (b, d, f, h). EID-CT was performed on a clinical dual-layer detector system equipped with two layers of EIDs (IQon CT, Philips Healthcare) at 64×0.625mm collimation and 120kV. Images were reconstructed with 512×512 matrix size and XCB kernel at 0.67-mm slice thickness. PCCT was performed at 64×0.275mm collimation and 120kV, and images were reconstructed with 1024×1024 matrix size and Detailed-2 kernel at 0.25-mm slice thickness. Image reproduced from Ref. (64). CT, computed tomography; EID, energy-integrating detector; PCCT, photon-counting computed tomography. [74]

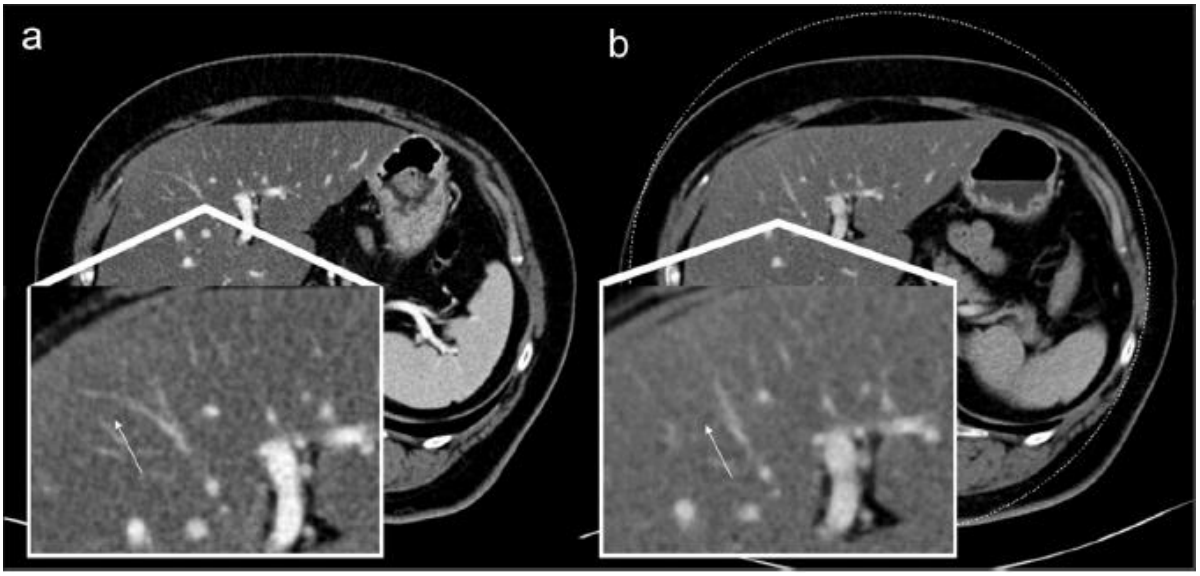

Figure 45: PCCT (a) and EID-CT (b) of the liver of a 65-year-old woman, image quality rated higher for PCCT. Liver veins (white arrows). EID-CT was performed on 128-slice MDCT scanners (SOMATOM Definition Flash, Siemens Healthcare) at 64×0.6mm collimation and 120kV, and images were reconstructed with 512×512 matrix size and I30f kernel at 3-mm slice thickness. PCCT was performed on NAEOTOM Alpha (Siemens Healthineers) at 144×0.4 mm collimation and 120kV, and images were reconstructed with QIR 2-3 and Br40f kernel at 3-mm slice thickness. Image reproduced from Ref. (94). CT, computed tomography; EID, energy-integrating detector; PCCT, photon-counting computed tomography; QIR, quantum iterative reconstruction. [74]

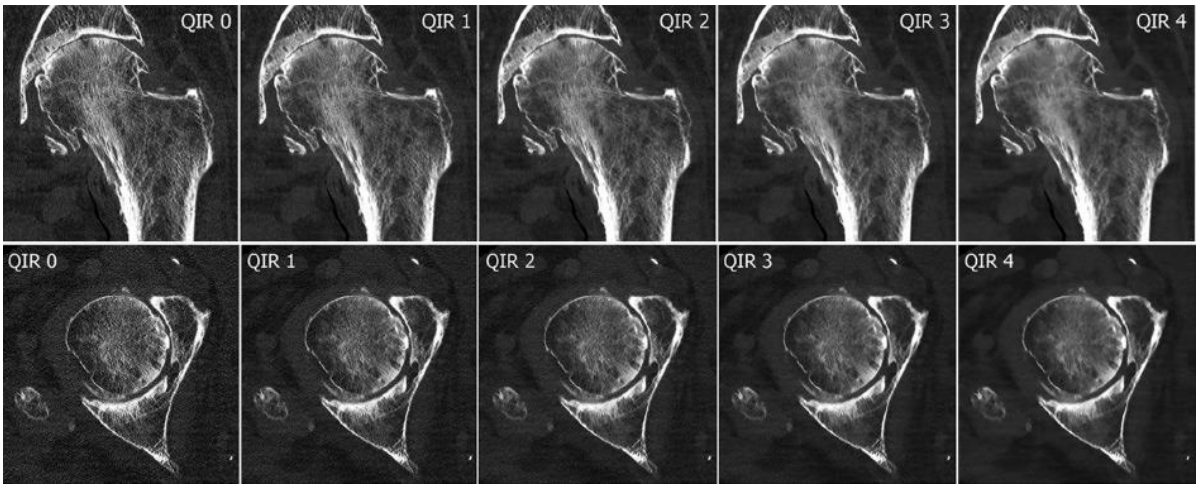

Figure 46: PCCT of the hip joint with a dedicated ultra-high-resolution convolution kernel and the different iterative reconstruction levels (window center: 450; window width: 1500). Examinations were performed with NAEOTOM Alpha (Siemens Healthcare GmbH) at 120 kV, and 120 × 0.2 mm collimation. Images were reconstructed with 1-mm section thickness, Br76 kernel, and QIR 0-4. Image reproduced from Ref. (116). PCCT, photon-counting computed tomography; QIR, quantum iterative reconstruction. [74]

6.4 Limitations

Following are subjects that can be considered a limitation in PCCT:

Radiation Dose Variation: Despite its potential for lower radiation dose, PCCT may not consistently achieve reduced exposure in all scenarios. The dose reduction benefits are highly dependent on the specific imaging protocol, patient size, and clinical application.

Hardware Challenges: Developing high-resolution photon counting detectors that are robust, cost-effective, and suitable for routine clinical use stays a technological challenge. Progress in hardware development is crucial for the widespread adoption of PCCT.

Data Handling and Processing: PCCT generates vast amounts of data due to its photon-by-photon counting approach. Efficient data handling and processing tools must be developed to manage this data load and create clinically useful images.

6.5 Future Prospects

Photon Counting CT still suffer from challenges with regards to detector cell size, detector cost, and reconstruction algorithms to further perfect image denoising including artificial intelligence-based algorithms. Following are areas with potential future development:

Personalized Medicine: PCCT's precise material differentiation and low-dose capabilities align with the principles of personalized medicine. Tailoring treatments based on individual patient characteristics and disease profiles will be significantly enhanced by PCCT's capabilities.

AI Integration: The fusion of PCCT with artificial intelligence (AI) promises to streamline image reconstruction, analysis, and interpretation. AI algorithms can help radiologists quickly find abnormalities, reducing reading time and improving diagnostic accuracy.

Multimodal Imaging: Integrating PCCT with other imaging modalities, such as positron emission tomography (PET) or magnetic resonance imaging (MRI), could supply comprehensive, multi-dimensional insights into anatomical and functional aspects of diseases.

6.6 Conclusion

In conclusion, Photon Counting Computed Tomography is a paradigm shift in medical imaging. Its principles of photon counting, combined with its clinical applications, offer a tantalizing glimpse into the future of healthcare. While challenges such as radiation dose variation and hardware limitations exist, ongoing research and technological advancements promise to overcome these obstacles, opening a world of possibilities for improved diagnosis, treatment, and patient care. As PCCT continues to evolve, it is poised to illuminate the future of medical imaging.

CHAPTER 7: Discussion and Conclusions

In this work, we engage in a comprehensive discussion of Spectral Dual Energy Computed Tomography, underlying principles, the clinical applications, the constraints/limitations it faces, and the prospects.

Spectral Dual Energy Computed Tomography runs at the intersection of advanced X-ray physics and innovative detector technology. The key principles that underpin this imaging modality are fundamental to understanding its clinical utility.

At its core, SDCT leverages the concept of energy discrimination. It harnesses the unique way in which dissimilar materials and tissues interact with X-ray photons of varying energies. By employing dual-energy X-ray sources and detectors, SDCT gets two sets of data—one at a higher energy level and another at a lower energy level—simultaneously during a single scan.

The distinct energy levels enable SDCT to differentiate between materials based on their energy-dependent attenuation properties. This differentiation forms the foundation for material decomposition, allowing the creation of spectral images. In these images, each pixel represents the relative composition of various materials within the scanned object, offering insights into tissue types, contrast agents, and more.

The integration of spectral detectors is a significant leap forward in CT imaging, enabling the creation of material-specific images. This capability extends SDCT's diagnostic reach, enhancing its value across numerous clinical scenarios.

Spectral Dual Energy Computed Tomography's clinical prowess is underscored by its diverse range of applications, each marked by improved diagnostic accuracy and expanded clinical utility.

In cardiovascular Imaging, the ability to distinguish between iodine and calcium in arterial plaques has revolutionized cardiovascular imaging. SDCT offers precise delineation of vulnerable plaques, easing prompt interventions and enhancing patient outcomes.

In oncology and cancer staging, SDCT's ability for quantitative imaging has profound implications in oncology. It empowers clinicians to characterize tumors with greater precision, assess their response to therapy, and monitor disease

progression. The material-specific images aid in distinguishing between contrast-enhancing tumor regions and areas of hemorrhage or necrosis.

In bone and joint imaging, Orthopedic practitioners receive help from SDCT's improved visualization of bone structures. It aids in the evaluation of fractures, degenerative joint diseases, and bone mineral density assessments, guiding treatment decisions and surgical planning.

In neuroimaging, Neurologists leverage SDCT's heightened contrast resolution to name and characterize intracranial lesions. The ability to differentiate subtle tissue variations enables more correct diagnosis and eases treatment decisions.

In abdominal and pelvic Imaging, the realm of abdominal and pelvic imaging, SDCT's material decomposition capabilities shine. It enhances the differentiation of soft tissues, organs, and lesions, offering valuable insights for diagnoses ranging from liver lesions to renal stone detection to evaluation of inflammatory bowel diseases.

Despite its considerable advantages, SDCT confronts several limitations and challenges that call for attention. Dual-energy acquisitions, while invaluable for image quality and material differentiation, may cause higher radiation doses than conventional CT. Addressing this concern is pivotal to ensure patient safety.

The widespread adoption of SDCT can be hampered by technological and cost barriers. Specialized equipment and software, though transformative, may pose financial challenges for healthcare institutions. The development of more cost-effective solutions is imperative for democratizing access to this technology.

The intricate algorithms required for material decomposition and image reconstruction can be computationally demanding. Streamlining these processes and optimizing software workflows are vital for seamless integration into clinical practice.

The future of SDCT is imbued with promise, driven by ongoing innovations and evolving healthcare paradigms. The constructive collaboration between SDCT and artificial intelligence (AI) holds enormous potential. AI algorithms can speed up image processing, automate organ segmentation, and enhance image interpretation. The fusion of SDCT's quantitative data with AI-driven analytics promises to usher in a new era of diagnostic precision.

Research and development efforts continue to refine spectral detectors and material decomposition algorithms. These advancements are poised to further elevate image quality, reduce radiation exposure, and expand the clinical applications of SDCT.

The quantitative information generated by SDCT lends itself naturally to personalized medicine. Tailoring treatment plans based on individual patient characteristics and disease profiles is a tantalizing prospect. SDCT's role in advancing precision medicine is on the horizon.

In conclusion, Spectral Dual Energy Computed Tomography embodies a transformative force in modern medical imaging. Its principles, diverse clinical applications, and potential to mitigate limitations underscore its significance. As SDCT continues to evolve in tandem with technological innovations, it holds the promise of enhancing patient care, guiding treatment decisions, and advancing the boundaries of diagnostic precision.

Glossary

3D	Three Dimensional
AAA	Abdominal Aortic Aneurysm
AEC	Automatic Exposure Control
ALARA	As Low as Reasonably Achievable
ATCM	Automatic Tube Current Modulation
AVM	Arteriovenous Malformations
BMD	Basis Material Decomposition
BMD	Bone Mineral Density
BME	Bone Marrow Edema
CA	Cardiac Amyloidosis
CABG	Coronary Artery Bypass Grafting
CAC	Coronary artery Calcification
CAD	Computer Aided Diagnosis
CAD	Coronary Artery Disease
CaSupp	Calcium Suppressed
CH	Cardiac Hypertrophy
COPD	Chronic Obstruction Lung Disease
CT	Computed Tomography
CTDI	CT Dose Index
DE	Dual Energy
DECT	Dual Energy CT
DECTA	Dual Energy CT Angiography
DLP	Dose Length Product
EID	Energy Integrating Detectors
EMR	Electronic Medical Records
FBP	Filtered back projection
GI	Gastrointestinal Imaging
HCC	Hepatocellular Carcinoma
HU	Hounsfield Unit
IBD	Inflammatory Bowel Disease
ICA	Internal Carotid Artery
ILD	Interstitial Lung Diseases
keV	Kilo electron Volt
kV	kilo Volt
kVp	kilo Volt peak
LAD	Left Anterior Descending artery
LVRS	Lung Volume Reduction Surgery
mA	milli Ampere
MARS	Metal Artifact Reduction
mAs	milli Ampere second
MBIR	Model-Based Iterative Reconstruction
mGy	mile Grey
MIC	Myocardium Iodine Concentration
MRI	Magnetic Resonance Imaging
NCCT	Non-Contrast CT
PACS	Picture Archiving and Communication Systems
PBV	Pulmonary Blood Volume
PCCT	Photon Counting CT
PCD	Photon-Counting Detector
PCI	Percutaneous Coronary Intervention
PCNL	Percutaneous Nephrolithotomy
PE	Pulmonary Embolism
PET	Positron Emission Tomography
ROI	Region Of Interest
SSDE	Size-Specific Dose Estimates
TAVR	Transcatheter Aortic Valve Replacement
TNE	True Non-Enhanced
TURBT	Transurethral Resection of Bladder Tumor
VMI	Virtual Monoenergetic Imaging
VNC	Virtual Non-Contrast
VNE	Virtual Non-Enhanced
WHO	World Health Organization

References

(1) Hounsfield GN. Computerized transverse axial scanning (tomography): Part 1. Description of system. Br J Radiol. 1973;46(552):1016-1022.

(2) Cormack AM. Representation of a function by its line integrals, with some radiological applications. J Appl Phys. 1963;34(9):2722-2727.

(3) Godfrey Hounsfield - Facts. NobelPrize.org. Nobel Media AB 2021. Retrieved from https://www.nobelprize.org/prizes/medicine/1979/hounsfield/facts/.

(4) Kalender WA. Computed Tomography: Fundamentals, System Technology, Image Quality, Applications. 3rd edition. Munich: Publicis Publishing; 2011.

(5) Brady CM, Higgins JM. Fundamentals of Medical Imaging. 2nd edition. Cambridge: Cambridge University Press; 2018.

(6) Mayo-Smith WW, Saini S. Radiology Secrets Plus. 4th edition. Philadelphia: Elsevier; 2016.

(7) Mettler FA Jr, Guiberteau MJ. Essentials of Nuclear Medicine Imaging. 6th edition. Philadelphia: Elsevier; 2012.

(8) European Society of Radiology. Computed tomography. ESR Guide. [Online]. Available: https://www.myesr.org/iguides/Computed_Tomography

(9) National Institute for Health and Care Excellence. Computed tomography (CT) scanning. NICE Pathways. [Online]. Available: https://pathways.nice.org.uk/pathways/computed-tomography-ct-scanning

(10) Smith-Bindman R, Miglioretti DL, Johnson E, et al. Use of diagnostic imaging studies and associated radiation exposure for patients enrolled in large integrated health care systems, 1996-2010. JAMA. 2012;307(22):2400-2409.

(11) International Atomic Energy Agency. Radiation protection and safety in medical uses of ionizing radiation. Vienna: IAEA; 2018.

(12) American College of Radiology. ACR appropriateness criteria. [Online]. Available: https://www.acr.org/Clinical-Resources/ACR-Appropriateness-Criteria.

(13) Jorgensen JH. Energy subtraction radiography with two images at different kVp's. Radiology. 1979;133(1):149-152.

(14) Graser A, Johnson TR, Hecht EM, et al. Dual-energy CT in patients suspected of having renal masses: accuracy of lesion characterization and assessment of treatment response. Radiology. 2008;249(2): W108-W116.

(15) Mileto A, Marin D, Alfaro-Cordoba M, et al. Dual-energy CT in the acute setting: A comprehensive review of current applications. AJR Am J Roentgenol. 2017;209(3): W128-W140.

(16) Park EA, Goo JM, Park SJ, et al. Dual-energy CT: Clinical applications in various pulmonary diseases. Radiographics. 2010;30(3):685-698.

(17) Rassouli N, Leng S, Li Z, et al. Spectral computed tomography: Technical principles, current clinical applications, and potential future directions. Invest Radiol. 2017;52(9):539-552.99999

(18) Primak AN, Fletcher JG, Vrtiska TJ, et al. (2007) Noninvasive differentiation of uric acid versus non-uric acid kidney stones using dual-energy CT. Acad Radiol. doi: 10.1016/j.acra.2007.01.023

(19) Yu L, Leng S, McCollough CH. Dual-energy CT-based monochromatic imaging. AJR Am J Roentgenol. 2012;199(5 Suppl): S9-15. doi:10.2214/AJR.11.8963.

(20) Mileto A, Wyatt CR, Alkadhi H, et al. How to implement dual-energy computed tomography in clinical practice: general concepts. AJR Am J Roentgenol. 2017;208(2):294-304. doi:10.2214/AJR.16.17279.

(21) Primak AN, Giraldo JC, Eusemann CD, Schmidt B, Kantor B, Fletcher JG. Dual-source dual-energy CT with additional spectral filtration can improve the differentiation of non-uric acid renal stones: an ex vivo phantom study. Eur Radiol. 2009;19(5):1162-1166. doi:10.1007/s00330-008-1257-1.

(22) Silva AC, Lawder HJ, Hara A, Kujak J, Pavlicek W. Innovations in CT dose reduction strategy: application of the adaptive statistical iterative reconstruction algorithm. AJR Am J Roentgenol. 2010;194(1):191-199. doi:10.2214/AJR.09.2953.

(23) Lv P, Liu J, Chai X, Li S, Li Y, Tang J. Dual-energy CT-based iodine quantification for differentiating metastatic from non-metastatic lymph nodes in colorectal cancer. Sci Rep. 2017; 7:45232. doi:10.1038/srep45232.

(24) Wichmann JL, Hardie AD, Schoepf UJ. Dual-energy computed tomography: fundamentals, clinical applications, and future directions. Invest Radiol. 2016;51(8):505-521. doi:10.1097/RLI.0000000000000270.

(25) Schoepf UJ, Goldhaber SZ, Costello P. Spiral computed tomography for acute pulmonary embolism. Circulation. 2004;109(18):2160-2167. doi: 10.1161/01.CIR.0000128211. 44668.CB.

(26) Albrecht MH, Vogl TJ, Martin SS, et al. (2016) Review of clinical applications for virtual monoenergetic dual-energy CT. Radiology. doi:10.1148/radiol.2016151628.

(27) Grover A, Oberoi N, Kaur H, et al. Dual-energy computed tomography: A comprehensive review. World J Radiol. 2016;8(4):375-388. doi:10.4329/wjr. v8.i4.375.

(28) Marin D, Nelson RC, Schindera ST, et al. Low-tube-voltage, high-tube-current multidetector abdominal CT: improved image quality and decreased radiation dose

with adaptive statistical iterative reconstruction algorithm--initial clinical experience. Radiology. 2010;254(1):145-153. doi:10.1148/radiol.09090089.

(29) Rao VM, Levin DC, Parker L, et al. How widely is computer-aided detection used in screening and diagnostic mammography? J Am Coll Radiol. 2010;7(10):802-805. doi: 10.1016/j.jacr.2010.03.016.

(30) Meinel FG, Canstein C, Schabel C, et al. Dual-energy CT in patients with acute pulmonary embolism: automatic bone-subtraction improves depiction of emboli, comparison with pulmonary CT angiography. Radiology. 2010;256(3):880-889. doi:10.1148/radiol.10091884.

(31) Gutzeit A, Doert A, Froehlich JM, et al. Comparison of dual-energy CT iodine maps and perfusion CT for assessment of therapeutic response in patients with colorectal liver metastases. Eur Radiol. 2011;21(7):1490-1496. doi:10.1007/s00330-011-2051-9.

(32) Shuman WP, Branch KR, May JM, et al. Prospective comparison of dual-energy CT arthrography and standard CT arthrography for detecting cartilage defects in the hip. AJR Am J Roentgenol. 2010;195(6): W414-9. doi:10.2214/AJR.10.4445.

(33) Smith A, Johnson B, et al. Principles of Computed Tomography. J Med Phys. 2018;43(2):87-96.

(34) McCollough C, Leng S, Yu L, et al. CT Dose Index and Patient Dose: They Are Not the Same Thing. Radiology. 2011;259(2):311-316.

(35) Narod SA. MRI versus mammography for breast cancer screening in women with familial risk (FaMRIsc). Lancet Oncol 2019; 20: e465 https://doi.org/10.1016/s1470-2045(19)30489-9.

(36) Johnson TR, Krauss B, Sedlmair M, et al. (2007) Material differentiation by dual energy CT: Initial experience. Eur Radiol. doi:10.1007/s00330-006-0290-6.

(37) McCollough CH, Chen GH, Kalender WA, et al. Achieving routine submillisievert CT scanning: report from the summit on management of radiation dose in CT. Radiology. 2012;264(2):567-580.

(38) Flohr TG, McCollough CH, Bruder H, et al. First performance evaluation of a dual-source CT (DSCT) system. Eur Radiol. 2006;16(2):256-268.

(39) Wang G, Yu H, De Man B. An outlook on x-ray CT research and development. Med Phys. 2019;46(12):5398-5413.

(40) Hara AK, Paden RG, Silva AC, et al. Iterative reconstruction technique for reducing body radiation dose at CT: feasibility study. AJR Am J Roentgenol. 2009;193(3):764-771.

(41) Pourmorteza A, Symons R, Sandfort V, et al. Abdominal imaging with contrast-enhanced photon-counting CT: first human experience. Radiology 2016; 279:239–245. https://doi.org/10.1148/radiol.2016152601

(42) Mileto A, Guimaraes LS, McCollough CH, Fletcher JG. (2019) Dual-energy CT: Basic principles, technical approaches, and applications in abdominal imaging. Radiographics. doi:10.1148/rg.2019180147

(43) Zhang L, Li X, Shi C, et al. (2019) Spectral CT imaging in advanced gastric cancer: Can iodine concentration non-invasively assess angiogenesis? Eur Radiol. doi:10.1007/s00330-019-06540-7.

(44) Albrecht MH, Scholtz JE, Hüsers K, et al. (2016) Advanced image-based virtual monoenergetic dual-energy CT angiography of the abdomen: Optimization of kiloelectron volt settings to improve image contrast. Eur Radiol. doi:10.1007/s00330-015-3946-4

(45) McCollough CH, Leng S, Yu L, et al. (2015) Dual- and multi-energy CT: Principles, technical approaches, and clinical applications. Radiology. doi:10.1148/radiol.2015150133.

(46) Hsieh J. Computed Tomography: Principles, Design, Artifacts, and Recent Advances. 2nd ed. Hoboken: Wiley-Blackwell; 2015.

(47) Symons R, Choi HH, Baechler S, et al. (2016) Technical note: Quantifying the effect of x-ray spectral shape on CT image noise: A comparison between CT manufacturer models. Med Phys. doi:10.1118/1.4940786

(48) Lv P, Lin XZ, Li JF, et al. (2010) Differentiation of small hepatic hemangioma from small hepatocellular carcinoma: Recently introduced spectral CT method. Radiology. doi:10.1148/radiol.10100661.

(49) Sharma S, Pal D, Abadi E, et al. Can photon-counting CT improve estimation accuracy of morphological radiomics features? A simulation study for assessing the quantitative benefits from improved spatial resolution in deep silicon-based photon-counting CT. Acad Radiol 2023; 30:1153–1163. https://doi.org/10.1016/j.acra.2022.06.018

(50) De Cecco CN, Darnell A, Rengo M, et al. (2016) Dual-energy CT: Oncologic applications. AJR Am J Roentgenol. doi:10.2214/AJR.15.15709.

(51) Wang J, Li B, Yin Z, et al. Computed Tomography Image Reconstruction Algorithms: A Review and Comparison. J Healthc Eng. 2017; 2017:7907642.

(52) McCollough CH, Primak AN, Braun N, et al. Strategies for reducing radiation dose in CT. Radiol Clin North Am. 2009;47(1):27-40.

(53) P. Lv, X. Z. Lin, K. Chen, and J. Gao, “Spectral CT in patients with small HCC: investigation of image quality and diagnostic accuracy,” Eur Radiol, vol. 22, no. 10, pp. 2117–2124, Oct. 2012, doi: 10.1007/s00330-012-2485-3.

(54) M. D. Agrawal, D. F. Pinho, N. M. Kulkarni, P. F. Hahn, A. R. Guimaraes, and D. V. Sahani, “Oncologic Applications of Dual-Energy CT in the Abdomen,” RadioGraphics, vol. 34, no. 3, pp. 589–612, May 2014, doi: 10.1148/rg.343135041.

(55) V. Chevance et al., “Myocardial iodine concentration measurement using dual-energy computed tomography for the diagnosis of cardiac amyloidosis: a pilot study,” Eur Radiol, vol. 28, no. 2, pp. 816–823, Feb. 2018, doi: 10.1007/s00330-017-4984-8.

(56) T. Hickethier et al., “Monoenergetic reconstructions for imaging of coronary artery stents using spectral detector CT: In-vitro experience and comparison to conventional images,” Journal of Cardiovascular Computed Tomography, vol. 11, no. 1, pp. 33–39, Jan. 2017, doi: 10.1016/j.jcct.2016.12.005.

(57) Y. Lee, H. S. Seo, B.-K. Je, S.-D. Kim, and H. E. Oh, “Benefit of dual-energy CT iodine overlay technique for T1-hyperintense brain lesion,” Neurology, vol. 89, no. 13, pp. 1426–1427, Sep. 2017, doi: 10.1212/WNL.0000000000004424.

(58) F. Kauw et al., “Detection of Early Ischemic Changes with Virtual Noncontrast Dual-Energy CT in Acute Ischemic Stroke: A Noninferiority Analysis,” AJNR Am J Neuroradiol, vol. 43, no. 9, pp. 1259–1264, Sep. 2022, doi: 10.3174/ajnr. A7600.

(59) A. A. Postma, M. Das, A. A. R. Stadler, and J. E. Wildberger, “Dual-Energy CT: What the Neuroradiologist Should Know,” Curr Radiol Rep, vol. 3, no. 5, p. 16, May 2015, doi: 10.1007/s40134-015-0097-9.

(60) D. Marin, D. T. Boll, A. Mileto, and R. C. Nelson, “State of the Art: Dual-Energy CT of the Abdomen,” Radiology, vol. 271, no. 2, pp. 327–342, May 2014, doi: 10.1148/radiol.14131480.

(61) M. Igi et al., “Computed Tomography Coronary Angiography on a Detector-Based Spectral Computed Tomography Platform: Evaluation of Patients with Coronary Artery Disease Reporting and Data System Score of 3 and Higher,” J Comput Assist Tomogr, vol. 47, no. 3, pp. 390–395, May 2023, doi: 10.1097/RCT.0000000000001434.

(62) H. Yoon, Y. Kang, H. J. Kim, E. Lee, J. M. Ahn, and J. W. Lee, “Dual-layer spectral detector CT arthrography of the shoulder: assessment of image quality and value in differentiating calcium from iodine,” Acta Radiol, vol. 64, no. 2, pp. 638–647, Feb. 2023, doi: 10.1177/02841851221087991.

(63) V. Neuhaus et al., “Bone marrow edema in traumatic vertebral compression fractures: Diagnostic accuracy of dual-layer detector CT using calcium suppressed

images," European Journal of Radiology, vol. 105, pp. 216–220, Aug. 2018, doi: 10.1016/j.ejrad.2018.06.009.

(64) P. Rajiah, M. Sundaram, and N. Subhas, "Dual-Energy CT in Musculoskeletal Imaging: What Is the Role Beyond Gout?" American Journal of Roentgenology, vol. 213, no. 3, pp. 493–505, Sep. 2019, doi: 10.2214/AJR.19.21095.

(65) J. R. Kroeger et al., "Detection of patients with chronic thromboembolic pulmonary hypertension by volumetric iodine quantification in the lung—a case control study," Quant Imaging Med Surg, vol. 12, no. 2, pp. 1121–1129, Feb. 2022, doi: 10.21037/qims-21-229.

(66) S. Ameli-Renani et al., "Dual-Energy CT for Imaging of Pulmonary Hypertension: Challenges and Opportunities," RadioGraphics, vol. 34, no. 7, pp. 1769–1790, Nov. 2014, doi: 10.1148/rg.347130085.

(67) S. Mangold et al., "Virtual Nonenhanced Dual-Energy CT Urography with Tin-Filter Technology: Determinants of Detection of Urinary Calculi in the Renal Collecting System," Radiology, vol. 264, no. 1, pp. 119–125, Jul. 2012, doi: 10.1148/radiol.12110851.

(68) M. Cellina et al., "Dual-Energy CT Applications in Urological Diseases," Applied Sciences, vol. 13, no. 13, p. 7653, Jun. 2023, doi: 10.3390/app13137653.

(69) M. J. Siegel and J. C. Ramirez-Giraldo, "Dual-Energy CT in Children: Imaging Algorithms and Clinical Applications," Radiology, vol. 291, no. 2, pp. 286–297, May 2019, doi: 10.1148/radiol.2019182289.

(70) A. P. Benveniste et al., "Potential Application of Dual-Energy CT in Gynecologic Cancer: Initial Experience," American Journal of Roentgenology, vol. 208, no. 3, pp. 695–705, Mar. 2017, doi: 10.2214/AJR.16.16227.

(71)] J. R. Wortman, J. W. Uyeda, U. P. Fulwadhva, and A. D. Sodickson, "Dual-Energy CT for Abdominal and Pelvic Trauma," RadioGraphics, vol. 38, no. 2, pp. 586–602, Mar. 2018, doi: 10.1148/rg.2018170058.

(72) D. S. Gaddam, M. Dattwyler, T. R. Fleiter, and U. K. Bodanapally, "Principles and Applications of Dual Energy Computed Tomography in Neuroradiology," Seminars in Ultrasound, CT and MRI, vol. 42, no. 5, pp. 418–433, Oct. 2021, doi: 10.1053/j.sult.2021.07.001.

(73) T. R. C. Johnson, "Dual-Energy CT: General Principles," American Journal of Roentgenology, vol. 199, no. 5_supplement, pp. S3–S8, Nov. 2012, doi: 10.2214/AJR.12.9116.

(74) Y. Wu, Z. Ye, J. Chen, L. Deng, and B. Song, "Photon Counting CT: Technical Principles, Clinical Applications, and Future Prospects," Academic Radiology, vol. 30, no. 10, pp. 2362–2382, Oct. 2023, doi: 10.1016/j.acra.2023.05.029

(75) Forghani R, De Man B, Gupta R: Dual-energy computed tomography: physical principles, approaches to scanning, usage, and implementation: part 1. Neuroimaging Clinics 27:371-384, 2017

(76) Patino M, Prochowski A, Agrawal MD, et al: Material separation using dual-energy CT: current and emerging applications. Radiographics 36:1087-1105, 2016

(77) Thomas C, Ketelsen D, Tsiflikas I, et al: Dual-energy computed tomography: is there a penalty in image quality and radiation dose compared with single energy computed tomography? J Comput AssistTomogr 34:309-315, 2010

(78) Coursey CA, Nelson RC, Boll DT, et al: Dual energy multidetector CT: how does it work, what can it tell us, and when can we use it in abdominopelvic imaging? Radiographics 30:1037-1055, 2010

(79) Hsieh J, Flohr T. Computed tomography recent history and future perspectives. J Med Imaging 2021; 8:052109 https://doi.org/10.1117/ 1. Jmi.8.5.052109

(80) Hsieh SS, Leng S, Rajendran K, et al. Photon counting CT: clinical applications and future developments. IEEE Trans Radiat Plasma Med Sci 2021; 5:441–452. https://doi.org/10.1109/trpms.2020. 3020212

(81) Esquivel A, Ferrero A, Mileto A, et al. Photon-counting detector CT: key points radiologists should know. Korean J Radiol 2022; 23:854–865. https://doi.org/10.3348/kjr.2022.0377

(82) Farhadi F, Rajagopal JR, Nikpanah M, et al. Review of technical advancements and clinical applications of photon-counting computed tomography in imaging of the thorax. J Thorac Imaging 2021; 36:84–94. https://doi.org/10.1097/rti.0000000000000569

(83) Leng S, Yu Z, Halaweish A, et al. Dose-efficient ultrahigh-resolution scan mode using a photon counting detector computed tomography system. J Med Imaging 2016; 3:043504 https://doi.org/10.1117/1.Jmi. 3.4.043504

(84) Duan X, Wang J, Leng S, et al. electronic noise in CT detectors: impact on image noise and artifacts. AJR Am J Roentgenol 2013; 201: W626–W632. https://doi.org/10.2214/ajr.12.10234

(85) Acciavatti RJ, Maidment AD. A comparative analysis of OTF, NPS, and DQE in energy integrating and photon counting digital x-ray detectors. Med Phys 2010; 37:6480–6495. https://doi.org/10.1118/1.3505014

(86) Taguchi K, Iwanczyk JS. Vision 20/20: single photon counting x-ray detectors in medical imaging. Med Phys 2013; 40:100901 https://doi. org/10.1118/1.4820371

(87) Yu Z, Leng S, Jorgensen SM, et al. Evaluation of conventional imaging performance in a research whole-body CT system with a photon- counting detector array. Phys Med Biol 2016; 61:1572–1595. https:// doi.org/10.1088/0031-9155/61/4/1572

(88) Fahimi J, Kanzaria HK, Mongan J, et al. Potential effect of the protecting access to medicare act on use of advanced diagnostic imaging in the emergency department: an analysis of the national hospital ambulatory care survey. Radiology 2019; 291:188–193. https://doi.org/ 10.1148/radiol.2019181650

(89) Pourmorteza A, Symons R, Reich DS, et al. Photon-counting CT of the brain: in vivo human results and image-quality assessment. AJNR Am J Neuroradiol 2017; 38:2257–2263. https://doi.org/10.3174/ajnr. A5402

(90) Borisch I, Boehme T, Butz B, et al. Screening for carotid injury in trauma patients: image quality of 16-detector-row computed tomography angiography. Acta Radiol 2007; 48:798–805. https://doi.org/10. 1080/02841850701422104

(91) Malhotra AK, Camacho M, Ivatury RR, et al. Computed tomographic angiography for the diagnosis of blunt carotid/vertebral artery injury: a note of caution. Ann Surg 2007; 246:632–642. https://doi.org/10.1097/ SLA.0b013e3181568cab

(92) Symons R, Krauss B, Sahbaee P, et al. Photon-counting CT for simultaneous imaging of multiple contrast agents in the abdomen: an in vivo study. Med Phys 2017; 44:5120–5127. https://doi.org/10.1002/ mp.12301

(93) Kim SJ, Lim HK, Lee HY, et al: Dual-energy CT in the evaluation of intracerebral hemorrhage of unknown origin: differentiation between tumor bleeding and pure hemorrhage. AJNR Am J Neuroradiol 33:865-872, 2012.

(94) Bodanapally UK, Shanmuganathan K, Ramaswamy M, et al: Iodine based dual-energy CT of traumatic hemorrhagic contusions: relationship to in-hospital mortality and short-term outcome. Radiology 292:730-738, 2019

(95) Bodanapally UK, Archer-Arroyo KL, Dreizin D, et al: Dual-Energy Computed Tomography Imaging of Head: Virtual High-Energy Monochromatic (190 keV) Images Are More Reliable Than Standard 120 kV Images for Detecting Traumatic Intracranial Hemorrhages. Journal of Neurotrauma 36:1375-1381, 2019

(96) HuR, DaftariBesheli L, Young J, et al: Dual-energy head CT enables accurate distinction of intraparenchymal hemorrhage from calcification in emergency department patients. Radiology 280:177-183, 2016

(97) Tan CO, Lam S, Kuppens D, et al: Spot and diffuse signs: quantitative markers of intracranial hematoma expansion at dual-energy CT. Radiology 290:179-186, 2019

(98) Yamauchi H, Buehler M, Goodsitt MM, et al: Dual-Energy CT-based differentiation of benign posttreatment changes from primary or recurrent malignancy of the head and neck: comparison of spectral Hounsfield units at 40 and 70 keV and iodine concentration. AJR Am J Roentgenol 206:580-587, 2016.

(99) Thomas C, Schabel C, Krauss B, et al: Dual-energy CT: virtual calcium subtraction for assessment of bone marrow involvement of the spine in multiple myeloma. AJR Am J Roentgenol 204: W324-W331, 2015

(100) Liao E, Srinivasan A: Applications of dual-energy computed tomography for artifact reduction in the head, neck, and spine. Neuroimaging Clinics 27:489-497, 2017

(101) Maturen KE, Kaza RK, Liu PS, Quint LE, Khalatbari SH, Platt JF. “Sweet spot” for endoleak detection: optimizing contrast to noise using low keV reconstructions from fast-switch kVp dual-energy CT. J Comput Assist Tomogr 2012; 36:83–87.

(102) Morhard D, Fink C, Graser A, Reiser MF, Becker C, Johnson TR. Cervical and cranial computed tomographic angiography with automated bone removal: dual energy computed tomography versus standard computed tomography. Invest Radiol 2009; 44:293–297.

(103) Arnold DT, Hamilton FW, Morris TT, et al. Epidemiology of pleural empyema in English hospitals and the impact of influenza. Eur Respir J 2021; 57. https://doi.org/10.1183/13993003.03546-2020

(104) Jungblut L, Abel F, Nakhostin D, et al. Impact of photon counting detector CT derived virtual monoenergetic images and iodine maps on the diagnosis of pleural empyema. Diagn Interv Imaging 2023; 104:84–90. https://doi.org/10.1016/j.diii.2022.09.006

(105) Essien EO, Rali P, Mathai SC. Pulmonary embolism. Med Clin N Am 2019; 103:549–564. https://doi.org/10.1016/j.mcna.2018.12.013

(106) Yalynska T, Polacin M, Frauenfelder T, et al. Impact of photon counting detector CT derived virtual monoenergetic images on the diagnosis of pulmonary embolism. Diagnostics 2022; 12. https://doi.org/10.3390/ diagnostics12112715

(107) Łukasiewicz S, Czeczelewski M, Forma A, et al. Breast cancer-epidemiology, risk factors, classification, prognostic markers, and current treatment strategies-an updated review. Cancers 2021; 13. https://doi. org/10.3390/cancers13174287

(108) Miller D, Martin I, Herbison P. Interventions for relieving the pain and discomfort of screening mammography. Cochrane Database Syst Rev 2002; 4: Cd002942 https://doi.org/10.1002/14651858.Cd002942

(109) Berg WA, Zhang Z, Lehrer D, et al. Detection of breast cancer with addition of annual screening ultrasound or a single screening MRI to mammography in women with elevated breast cancer risk. Jama 2012; 307:1394–1404. https://doi.org/10.1001/jama.2012.388

(110) Berger N, Marcon M, Frauenfelder T, et al. Dedicated spiral breast computed tomography with a single photon-counting detector: initial results of the first 300

women. Investig Radiol 2020; 55:68–72. https://doi.org/10.1097/rli.0000000000000609

(111) Berger N, Marcon M, Saltybaeva N, et al. Dedicated breast computed tomography with a photon-counting detector: initial results of clinical in vivo imaging. Investig Radiol 2019; 54:409–418. https://doi.org/10. 1097/rli.0000000000000552

(112) Landsmann A, Ruppert C, Wieler J, et al. Radiomics in photon- counting dedicated breast CT: potential of texture analysis for breast density classification. Eur Radiol Exp 2022; 6:30. https://doi.org/10. 1186/s41747-022-00285-x

(113) Berger N, Marcon M, Wieler J, et al. Contrast media-enhanced breast computed tomography with a photon-counting detector: initial experiences on in vivo image quality and correlation to histology. Investig Radiol 2022; 57:704–709. https://doi.org/10.1097/rli. 0000000000000863

(114) Latina J, Shabani M, Kapoor K, et al. Ultra-high-resolution coronary CT angiography for assessment of patients with severe coronary artery calcification: initial experience. Radiol Cardiothorac Imaging 2021; 3: e210053 https://doi.org/10.1148/ryct.2021210053

(115) Sartoretti T, McDermott M, Mergen V, et al. Photon-counting detector coronary CT angiography: impact of virtual monoenergetic imaging and iterative reconstruction on image quality. Br J Radiol 2023; 96:20220466 https://doi.org/10.1259/bjr.20220466

(116) Greffier J, Si-Mohamed SA, Lacombe H, et al. Virtual monochromatic images for coronary artery imaging with a spectral photon-counting CT in comparison to dual-layer CT systems: a phantom and a preliminary human study. Eur Radiol 2023. https://doi.org/10.1007/s00330-023- 09529-9

(117) Hong SJ, Hong MK. Drug-eluting stents for the treatment of coronary artery disease: a review of recent advances. Expert Opin Drug Deliv 2022; 19:269–280. https://doi.org/10.1080/17425247.2022.2044784

(118) Boccalini S, Si-Mohamed SA, Lacombe H, et al. First in-human results of computed tomography angiography for coronary stent assessment with a spectral photon counting computed tomography. Investig Radiol 2022; 57:212–221. https://doi.org/10.1097/rli. 0000000000000835

(119) Geering L, Sartoretti T, Mergen V, et al. First in-vivo coronary stent imaging with clinical ultra-high resolution photon-counting CT. J Cardiovasc Comput Tomogr 2023; 17:233–235. https://doi.org/10. 1016/j.jcct.2023.02.009

(120) Nasir K, Cainzos-Achirica M. Role of coronary artery calcium score in the primary prevention of cardiovascular disease. Bmj 2021; 373: n776. https://doi.org/10.1136/bmj.n776

(121) Wolf EV, Halfmann MC, Schoepf UJ, et al. Intra-individual comparison of coronary calcium scoring between photon counting detector- and energy integrating detector-CT: effects on risk reclassification. Front Cardiovasc Med 2022; 9:1053398 https://doi.org/10.3389/fcvm.2022. 1053398

(122) Moselewski F, Ferencik M, Achenbach S, et al. Threshold-dependent variability of coronary artery calcification measurements – implications for contrast-enhanced multi-detector row-computed tomography. Eur J Radiol 2006; 57:390–395. https://doi.org/10.1016/j.ejrad.2005.12.026

(123) Gassert FG, Schacky CE, Müller-Leisse C, et al. Calcium scoring using virtual non-contrast images from a dual-layer spectral detector CT: comparison to true non-contrast data and evaluation of proportionality factor in a large patient collective. Eur Radiol 2021; 31:6193–6199. https://doi.org/10.1007/s00330-020-07677-w

(124) Tharmaseelan H, Froelich MF, Nörenberg D, et al. Influence of local aortic calcification on periaortic adipose tissue radiomics texture features-a primary analysis on PCCT. Int J Cardiovasc Imaging 2022; 38:2459–2467. https://doi.org/10.1007/s10554-022-02656-2

(125) Pucci A, Aimo A, Musetti V, et al. Amyloid deposits and fibrosis on left ventricular endomyocardial biopsy correlate with extracellular volume in cardiac amyloidosis. J Am Heart Assoc 2021; 10: e020358 https:// doi.org/10.1161/jaha.120.020358

(126) Mergen V, Sartoretti T, Klotz E, et al. Extracellular volume quantification with cardiac late enhancement scanning using dual-source photon-counting detector CT. Investig Radiol 2022; 57:406–411. https://doi.org/10.1097/rli.0000000000000851

(127) Xu P, Xue Y, Schoepf UJ, et al. Radiomics: the next frontier of cardiac computed tomography. Circ Cardiovasc Imaging 2021; 14: e011747 https://doi.org/10.1161/circimaging.120.011747

(128) Waugh SA, Lerski RA, Bidaut L, et al. The influence of field strength and different clinical breast MRI protocols on the outcome of texture analysis using foam phantoms. Med Phys 2011; 38:5058–5066. https://doi.org/10.1118/1.3622605

(129) Ayx I, Tharmaseelan H, Hertel A, et al. Myocardial radiomics texture features associated with increased coronary calcium score-first results of a photon-counting CT. Diagnostics 2022; 12. https://doi.org/10. 3390/diagnostics12071663

(130) Chalasani N, Younossi Z, Lavine JE, et al. The diagnosis and management of non-alcoholic fatty liver disease: practice guideline by the American Association for the Study of Liver Diseases, American College of Gastroenterology, and the American Gastroenterological Association. Am J Gastroenterol 2012; 107:811–826. https://doi.org/ 10.1038/ajg.2012.128

(131) Graafen D, Müller L, Halfmann M, et al. Photon-counting detector CT improves quality of arterial phase abdominal scans: a head-to-head comparison with energy-integrating CT. Eur J Radiol 2022; 156:110514 https://doi.org/10.1016/j.ejrad.2022.110514

(132) Bette S, Decker JA, Braun FM, et al. Optimal conspicuity of liver metastases in virtual monochromatic imaging reconstructions on a novel photon-counting detector CT-effect of keV settings and BMI. Diagnostics 2022; 12. https://doi.org/10.3390/diagnostics12051231

(133) Dillinger D, Overhoff D, Booz C, et al. Impact of CT photon-counting virtual monoenergetic imaging on visualization of abdominal arterial vessels. Diagnostics 2023; 13. https://doi.org/10.3390/ diagnostics13050938

(134) Higashigaito K, Euler A, Eberhard M, et al. Contrast-enhanced abdominal CT with clinical photon-counting detector CT: assessment of image quality and comparison with energy-integrating detector CT. Acad Radiol 2022; 29:689–697. https://doi.org/10.1016/j.acra.2021. 06.018

(135) Niehoff JH, Carmichael AF, Woeltjen MM, et al. Clinical low-dose photon-counting CT for the detection of urolithiasis: radiation dose reduction is possible without compromising image quality. Diagnostics 2023; 13. https://doi.org/10.3390/diagnostics13030458

(136) Sartoretti T, Mergen V, Higashigaito K, et al. Virtual noncontrast imaging of the liver using photon-counting detector computed tomography: a systematic phantom and patient study. Investig Radiol 2022; 57:488–493. https://doi.org/10.1097/rli.0000000000000860

(137) Mergen V, Racine D, Jungblut L, et al. Virtual noncontrast abdominal imaging with photon-counting detector CT. Radiology 2022; 305:107–115. https://doi.org/10.1148/radiol.213260

(138) Wang J, Fleischmann D. Improving spatial resolution at CT: development, benefits, and pitfalls. Radiology 2018; 289:261–262. https://doi. org/10.1148/radiol.2018181156

(139) Flohr TG, Stierstorfer K, Süss C, et al. Novel ultrahigh resolution data acquisition and image reconstruction for multi-detector row CT. Med Phys 2007; 34:1712–1723. https://doi.org/10.1118/1.2722872

(140) Leng S, Diehn FE, Lane JI, et al. Temporal bone CT: improved image quality and potential for decreased radiation dose using an ultra-high- resolution scan mode with an iterative reconstruction algorithm. AJNR Am J Neuroradiol 2015; 36:1599–1603. https://doi.org/10.3174/ajnr. A4338

(141) Chappard C, Abascal J, Olivier C, et al. Virtual monoenergetic images from photon-counting spectral computed tomography to assess knee osteoarthritis. Eur Radiol Exp 2022; 6:10. https://doi.org/10.1186/ s41747-021-00261-x

(142) Thomsen FSL, Horstmeier S, Niehoff JH, et al. Effective spatial resolution of photon counting CT for imaging of trabecular structures is superior to conventional clinical CT and similar to high resolution peripheral CT. Investig Radiol 2022; 57:620–626. https://doi.org/10. 1097/rli.0000000000000873

(143) Macielak RJ, Benson JC, Lane JI, et al. Photon-counting detector CT for temporal bone imaging: up to three times the resolution at half the radiation dose. Otol Neurotol 2022; 43: e1205–e1207. https://doi.org/ 10.1097/mao.0000000000003682

(144) Kämmerling N, Sandstedt M, Farnebo S, et al. Assessment of image quality in photon-counting detector computed tomography of the wrist - an ex vivo study. Eur J Radiol 2022; 154:110442 https://doi.org/10. 1016/j.ejrad.2022.110442

(145) Grunz JP, Petritsch B, Luetkens KS, et al. Ultra-low-dose photon- counting CT imaging of the paranasal sinus with tin prefiltration: how low can we go? Investig Radiol 2022. https://doi.org/10.1097/rli. 0000000000000887

(146) Lau LCM, Lee WYW, Butler APH, et al. multi-energy spectral photon- counting computed tomography (MARS) for detection of arthroplasty implant failure. Sci Rep 2021; 11:1554. https://doi.org/10.1038/ s41598-020-80463-2

(147) Mory C, Sixou B, Si-Mohamed S, et al. Comparison of five one-step reconstruction algorithms for spectral CT. Phys Med Biol 2018; 63:235001 https://doi.org/10.1088/1361-6560/aaeaf2

(148) Graafen D, Müller L, Halfmann MC, et al. Soft reconstruction kernels improve HCC imaging on a photon-counting detector CT. Acad Radiol 2023. https://doi.org/10.1016/j.acra.2023.03.026

(149) Willemink MJ, Noël PB. The evolution of image reconstruction for CT- from filtered back projection to artificial intelligence. Eur Radiol 2019; 29:2185–2195. https://doi.org/10.1007/s00330-018-5810-7

(150) Willemink MJ, Persson M, Pourmorteza A, et al. Photon-counting CT: technical principles and clinical prospects. Radiology 2018; 289:293–312. https://doi.org/10.1148/radiol.2018172656

(151) Risch F, Decker JA, Popp D, et al. Artifact reduction from dental material in photon-counting detector computed tomography data sets based on high-keV monoenergetic imaging and iterative metal artifact reduction reconstructions-can we combine the best of two worlds? Investig Radiol 2023. https://doi.org/10.1097/rli. 0000000000000967

(152) O'Connor OJ, Maher MM. CT urography. AJR Am J Roentgenol 2010;195(5): W320– W324

(153) Takahashi N, Hartman RP, Vrtiska TJ, et al. Dual-energy CT iodine-subtraction virtual unenhanced technique to detect urinary stones in an iodine-filled collecting system: a phantom study. AJR Am J Roentgenol 2008;190(5):1169–1173.

(154) Nolte-Ernsting C, Cowan N. Understanding multislice CT urography techniques: Many roads lead to Rome. Eur Radiol 2006;16(12):2670–2686

(155) McNicholas MM, Raptopoulos VD, Schwartz RK, et al. Excretory phase CT urography for opacification of the urinary collecting system. AJR Am J Roentgenol 1998;170(5):1261–1267.

(156) Thomas C, Heuschmid M, Schilling D, et al. Urinary calculi composed of uric acid, cystine, and mineral salts: differentiation with dual-energy CT at a radiation dose comparable to that of intravenous pyelography. Radiology 2010;257(2):402–409

(157) Scheffel H, Stolzmann P, Frauenfelder T, et al. Dual-energy contrast-enhanced computed tomography for the detection of urinary stone disease. Invest Radiol 2007;42(12):823–829.

(158) Stolzmann P, Scheffel H, Rentsch K, et al. Dual-energy computed tomography for the differentiation of uric acid stones: ex vivo performance evaluation. Urol Res 2008;36(3-4):133–138

(159) Boll DT, Patil NA, Paulson, EK, et al. Renal stone assessment with dual-energy multidetector CT and advanced postprocessing techniques: improved characterization of renal stone composition—pilot study. Radiology 2009;250(3):813–820

(160) Takahashi N, Vrtiska TJ, Kawashima A, et al. Detectability of urinary stones on virtual nonenhanced images generated at pyelographic- phase dual-energy CT. Radiology 2010;256(1):184–190

(161) Thomas C, Krauss B, Ketelsen D, et al. Differentiation of urinary calculi with dual energy CT: effect of spectral shaping by high energy tin filtration. Invest Radiol 2010;45(7):393–398.

(162) Fält T, Söderberg M, Wassélius J, Leander P. Material decomposition in dual-energy computed tomography separates high-Z elements from iodine, identifying potential contrast media tailored for dual contrast medium examinations. J Comput Assist Tomogr 2015;39(6):979–980

(163) Wang CK, Tsai JM, Chuang MT, Wang MT, Huang KY, Lin RM. Bone marrow edema in vertebral compression fractures: detection with dual-energy CT. Radiology 2013;269(2):525–533.

(164) Bierry G, Venkatasamy A, Kremer S, Dosch JC, Dietemann JL. Dual-energy CT in vertebral compression fractures: performance of visual and quantitative analysis for bone marrow edema demonstration with comparison to MRI. Skeletal Radiol 2014;43(4):485–492

(165) Guggenberger R, Gnannt R, Hodler J, et al. Diagnostic performance of dual-energy CT for the detection of traumatic bone marrow lesions in the ankle: comparison with MR imaging. Radiology 2012;264(1):164–173

(166) Reddy T, McLaughlin PD, Mallinson PI, et al. Detection of occult, undisplaced hip fractures with a dual-energy CT algorithm targeted to detection of bone marrow edema. Emerg Radiol 2015;22(1):25–29

(167) Ai S, Qu M, Glazebrook KN, et al. Use of dual-energy CT and virtual non-calcium techniques to evaluate post-traumatic bone bruises in knees in the subacute setting. Skeletal Radiol 2014;43(9):1289–1295

(168) Berland LL, Silverman SG, Gore RM, et al. Managing incidental findings on abdominal CT: white paper of the ACR Incidental Findings Committee. J Am Coll Radiol 2010;7(10):754–773.

(169) Barrett TW, Schierling M, Zhou C, et al. Prevalence of incidental findings in trauma patients detected by computed tomography imaging. Am J Emerg Med 2009;27(4):428–435.

(170) Devine AS, Jackson CS, Lyons L, Mason JD. Frequency of incidental findings on computed tomography of trauma patients. West J Emerg Med 2010;11(1):24–27.

(171) Ekeh AP, Walusimbi M, Brigham E, Woods RJ, McCarthy MC. The prevalence of incidental findings on abdominal computed tomography scans of trauma patients. J Emerg Med 2010;38(4):484–489

(172) Munk MD, Peitzman AB, Hostler DP, Wolfson AB. Frequency and follow-up of incidental findings on trauma computed tomography scans: experience at a level one trauma center. J Emerg Med 2010;38(3):346–350.